University of Nebraska - Lincoln
DigitalCommons@University of Nebraska - Lincoln

Nebraska Department of Transportation Research Reports

Nebraska LTAP

9-2016

Performance of Advance Warning Systems in a Coordinated System

Li Zhao
University of Nebraska-Lincoln, lizhao@unl.edu

Laurence R. Rilett
University of Nebraska-Lincoln, lrilett2@unl.edu

Ernest Tufuor
University of Nebraska - Lincoln, ernest.tufuor@huskers.unl.edu

Waleed Khan
University of Nebraska - Lincoln

Christopher LeFrois
University of Nebraska - Lincoln, chrislefrois@unl.edu

Follow this and additional works at: https://digitalcommons.unl.edu/ndor

 Part of the Transportation Engineering Commons

Zhao, Li; Rilett, Laurence R.; Tufuor, Ernest; Khan, Waleed; and LeFrois, Christopher, "Performance of Advance Warning Systems in a Coordinated System" (2016). *Nebraska Department of Transportation Research Reports*. 187.
https://digitalcommons.unl.edu/ndor/187

This Article is brought to you for free and open access by the Nebraska LTAP at DigitalCommons@University of Nebraska - Lincoln. It has been accepted for inclusion in Nebraska Department of Transportation Research Reports by an authorized administrator of DigitalCommons@University of Nebraska - Lincoln.

Nebraska Transportation Center

MID-AMERICA TRANSPORTATION CENTER

NDOR Nebraska Department of Roads

Report SPR-P1(15) M024

Final Report
26-1121-0019-001

Performance of Advance Warning Systems in a Coordinated System

Li Zhao
Graduate Research Assistant, Ph.D. Candidate
Department of Civil Engineering
University of Nebraska-Lincoln

Laurence R. Rilett, Ph.D., PE
Distinguished Professor

Ernest Tufuor
Graduate Research Assistant

Waleed Khan
Graduate Research Assistant

Christopher LeFrois
ITS Sr. Transportation Technology Engineer

2016

Nebraska Transportation Center
262 WHIT
2200 Vine Street
Lincoln, NE 68583-0851
(402) 472-1975

"This report was funded in part through grant[s] from the Federal Highway Administration [and Federal Transit Administration], U.S. Department of Transportation. The views and opinions of the authors [or agency] expressed herein do not necessarily state or reflect those of the U.S. Department of Transportation."

Performance of Advance Warning Systems in a Coordinated System

Li Zhao
Graduate Research Assistant, Nebraska Transportation Center
Ph.D. Candidate, Department of Civil Engineering
University of Nebraska-Lincoln

Laurence R. Rilett, Ph.D, PE
Keith W. Klaasmeyer Chair in Engineering and Technology
Director, Nebraska Transportation Center
Distinguished Professor, Department of Civil Engineering
University of Nebraska-Lincoln

Ernest Tufuor
Graduate Research Assistant
Department of Civil Engineering
University of Nebraska-Lincoln

Waleed Khan
Graduate Research Assistant
Department of Civil Engineering
University of Nebraska-Lincoln

Christopher LeFrois
ITS Sr. Transportation Technology Engineer
Nebraska Transportation Center
University of Nebraska-Lincoln

A Report on Research Sponsored by

Nebraska Department of Roads

Mid-America Transportation Center

University of Nebraska-Lincoln

September 2016

Technical Report Documentation Page

1. Report No. SPR-P1(15) M024	2. Government Accession No.	3. Recipient's Catalog No.
4. Title and Subtitle Performance of Advance Warning Systems in a Coordinated System		5. Report Date September 2016
		6. Performing Organization Code
7. Author(s) Li Zhao, Laurence R. Rilett, Ernest Tufuor, Waleed Khan, and Christopher LeFrois		8. Performing Organization Report No. 26-1121-0019-001
9. Performing Organization Name and Address Nebraska Transportation Center 2200 Vine St. 262 Whittier Research Center Lincoln, NE 68583-0851		10. Work Unit No. (TRAIS)
		11. Contract or Grant No.
12. Sponsoring Organization Name and Address Nebraska Department of Roads 1500 Nebraska Highway 2 Lincoln, Nebraska 68509-4567		13. Type of Report and Period Covered Draft Report
		14. Sponsoring Agency Code
15. Supplementary Notes		

16. Abstract

The Advance Warning System (AWS), developed by the Nebraska Department of Roads (NDOR) has proven to be effective at improving traffic safety at isolated signalized intersections. However, the effectiveness of the system has not been analyzed at signalized intersections operating in a coordinated mode. This project analyzed AWS on arterials where the signals operate in a coordinated mode. The test bed consisted of nine sites, which are located at five successive coordinated signalized intersections on Highway 281 in Grand Island, Nebraska. A non-intrusive data collection system was used to collect a continuous traffic stream of data up to 1200 ft upstream of the stop-line at a given intersection. The analysis showed that with the AWS, the dilemma zone entrapment rate was, on average, 81% smaller than what would have been expected if the AWS was not installed. The accelerating/decelerating analysis showed that 94% of the average acceleration/deceleration rates were within the comfortable range, 69.7% of the vehicles slowed down after the start of the AWS signal, and 92.1% of vehicles slowed down after the start of amber. The red-light running analysis showed that the percentage of red-light running occurrence ranged from 0.9% to 2.0%, with an average of 1.5% and a standard deviation of 0.4%. These results indicated that most of the vehicles were in compliance. The simulation-based conflict analysis showed that, on average, there was a 55%, 12%, and 51% reduction in rear-end, lane-change, and crossing conflicts, respectively, for all nine sites, when the AWS system was applied. The overall results suggested that the AWS was effective at alerting drivers to the impending end of the green signal, which resulted in a reduction of conflicts and a safer corridor.

17. Key Words		18. Distribution Statement	
19. Security Classification (of this report) Unclassified	20. Security Classification (of this page) Unclassified	21. No. of Pages 122	22. Price

Table of Contents

List of Figures

List of Tables

Acknowledgments

We would like to acknowledge the help of the city of Grand Island with the data collection. We also want to acknowledge the contributions of the Nebraska Transportation Center staff who provided technical support.

Disclaimer

The contents of this report reflect the views of the authors, who are responsible for the facts and the accuracy of the information presented herein. This document is disseminated under the sponsorship of the Nebraska Department of Roads. The contents do not necessarily reflect the official views or policies of the Nebraska Department of Roads. This report does not constitute a standard, specification, regulation, product endorsement, or an endorsement of manufacturers.

Abstract

The Advance Warning System (AWS), developed by the Nebraska Department of Roads (NDOR) has proven to be effective at improving traffic safety at isolated signalized intersections. However, the effectiveness of the system has not been analyzed at signalized intersections operating in a coordinated mode.

This project analyzed AWS on arterials where the signals operate in a coordinated mode. The test bed consisted of nine sites, which were located at five successive coordinated signalized intersections on Highway 281 in Grand Island, Nebraska. A non-intrusive data collection system was used to collect a continuous traffic stream of data up to 1200 ft upstream of the stop-line at a given intersection.

The analysis showed that with the AWS, the dilemma zone entrapment rate was, on average, 81% smaller than what would have been expected if the AWS was not installed. The accelerating/decelerating analysis showed that 94% of the average acceleration/deceleration rates were within the comfortable range, 69.7% of the vehicles slowed down after the start of the AWS signal, and 92.1% of vehicles slowed down after the start of amber. The red-light running analysis showed that the percentage of red-light running occurrence ranged from 0.9% to 2.0%, with an average of 1.5% and a standard deviation of 0.4%. These results indicated most of the vehicles were in compliance. The simulation-based conflict analysis showed that, on average, there was a 55%, 12%, and 51% reduction in rear-end, lane-change, and crossing conflicts, respectively, for all nine sites, when the AWS system was applied.

The overall results suggested that: 1) the AWS was effective at alerting drivers to the impending end of the green signal, and 2) the impacted driver, for the most part, slowed down when the AWS was activated.

Chapter 1 Introduction

1.1 Background

As a driver approaches a signalized intersection and the signal transitions from green to amber, she or he has to make a decision on whether to stop or proceed through the intersection. Historically, there were situations where neither option could be completed safety and/or legally. The approach area where this occurred is known as a dilemma zone. In theory, it is possible to eliminate the dilemma zone through proper timing of the signal. However, the stochastic nature of driving means that some drivers will invariably make the wrong choice. For example, some drivers may stop abruptly when they should proceed, and in doing so, increase the risk of a rear-end collision. As well, drivers might proceed through the intersection when they should stop, which increases the risk of red-light running and the possibility of a right-angle collision.

A great deal of effort is focused on dilemma zone mitigation especially at high-speed signalized intersections. The common mitigation methods are the: (1) Advanced Detection Systems (ADS), (2) Advance Warning-flasher System (AWS), and (3) Actuated Advance Warning System (AAWS), which is a combination of both the ADS and AWS. These different mitigation options have been documented to reduce the problem previously described and to improve safety (1-5). The communication occurs via flashing signal heads and warning signs to warn drivers that they should be prepared to stop as they approach a signalized intersection. There are a variety of warning sign and flasher combinations being used in practice.

NDOR was one of the first state transportation agencies to implement ADS at isolated intersections. These systems provide information to drivers indicating that they should be prepared to stop as they approach a traffic signal because the signal is about to transition from green to amber (and to red). The decision on whether to provide information to the drivers is a

function of a number of parameters including the presence of vehicles on the roadway (identified via an upstream detector), the phase sequence, and where in the cycle the current signal timing plan is operating. While a number of states have adopted similar systems, the NDOR operating algorithm is unique to Nebraska. The successes of the NDOR system at improving intersection safety at isolated signalized intersections operating in the fully-actuated mode have been documented (1, 5).

1.2 Problem Statement

Most research on the effectiveness of the AAWS for reducing dilemma zone problems has been conducted at rural isolated high-speed signalized intersections. That is, the systems have been deployed (and evaluated) at locations outside of the city limits where the approach speeds are greater than 40 mph. Because these signals operate in the uncoordinated mode, the transportation operators have the freedom to extend green time in accordance with the oncoming traffic. This ability, by definition, does not exist in coordinated systems. For this reason, many agency operators are skeptical of their effectiveness.

However, as cities grow, these systems that were initially deployed at isolated locations can become part of a coordinated corridor. In a coordinated setting, while green extension(s) are not appropriate, the use of AAWS remains an option. The other issue in a coordinated corridor with closely spaced intersections is that traffic will arrive in platoons. This can be contrasted to the isolated intersection scenario where the traffic arrives randomly. Therefore, the impact of the information provided by the AAWS to an individual driver can be different than the impact of the same information on a platoon of vehicles. Intuitively, the safety risk that a platoon of vehicles having to make a stop or go decision could potentially be much higher depending on the signal coordination plan.

The intention of this project is to conduct a field evaluation of an AWS when deployed in a coordinated setting. More specifically, this study will assess the safety and operational impacts associated with combining the advance warning flasher with signal coordination on Highway 281 in Grand Island, Nebraska.

1.3 Research Objectives

It is common practice in traffic control not to combine dilemma zone protection and signal coordination systems because the fixed time of coordinated signals typically overrides any detectors providing dilemma zone protection. As a city grows, isolated AWS becomes part of a coordinated signal corridor. In addition, some city agencies have chosen to implement AWS corridor-wide. In these jurisdictions it is hypothesized that using an AWS in a coordinate traffic signal system may have some benefit and will not result in riskier driver behavior such as red-light running and abrupt stopping. The main objective of this research is twofold:

(1) quantify the effectiveness of AWS in terms of safety and efficiency on a coordinated arterial system, and

(2) develop guidelines for the installation or removal of the AWS.

This research is directly related to the US DOT's Strategic Goal of "enhancing safety." Additionally, motor vehicle traffic crashes exact a severe toll in loss of life, injuries, property damage, and reduced productivity. The findings of this research will improve the region's economic competitiveness by helping identify where implementation of the NDOR system is likely to be beneficial and thus promote better allocation of highway funds.

1.4 Research Approach and Methods

The research approach involved a detailed operational analysis of AWS using field data in order to monitor the performance of the AWS. Traffic characteristics, including vehicle speed

profiles with a particular emphasis on vehicle acceleration profiles both immediately before and after the advanced warning signs became active, were observed. A calibrated microsimulation model was developed. This simulation model can be used to identify the situations under which AWS in coordinated systems will be most successful. The model was calibrated to the observed speed profiles obtained in the operation analysis of the empirical data.

1.5 Organization of the Report

There are six chapters in this report. Chapter 1 contains an introduction of the problem and the objectives of the project. Chapter 2 provides a summary of the literature review of AWS operations and relevant safety studies. Chapter 3 details the study sites, the data collection system, the data collection process, and the data format. Chapter 4 presents the analytical results of the traffic conditions including hourly traffic volume, effective green time, speed, heavy vehicle percentages, vehicle trajectories, etc. Chapter 5 analyzes the operational performance of the AWS with an emphasis on platoon dispersion and arrival flow profiles. Chapter 6 analyzes the data at signalized intersections with an emphasis on red-light running rates and dilemma zone entrapment, and discusses the safety issues at signalized, high-speed intersections with AWS. Chapter 7 develops a simulation model to study the potential conflicts at different intersections. Chapter 8 summarizes the findings and provides recommendations for targeting the objectives in this project.

Chapter 2 The Operation of an Advanced Warning System (AWS)

A dilemma zone exists at a high-speed signalized intersection if a driver can neither stop safely nor proceed safely through the intersection when the signal transitions from green to amber (4). Crashes at high-speed signalized intersections are particularly horrific because of the high speeds involved and the fact that many crashes are at right-angles (e.g., "T-bone" crashes). Fortunately, it is possible to eliminate the dilemma zone through proper timing of the traffic signal at an intersection. These signal timing methodologies are widely used in the U.S. Unfortunately, due to the stochastic nature of drivers' behavior and their vehicles, some drivers will make an incorrect choice putting themselves and others at risk for a crash. For example, the drivers may misjudge the distances involved, they may have slower perception reaction times than the design standards, or their vehicles may lack the necessary braking power required. Because drivers exhibit distinct differences in their desires and/or abilities to stop at the onset of the amber indication, they are potentially at risk of being in a crash if they choose incorrectly. For example, some drivers may stop abruptly when they should proceed and thereby increase the risk of a rear-end collision. Other drivers might proceed through the intersection when they should have stopped. By entering the intersection after the amber signal is finished (e.g., running the red light), they increase the possibility of a right-angle collision with vehicles entering the intersection from the cross road.

A great deal of research has been focused on helping drivers make the correct decision to stop or proceed at signalized intersections. This is because of the high negative impact on safety and operations, especially at high-speed signalized intersections (1, 2, 4, 5) when drivers choose incorrectly. The mitigation efforts include: (1) reducing the likelihood of a driver making the wrong choice by extending the amount of green time (e.g., green extension); (2) increasing the

awareness of the driver that the green indication will be changing from green to amber in the near future, thus allowing them a greater probability of the driver choosing the appropriate action; or 3) a combination of both option 1 and 2. The common methods of providing dilemma zone protection at high-speed signalized intersections are the use of advanced detection, advance warning flashers, or a combination of both advance detection and advance warning flashers.

2.1 NDOR Advance Warning System (AWS) and NDOR Actuated AWS

2.1.1 NDOR AWS

The Nebraska Department of Roads (NDOR) developed a system, referred to as the NDOR Advance Warning System (AWS), which combines advance detectors and advance warning flashers. The NDOR AWS assembly is shown in figure 2.1. It includes a pair of flashing beacons mounted above a warning sign with the text “PREPARE TO STOP WHEN FLASHING.” Below the warning sign, the name of the cross street in the downstream intersection will generally be provided.

Figure 2.1 Advance Warning System (AWS) assembly on NB 281 in Grand Island, NE

The AWS sign is positioned on both sides of the road and placed at a safe distance from the downstream intersection. In addition, the AWS is connected to the intersection signal controller so that when the downstream signal is about to transition from green to amber, the flasher is turned on to warn the approaching drivers of the impending phase change. Based on NDOR standards, the AWS signal heads are designed to begin flashing five to seven seconds prior to the onset of the amber indication at the downstream signalized intersection (1).

Once the AWS beacons begin to flash, the green interval will continue for a period of time, known as the "lead flash" (1). The duration of the lead flash is the travel time between the AWS location and the stop-line for a vehicle traveling at the design speed, which is calculated using eq. 2.1.

$$t = \frac{D_M}{V} \tag{2.1}$$

Where t = the duration of the lead flash (seconds)

D_M = distance from the AWS location to the stop-line (feet)

V = design speed (ft/s)

2.1.2 NDOR Actuated AWS

The design algorithm of the NDOR actuated AWS (AAWS) combines the functionality of advance detection and advance warning, and uses a short maximum allowable headway (MAH) to extend the green at isolated intersections (1). The system has one advance detector in each approach lane as well as an AWS assembly positioned on both sides of the roadway approach downstream of the advance detector. In addition, stop line detection is also provided in the through lanes and left-turn bays. The range of stop-line detection is 30 to 40 feet in the left-turn bays. The advance detector operates in the pulse mode, which means that each vehicle

crossing the detector transmits a single pulse to the controller, regardless of the time that the vehicle spends in the detection area. The stop line detectors operate in the presence mode (e.g., a continuous call is transmitted to the controller as long as a vehicle is within the detection area), but are not active during the extendible portion of the green interval (1).

The NDOR AAWS is based on the concept of the NDOR dilemma zone, as shown in figure 2.2. The beginning of a vehicle's dilemma zone is the stopping distance (1), i.e. D_{bz}, where a vehicle can complete a stop at the stop-line assuming maximum deceleration. The end of the dilemma zone is the stop-line of the intersection (1), i.e. D_{ez}, as can be seen in figure 2.2.

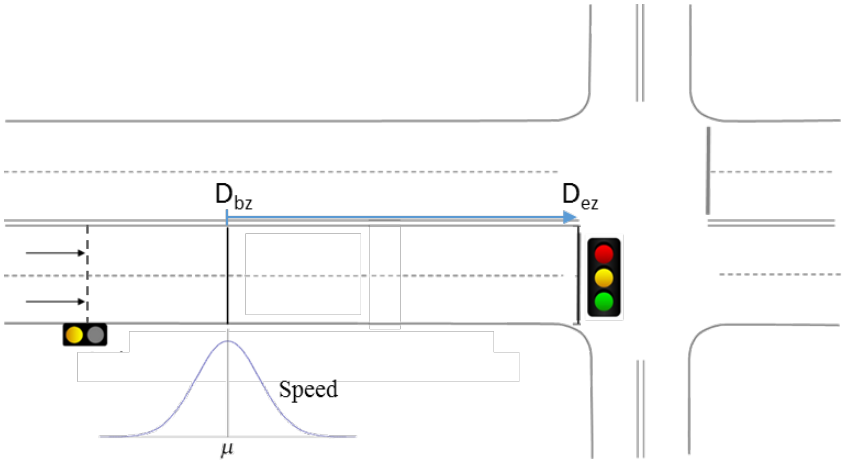

Figure 2.2 Dilemma zone definition by NDOR – speed protection

2.2 AWS Safety Studies

Several researchers have undertaken projects aimed at quantifying the safety and operational effectiveness of AWS installations at high-speed isolated signalized intersections. In terms of safety, AWS appears to lower left-turn, right angle, and in some instances, rear-end crashes (6-10). In addition, Agent and Pigman (9) and Knodler and Hurwitz (4) found that the use of AWS should be limited to locations with existing vehicle crash problems or a high

potential for them to develop. Gibby et al. (7) provided more detail indicating that high-speed approaches equipped with AWS had significantly lower total, left-turn, right-angle, and rear-end approach crash rates than those without AWSs. Gibby et al. (7) also observed significantly lower ratios of night-time crashes. The research performed by Klugman et al. (8) in Minnesota concluded that the use of AWS devices could be effective at reducing right-angle and rear-end accidents under certain situations, but they do not automatically increase the safety of all intersections and all situations.

Sayed et al. (10) provided a detailed crash analysis and indicated that AWS intersections showed 10% fewer total crashes and 12% fewer severe crashes. Negligible reductions were observed with respect to rear-end crashes. The crash reduction was not statistically significant at the 95% level. Sayed et al. (10) also found a correlation between the crash frequency of AWS sites and the minor street traffic volumes. It was observed that when the minor street traffic volumes are low, sites with AWS had a higher frequency of crashes than non-AWS sites. In contrast, as traffic volumes in minor streets increased, the crash frequency for AWS-equipped intersections was found to be lower than at non-AWS sites. The results indicated that an AWS was effective at locations with a minor street annual average daily traffic (AADT) of 13,000 vehicles per day (vpd) or greater.

In terms of operations, Farraher et al. (11) collected data on red-light-running and vehicle speeds at isolated intersections equipped with an AWS. They observed an overall reduction of 29% in red-light-running, a 63% reduction in truck red-light-running, and an 18.2% reduction in the speed of trucks. Although the data indicates that AWS was effective at the sites studied, the number of overall violators and their speeds remained unacceptably high (11). Pant and Xie (12) compared the way drivers respond to various types of AWS at isolated intersections. The study

was based on a speed and intersection conflict analysis and the effectiveness of the three advance warning systems presented above. The authors found that two types (e.g., a warning sign with the text “Prepare to Stop When Flashing” complemented by a pair of flashing yellow beacons, and a warning sign with a schematic of a traffic signal and complemented by a pair of flashing yellow beacons) increased vehicular speeds. This increase in speed was attributed to drivers attempting to “sneak through” the yellow signal phases.

2.3 Safety Studies of Actuated Advanced Warning Systems (AAWS)

Transportation agencies may use a variety of dilemma zone protection systems that combine features of both advance detection and advance warning flashers. These modified systems are referred to in this report as actuated advanced warning systems (AAWS) (1).

2.3.1 Advance Warning for End-Of-Green System (AWEGS)

Messer et al. (2) developed the Advance Warning for End-Of-Green System (AWEGS) for high-speed (≥ 45mph) traffic signals in Texas. The AWEGS uses a combination of advance detection and advance warning flashers. Three architectures (e.g., Levels 0, 1, and 2) of AWEGS were examined during the course of this study. The level 1 technology used “trailing overlaps” to provide a fixed amount of advance warning of the end-of-green phase, but this method was rejected because it eliminated the existing dilemma zone protection. The level 1 technology used average speed and predicted when the traffic-actuated controller would gap-out. The level 2 AWEGS added a feature that was capable of identifying aggregate vehicle classification (e.g., car, truck) and an individual speed measurement to better estimate when the signal controller would gap-out. The AWEGS was found to reduce red-light running by 38-42% during the targeted first 5 seconds of red (13). The level 2 architecture was the preferred option because it

provided extra dilemma zone protection for trucks and high-speed passenger cars while simultaneously reducing delay.

2.3.2 NDOR AAWS

The system continually monitors traffic at an upstream detector as well as at stop line detectors to predict the onset of the yellow indication, and provides information to drivers (via flashing signal heads and a warning sign) regarding whether they should be prepared to stop as they approach a traffic signal.

The system has been documented as being effective at improving traffic safety at isolated signalized intersections where the controller operates in the fully actuated mode. A study evaluating the safety effectiveness of the NDOR actuated AWS at high-speed isolated intersections showed crash reduction rates of 0.5% for heavy vehicle crashes, 1.2% for rear-end crashes, 43.6% for right-angle crashes, 11.3% for injury crashes, and 8.2% for all crashes combined (5). However, this system has not been examined in the context of a coordinated arterial system.

2.4 Summary

Most of the research on the effectiveness of the advance warning systems to date was conducted at isolated intersections. For example, via the green extensions at the isolated signalized intersection, AAWS has been shown to be effective in slowing drivers down when it is active.

As this project studied the use of the NDOR AWS in a corridor that operates under coordinate control, the NDOR AAWS would not be appropriate. Consequently, there was no advance detection on any approach on the corridor. Instead, the NDOR AWS was initiated by a pre-determined time period (i.e., the lead flash time) about 7-8 seconds prior to the start of the

phase change from green to amber at the intersections. This is because in a coordinated system, all the intersections share a common cycle length. This limits the ability of the traffic agency to extend the green phase at a certain single intersection. Thus, it is unclear if AWS in this situation is still effective.

Chapter 3 Data Collection and Reduction

This chapter details the data collection process at the AWS test bed in Grand Island, Nebraska. The data collection system was designed from December 2015 to February 2016. A preliminary data study was conducted from March 6, 2016 through April 10, 2016. An extensive data collection effort was conducted from April 12, 2016 through June 23, 2016. The entire data collection process will be introduced in the following subsections.

3.1 Data Collection System

3.1.1 Mobile Trailer Data Collection (MTDC) System

The Nebraska Transportation Center (NTC) mobile trailer data collection (MTDC) system, as shown in figure 3.1, was utilized in the data collection. The MTDC system consisted of two Wavetronix smartsensor Advances (ADs), one Wavetronix smartsensor high definition (HD), and two internet protocol (IP) cameras. These were all installed on the trailer mast. The AD sensors utilize digital wave radar technology to track the vehicles upstream and downstream of the trailer and record vehicles' time, speed, lane, and distance. They can track vehicles over a distance of 600 feet in both the upstream and downstream directions. The videos cover the range of the AD sensors and are used to confirm traffic behavior and eliminate false calls. The HD sensor counts vehicles and records vehicle length and vehicle speed as the vehicles pass through the detection zone adjacent to the trailer.

Figure 3.1 Mobile trailer data collection (MTDC) system

All the sensors are powered by batteries stored in the trailer cabinet, located near the trailer wheels. These are automatically charged by a solar panel. Located in the trailer cabinet is the local server that consists of a laptop and a digital hard drive. The data from different devices are sent to the server and are saved into the hard drive automatically. Note that the time stamp for all the sensors are synchronized to the server in the trailer cabinet. Thus, the different data sources have the same time baseline.

3.1.2 Traffic Signal Phase Identification (TSPI) System

The signal phases and the AWS timing are identified by utilizing non-invasive current sensors attached to the traffic signal circuit in the traffic control cabinet. This TSPI system was developed by NTC and uses both C++ and python programming. As shown in figure 3.2, the sensors were attached to the power lines within the traffic cabinet. The current sensor is connected to an Arduino Pro Mini microcontroller. The Arduino Pro Mini has an analog to digital converter that converts the current sensors' reading to a digital value. When a large change in current is detected it is compared to the threshold values set in the program to determine if the traffic signal has transitioned to a new phase.

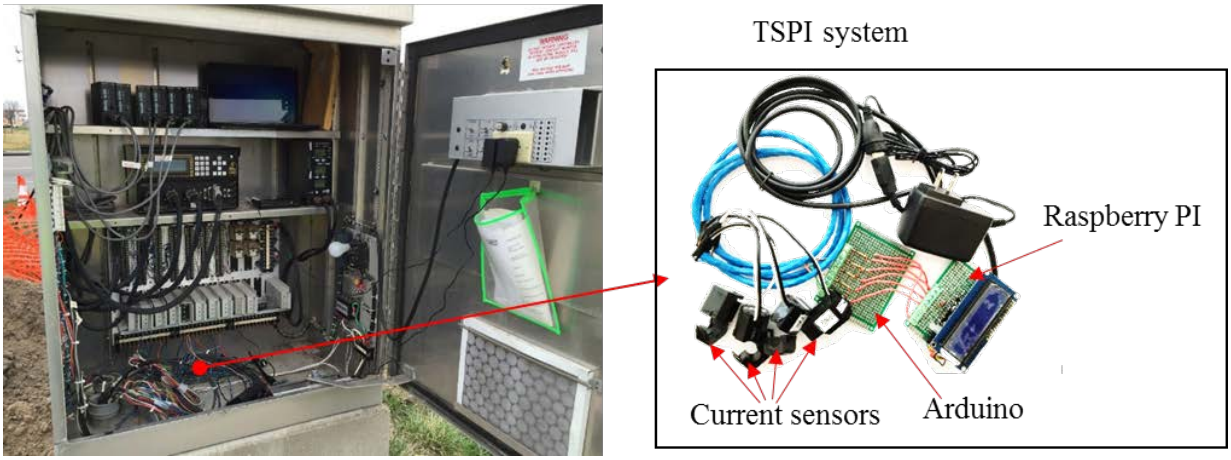

Figure 3.2 TSPI in the traffic cabinet close to the intersection

After processing the data for each of the attached current sensors, the status of the traffic signal phase is then passed on to a Raspberry PI connected to the Arduino via a USB connection. The Raspberry PI then checks for a change in status. If a change is detected, it records this change, along with a time stamp, in the data file.

The TSPI system is comprised of the following components.

1) Current Sensor: the CR3110-3000 current sensors are used to detect the electrical current from the power lines. Large current change indicates a phase change. This is a split core transformer and can support a maximum current of 75 amps.
2) Arduino: the Arduino Pro Mini is a microcontroller utilizing an ATmega328 chip. It was selected for its small size and its onboard analog to digital converter. There are 6 analog input pins allowing up to 6 current sensors being attached to the Pro Mini. It operates at 16 MHz (i.e., 1 instruction every 62.5 ns). The Analog pins can be sampled at a rate of 100 µs. Because the Arduino Pro Mini operates at 5 volts the analog pins need to be protected from voltages over 5 volts by utilizing Zener diodes. Ceramic capacitors are used to filter any noise in the system. The Arduino sends the status of the traffic signals every 100 ms via a USB cable to the Raspberry PI.
3) Raspberry PI: the Raspberry PI minicomputer is used to store the on and off times of the phases. Upon receiving the data from the Arduino, the Raspberry PI checks the data to see if any of the signals have changed their states. If there is a change, a time stamp is taken and this data is recorded into the file. There are separate files for each of the 6 connected sensors. In addition, a real time clock is added to the Raspberry PI so that it could be synchronized to the master clocks. The files were accessed from the Raspberry PI via a browser connected to the same local network.

3.2 Sensor Performance Evaluation

Figure 3.3 (a) shows a screen shot of the user interfaces of the Wavetronix smartsensors while they are collecting data. The left side interface (e.g., labeled “AD_upstream”) shows the output from the AD sensor that targets the traffic upstream of the trailer. Each data record (e.g.,

line) consists of the range, speed, and ETA (i.e., Estimated Time to Arrival) of an identified vehicle that is moving toward the sensor location. The right side interface (e.g., labeled "AD_downstream") is from the AD sensor that targets the traffic downstream of the trailer. Each data record (e.g., line) consists of the range and speed of the identified vehicle that is moving away from the sensor location. Note that in this case ETA is not applicable and is shown as a series of dashes. The middle interface (e.g., labeled "HD") is from the HD sensor, where each data record represents a vehicle passing by the sensor location. The time of detection, instantaneous speed, length of vehicle, and distance to the sensor location are all collected and stored.

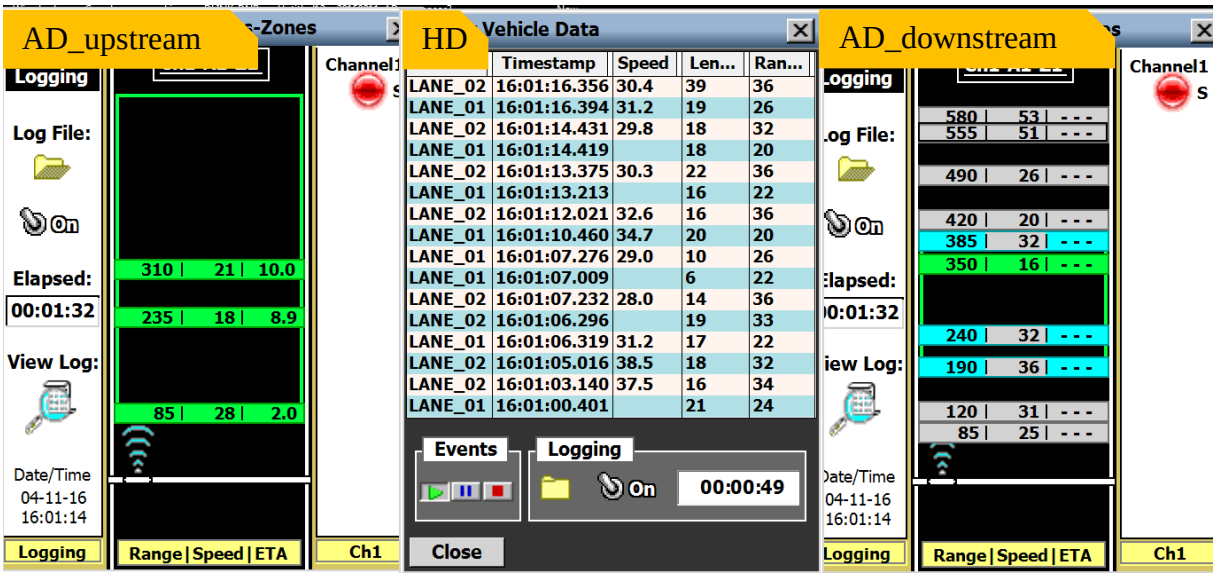

(a) Real-time data collection by Wavetronix ADs (right and left) and HD (middle) interfaces

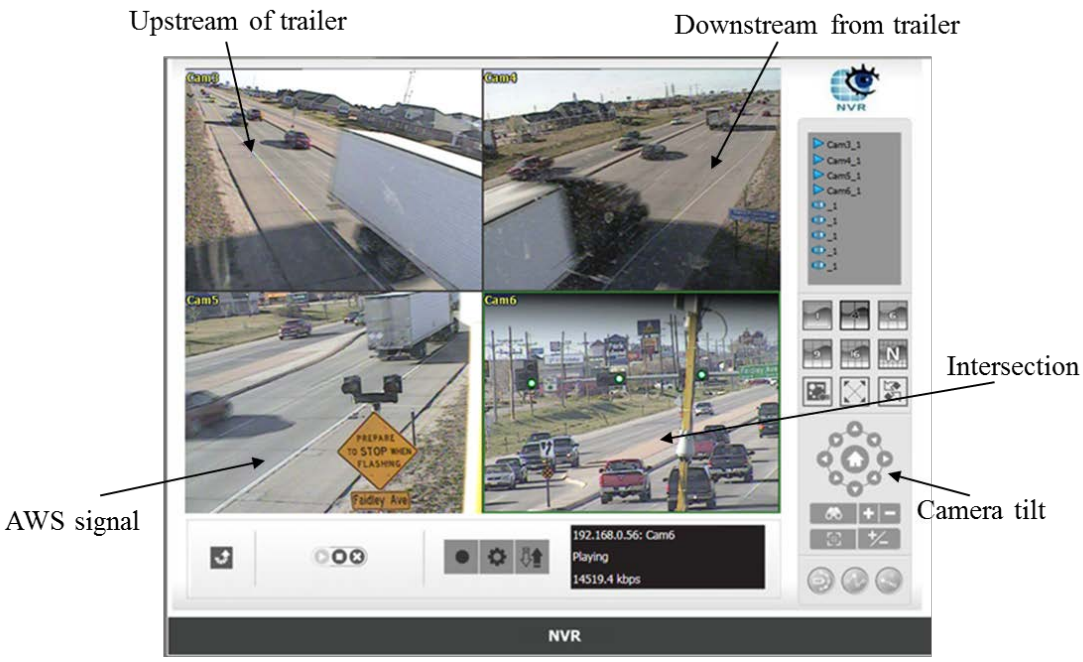

(b) Real-time video recording of the approach lane and intersection

Figure 3.3 Sensor interface - onsite data collection interface

Figure 3.3(b) shows a screen shot of the camera control server. The server is used to assemble the views from the four cameras. It may be seen that the upper left and upper right cameras cover the views upstream and downstream of the trailer, respectively. The lower two cameras focused on the AWS signal heads (lower left) and the intersection signal heads (lower right). Note that the angles of all the camera heads can be adjusted using the panel shown on the right hand of the screen (e.g., labeled “Camera tilt”).

In addition to the real-time data collection, the performance specifications of the Wavetronix AD and HD sensors, as reported by manufacturer, are shown in figure 3.4. Note that the specification for the percentages of small vehicles and large vehicles identified by the AD sensor within 400 ft of the trailer location are 90% and 95%, respectively. This means the two upstream and downstream sensors have an effective 800 ft vehicle tracking range with at least

90% accuracy. Speed accuracy is within 5 mph for 90% of the measurements for both the AD sensor and the HD sensor.

Wavetronix AD Performance	
Maximum mounting distance from center of lanes	50 ft (15.2 m)
Maximum mounting height	40 ft (12.2 m)
Detection area	50 to 600 ft (15.2 to 182.9 m)
Percentage of vehicles detected before 400 ft (121.9 m)	all motor vehicles 90%; large vehicles 95%
Detection accuracy	large vehicles 98%; all motor vehicles 95%
Range accuracy	±10 ft (3 m) for 90% of measurements
Speed accuracy	±5 mph (8 kph) for 90% of measurements
ETA accuracy	±1 sec. for 85% of measurements

Wavetronix HD Performance	
Typical per-direction volume accuracy	98%–99%
Minimum per-direction volume accuracy	95%
Typical per-lane volume accuracy	98%–99%
Minimum per-lane volume accuracy	90%
Minimum separation between two vehicles	5.5 ft. (1.67 m)
Per-lane average speed accuracy	±3 mph (5kph)
Per-vehicle speed measurement accuracy	±5mph (8 kph) for 90% of measurements
Method of speed measurement	dual radar speed trap
Typical classification accuracy	90%
Minimum classification accuracy	80%

Figure 3.4 Performance of Wavetronix smartsensors provided by product manufacturer

In a previous study (14), 55 test runs were performed with a portable GPS to validate the accuracy of Wavetronix AD. The speed difference of the two sensors were used to measure accuracy. It was found that the error is distributed with the mean close to 0.01 mph and the standard deviation at 1.39 mph. This indicates the Wavetronix AD sensor provides acceptable values for speed and distance.

The Wavetronix HD has been widely used in traffic vehicle count and speed detection. A study of evaluation of the non-intrusive Wavetronix HD for traffic detection (15) has found that the volume accuracy is within 2 percent in free flow conditions. The error determined in the 30 min average speed between the HD sensor and the manual measurement was 0.6 mph. The length-based vehicle classification had an error of 2.3 percent for passenger cars and an error of 15.3 percent for trucks, compared with the Piezo-Loop-Piezo baseline. The overall error for all vehicles is approximately 3.0 percent.

The sensors in the Raspberry PI system were sampled every $1/10^{th}$ milliseconds for 10 milliseconds. Its performance is rated for an error margin of 1% to 1.7%, depending on the strength of the electric power of the traffic signal (e.g., incandescent bulb or LED bulb). In the study sites at the 281 Highway corridor, all the traffic signals have LED bulbs.

3.3 Test Sites

3.3.1 Site Selection

The specific signalized intersections in the test bed that were studied were identified using the selection criteria, which included:

1) intersections equipped with NDOR AWS;

2) signal-coordinated corridors;

3) vehicle platoons formed during each cycle;

4) ability to set-up data collection trailers and access to a traffic controller cabinet; and

5) cooperation from local transportation agencies.

Based on input from the NDOR Technical Advisory Committee, the north-south Highway 281 corridor between US Route 30 and Nebraska Route 2 in Grand Island, NE, was selected as the study area. The test sites are shown in figure 3.5. This N-S corridor consisted of

five signalized intersections, each of which was instrumented with the NDOR AWS. In total, 4 NB and 5 SB approaches were studied in detail, as shown by the red rectangle in figure 3.5, where the name and direction of the approach are labeled. The test bed serves as a major N-S arterial corridor and is located in the western section of the city of Grand Island. Note that Highway 281 intersects Interstate 80 approximately 8 miles south of Grand Island.

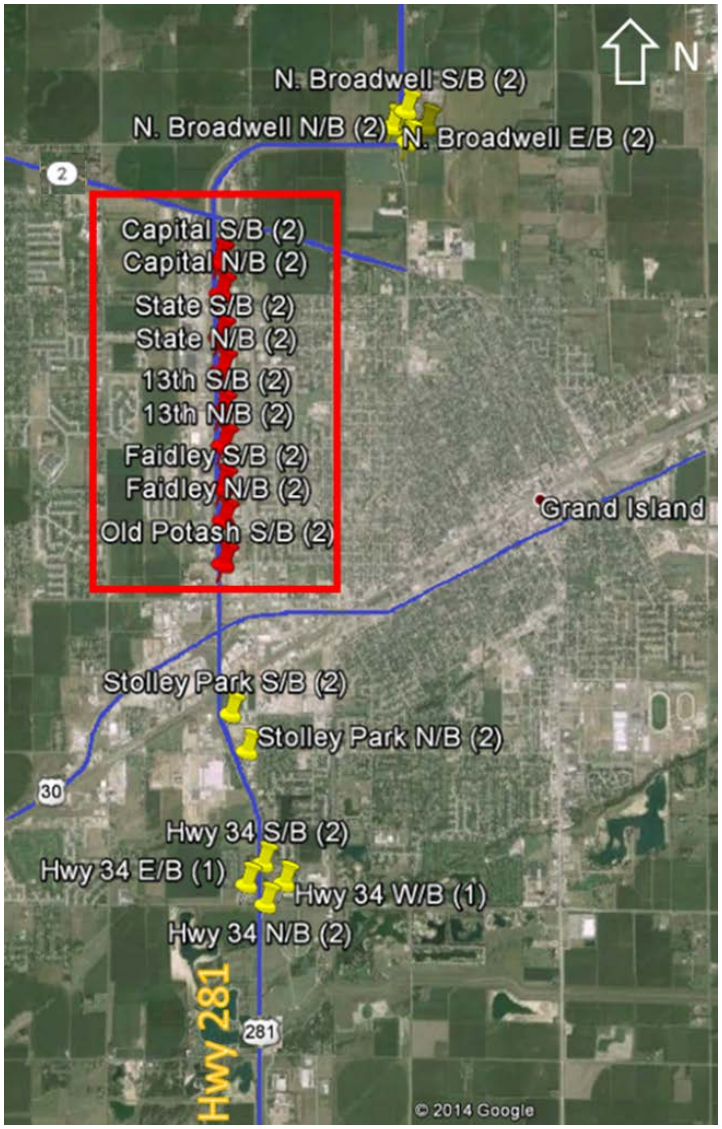

Figure 3.5 Site selection map in Grand Island (the number 1 or 2 in the parentheses indicates the number of the warning flashers at both sides of the approach)

3.3.2 MTDC Location

For each site, the data collection mobile trailer was placed between the AWS and 300~350 ft upstream of the stop-line, as illustrated in figure 3.6. The two Wavetronix AD sensors cover approximately 600 ft of the upstream approach, including the AWS, and approximately 600 ft of the downstream approach, including the stop-line. The distance of the AWS location and the actual mobile trailer placement for each of the nine sites are shown in table 3.1.

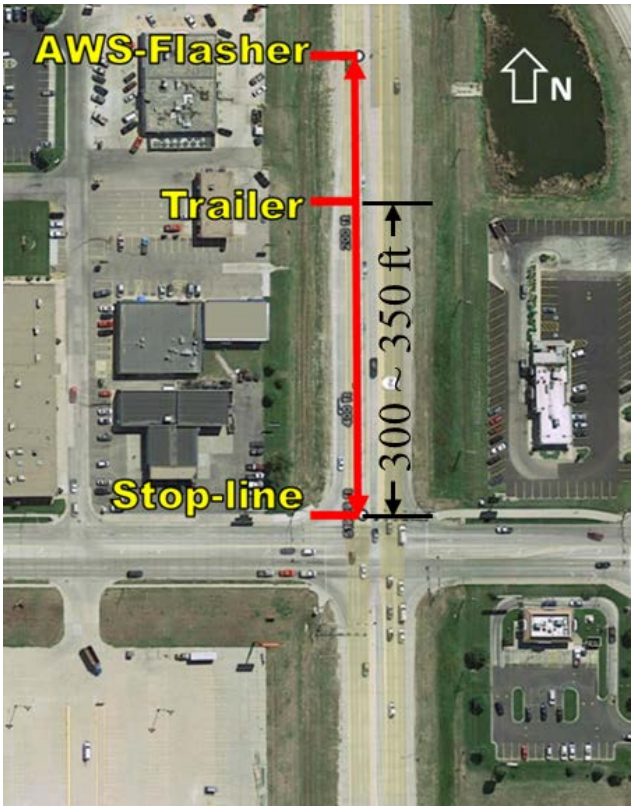

Figure 3.6 Trailer placement on the roadside of the approach at the study sites

Table 3.1 Information on approaches

Crossroad	Location	Speed Limit	Flasher[1]	Trailer[1]
Capital	SB	45 mph	507 ft	310 ft
	NB	45 mph	495 ft	315 ft
State St.	SB	45 mph	550 ft	307 ft
	NB	45 mph	519 ft	306 ft
13th St.	SB	45 mph	554 ft	314 ft
	NB	45 mph	535 ft	327 ft
Faidley	SB	45 mph	528 ft	330 ft
	NB	45 mph	528 ft	351 ft
Old Potash	SB	45 mph	526 ft	302 ft

[1] Distance measured upstream from stop-line

3.3.3 Signal Control

The signal timing plan for this test bed was provided by the city of Grand Island. The five signalized intersections in the study have the same 8-phase signal plan. The phase diagram is shown in figure 3.7. The left-turn phases (phases 1, 3, 5, and 7) are actuated, the major through phases (phases 2 and 6) are coordinated, and the minor through phases (phases 4 and 8) operate in minimum recall mode. The exceptions are that phases 3 and 7 at the Faidley intersection are not used, and phases 4 and 8 at the Old Potash intersection are actuated.

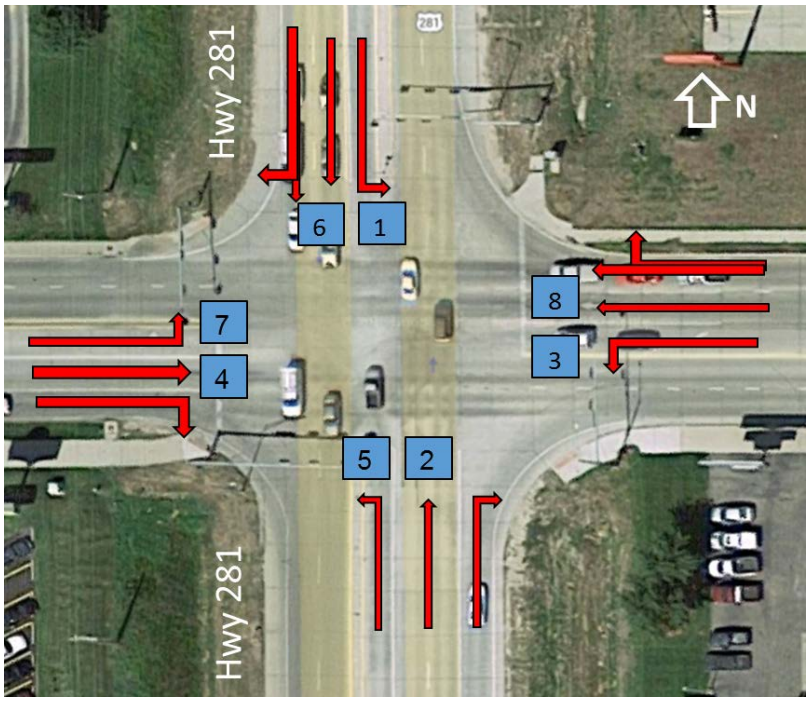

Figure 3.7 The 8-phase signal plan at the test intersection

Because the N-S through phases are not actuated, the intersections operate under semi-actuated control. In other words, detectors are only used for optimizing the signal timing of the minor streets. The phases associated with the major road (i.e., N-S of Hwy 281 corridor) through movements are operated in a "non-actuated" mode. That is, these phases are not provided detection information. In this type of operation, the controller is programmed to dwell in the non-actuated phase and, thereby, sustain a green time for the highest flow movements (i.e., the N-S through movements). The minor movement phases (e.g., E-W) start only after a call for their service is received by the controller.

The AWS signal flashers for the N-S through movements are coordinated with phase 2 and phase 6, respectively. When the downstream signal is approximately 7-8 seconds from beginning the transition from green to amber, the flasher is turned on to warn the approaching

drivers of the impending phase change. As discussed previously, this period of advance warning flashing is called lead flash, which is illustrated in figure 3.8. The AWS flasher will remain active until the end of the red indication for the N-S through traffic phase.

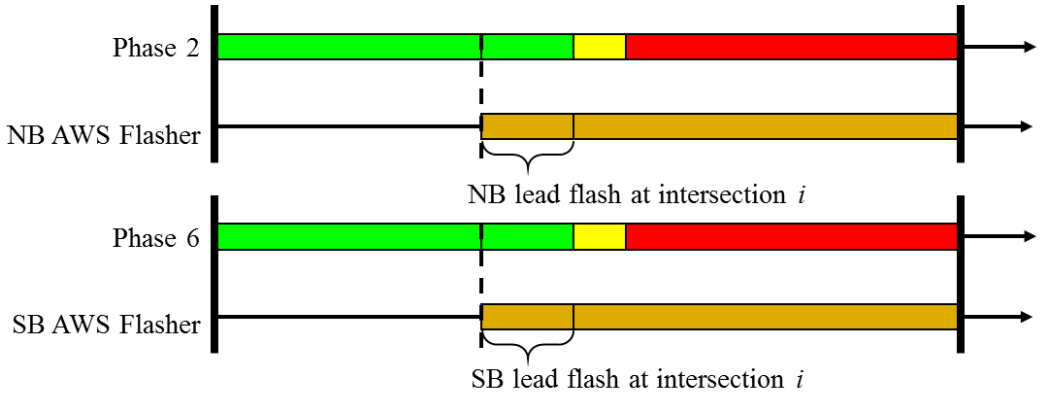

Figure 3.8 Schematic of an AWS timing coordination on N-S corridor

Because the signals in the test bed operate on an 8-phase signal plan, the NB and SB through green phases do not necessarily end at the same time. If the southbound and northbound green phases do not end at the same time, the AWS flashers on the NB and SB approaches will not start at the same time. However, the lead flash time periods are kept constant for each of the nine sites, as they are fixed lengths and begin prior to the end of the green (or the start of the amber).

It should be noted that because the corridor intersections are coordinated, all of their signal plans have a common cycle length. In this corridor, the coordination cycle length is 79 seconds for all the intersections. Other signal time information for each site is provided in table 3.2. Note that the lead flash time is measured on site by the TSPI system, as discussed in section

3.1.2. The universal parameters (e.g., yellow, all-red, cycle length) were obtained from the signal timing report provided by the city of Grand Island and were confirmed in the field.

Table 3.2 Signal time for each site

Site	Loc.	Cycle Length	Lead Flash*	Yellow	All-red
Capital	SB	79 s	7 s	4.5 s	1.5 s
	NB	79 s	7 s	4.5 s	1.5 s
State St.	SB	79 s	8 s	4.5 s	1.5 s
	NB	79 s	8 s	4.5 s	1.5 s
13th St.	SB	79 s	7 s	4.5 s	1.5 s
	NB	79 s	7 s	4.5 s	1.5 s
Faidley	SB	79 s	7 s	4.5 s	2 s
	NB	79 s	7 s	4.5 s	2 s
Old Potash	SB	79 s	7 s	4.5 s	2 s

3.4 Data Format

There are four types of data that were collected. The MTDC data and the TSPI data were all automatically saved in text files. In addition, the video data were backed up in a NVR-software-readable format. Figure 3.9 shows the screen shots of the raw data from the data collection system. Figure 3.9 (a) shows the Wavetronix AD (upstream and downstream) data, figure 3.9 (b) shows the Wavetronix HD data, and figure 3.9 (c) shows the Raspberry PI data that takes care of the signal phase of green, yellow, and red in the intersection and the flasher time of the AWS, respectively.

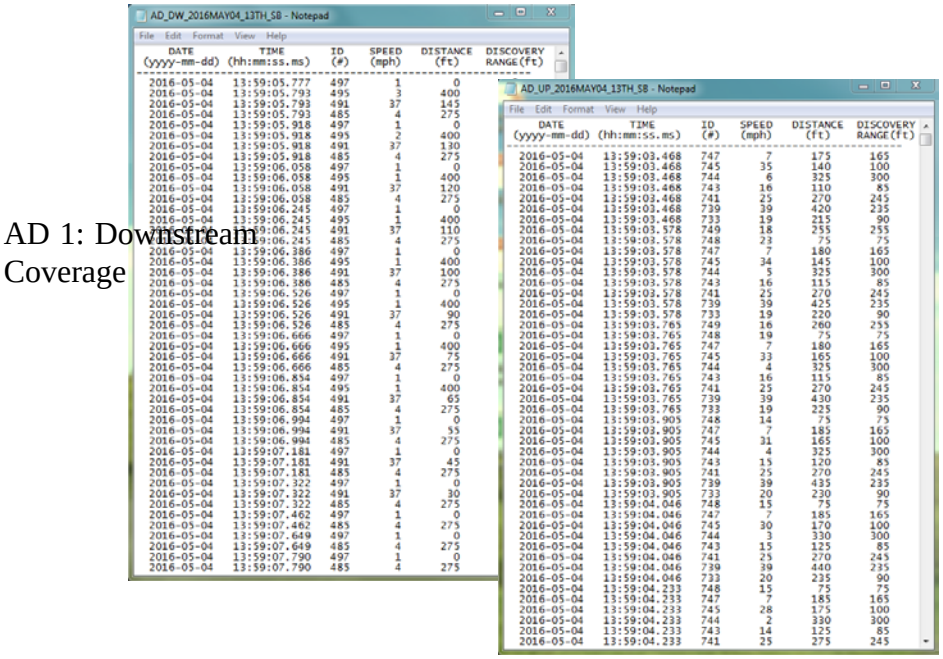

(a) Wavetronix AD

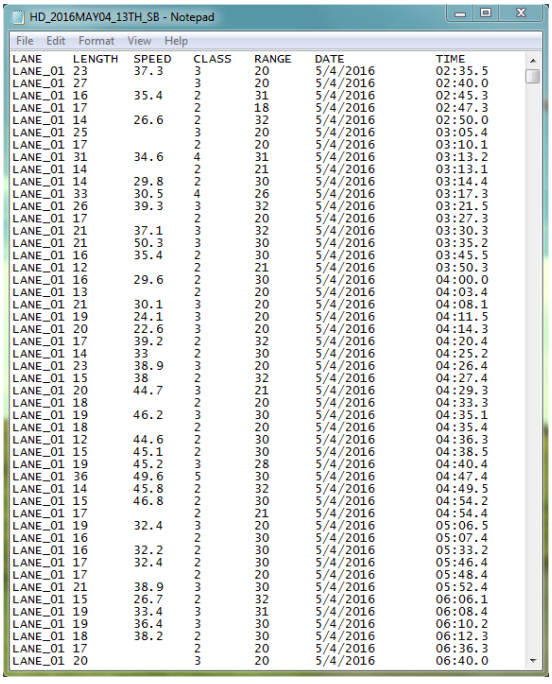

(b) Wavetronix HD

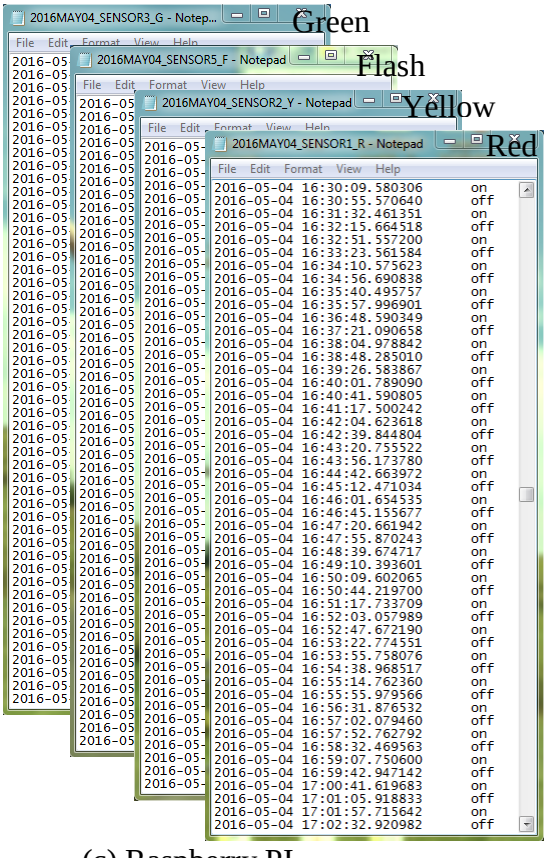

(c) Raspberry PI

Figure 3.9 Raw data sample from the data collection system

3.5 Data Reduction

In total, 277 hours of data from the nine sites were collected. As the daytime driver behavior was the focus of this study, the analysis duration was constrained to the time period between 06:00:00 and 22:00:00. Because the data were collected continuously over 24 hours, the night period (e.g., 22:00:00 – 06:00:00 next day) was included in the raw data. This data was not considered in the analysis. The resulting total effective data analysis time is 189 hours. The information on the data collection at each site is shown in table 3.3. The files from ADs (upstream and downstream), HD, Video, and Raspberry PI signals were named by date and the minor street of the site. All the test data files were stored in .txt format.

3.6 Summary

This chapter discussed the test site location, the data collection devices, and the data collection systems (i.e., MTDC system and TSPI system) that were used in the study. Chapter 4 will provide a preliminary analysis of the data.

Table 3.3 Data collection period

No.	Street Name	Direction	Link Length	Collection Date	Total Hours	Overnight*
1	Capital	SB		5/15, 5/17, 5/18	25 hrs	-8
2		NB	2677 ft	5/13, 5/14, 5/15	44 hrs	-16
3	State St.	SB		5/18, 5/19, 5/20	43 hrs	-16
4		NB	2603 ft	5/27, 5/28	26 hrs	-8
5	13th St.	SB		5/4, 5/5	28 hrs	-8
6		NB	2596 ft	4/22, 4/23	24 hrs	-8
7	Faidley	SB		4/3, 4/8	12 hrs	
8		NB	2680 ft	4/11, 4/12, 4/13	28.5 hrs	-8
9	Old-Potash	SB		6/3, 6/4, 6/22, 6/23	46.5 hrs	-16

*Overnight indicates the data recording period included the duration of 22:00 - 6:00 (next day), thus should minus 8 hours per time

Chapter 4 Preliminary Data Analysis and Vehicle Trajectory

This chapter analyzes the Grand Island data that were collected, as described in chapter 3. The goal was to study the operational effectiveness of the AWS and to identify if the NDOR AWS was operating in an effective and safe manner on a coordinated arterial. To achieve the goal, a preliminary data analysis was conducted to obtain the basic information of the traffic flow and operational conditions at the study sites. The preliminary analysis is the focus of this chapter.

4.1 Preliminary Analysis of Key Traffic Parameters

4.1.1 Green Time

The green time duration for a given approach is calculated as the difference between the time of a recorded “off” signal and the time of a recorded “on” signal. The output of the TSPI system was used to calculate green time. Note in this research the phase of interest is the NB and SB straight through movements, as applicable, for each test site. Figure 4.1 (a) and figure 4.1 (b) show the green time as a function of the time of day for the SB Capital approach and SB Old Potash approach, respectively. Note that these two graphs are representative of all nine sites. The green time distribution for the other seven approaches may be found in Appendix A. It may be seen that the period from 10 pm to 6 am the following day has the longest green time on average. The green time during the daytime period (7 am to 7 pm) is generally shorter. This phenomenon occurs because the signals are in semi-actuated control. At night there is not a lot of cross street traffic so the N-S green time is higher. As the cross street traffic increases during the day time, the corresponding N-S green time decreases.

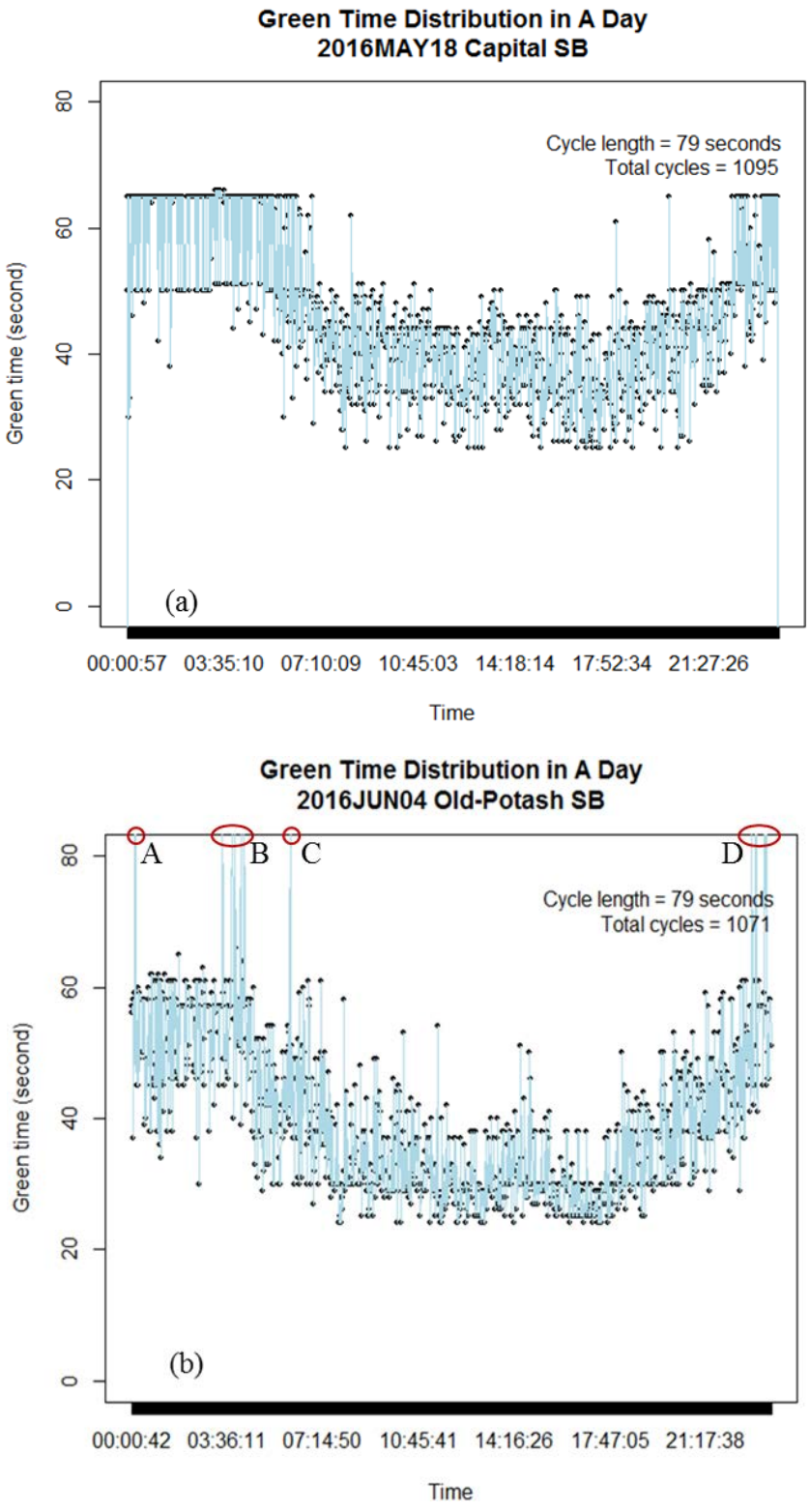

Figure 4.1 Distribution of the length of green time over a day for (a) SB Capital approach, and (b) SB Old Potash approach

It should be noted that sometimes the TSPI system misses a green time recording. In that case, the estimated green time is unreasonably high, as shown by circles A, B, C, and D in figure 4.1 (b). In this situation the green time is set to the average green time of the phases before and after the one in question.

Table 4.1 summarizes the statistics of the green time distribution at each site. Appendix A contains the distribution plot for all nine sites. It may be seen that the night time (e.g., 8 pm to 6 am in the next day) has a greater length of average green time than the day time (e.g., 6 am to 8 pm). This is due to the low traffic flow during the night on the minor cross street where the signal is semi-actuated, which leads to a shorter green time of the minor phases (E-W) and a longer green time of the major phases (N-S). Similarly, during the day time, traffic flow rate is comparatively high. Therefore, the green time on the minor phases is longer and results in a comparatively shorter green time on the major arterial.

Table 4.1 Statistic summary of green time

Site	Time period	Obs.	Max. (s)	Min. (s)	Mean (s)	Sd. (s)
Capital SB	Day (6:00-20:00)	730	66	24	37.6	8.9
	Night (20:00-6:00 next day)	365	66	30	57.4	9.3
Capital NB	Day(6:00-20:00)	729	51	21	40.3	10.7
	Night (20:00-6:00 next day)	364	66	24	52.2	10.4
State SB	Day(6:00-20:00)	729	60	24	32.6	11.6
	Night (20:00-6:00 next day)	364	69	24	50.3	11.9
State NB	Day(6:00-20:00)	730	60	27	35.2	11.3
	Night (20:00-6:00 next day)	365	69	30	48.6	10.2
13^{th} SB	Day(6:00-20:00)	729	63	27	38.3	10.3
	Night (20:00-6:00 next day)	364	63	36	52.0	9.6
13^{th} NB	Day(6:00-20:00)	729	63	24	38.5	12.8
	Night (20:00-6:00 next day)	363	63	36	56.7	8.8
Faidley SB	Day(6:00-20:00)	274	51	12	31.7	12.6
	Night (20:00-6:00 next day)*	-	-	-	-	-
Faidley NB	Day(6:00-20:00)	647	57	21	33.4	9.1
	Night (20:00-6:00 next day)	323	63	36	50.6	11.2
Old-Po. SB	Day(6:00-20:00)	714	54	24	30.7	8.9
	Night (20:00-6:00 next day)	357	63	30	51.4	10.5

*lack of data on that day (see Appendix A(g))

A disadvantage of the semi-actuated operation is that continuous demand on the phases associated with one or more minor movements can cause excessive delay to the major road through movements if the maximum green and passage time parameters are not appropriately set. This issue will be examined further in the following sections.

4.1.2 Traffic Volume

Figure 4.2 shows traffic flow as a function of the time of day from 0:00 to 23:59 (i.e., midnight). Figure 4.2 (a) shows the relationship between traffic volumes as a function of the time of day at the Capital NB site on Saturday, May 14, 2016. Figure 4.2 (b) shows the same relationship for the Old-Potash SB site on Wednesday, June 22, 2016. As would be expected, there is a definite afternoon peak for both sites. The latter shows typical weekday peaking (e.g., morning, lunch, and afternoon). The former indicates a typical weekend pattern where there is one peak in the afternoon and volumes are lower than a weekday.

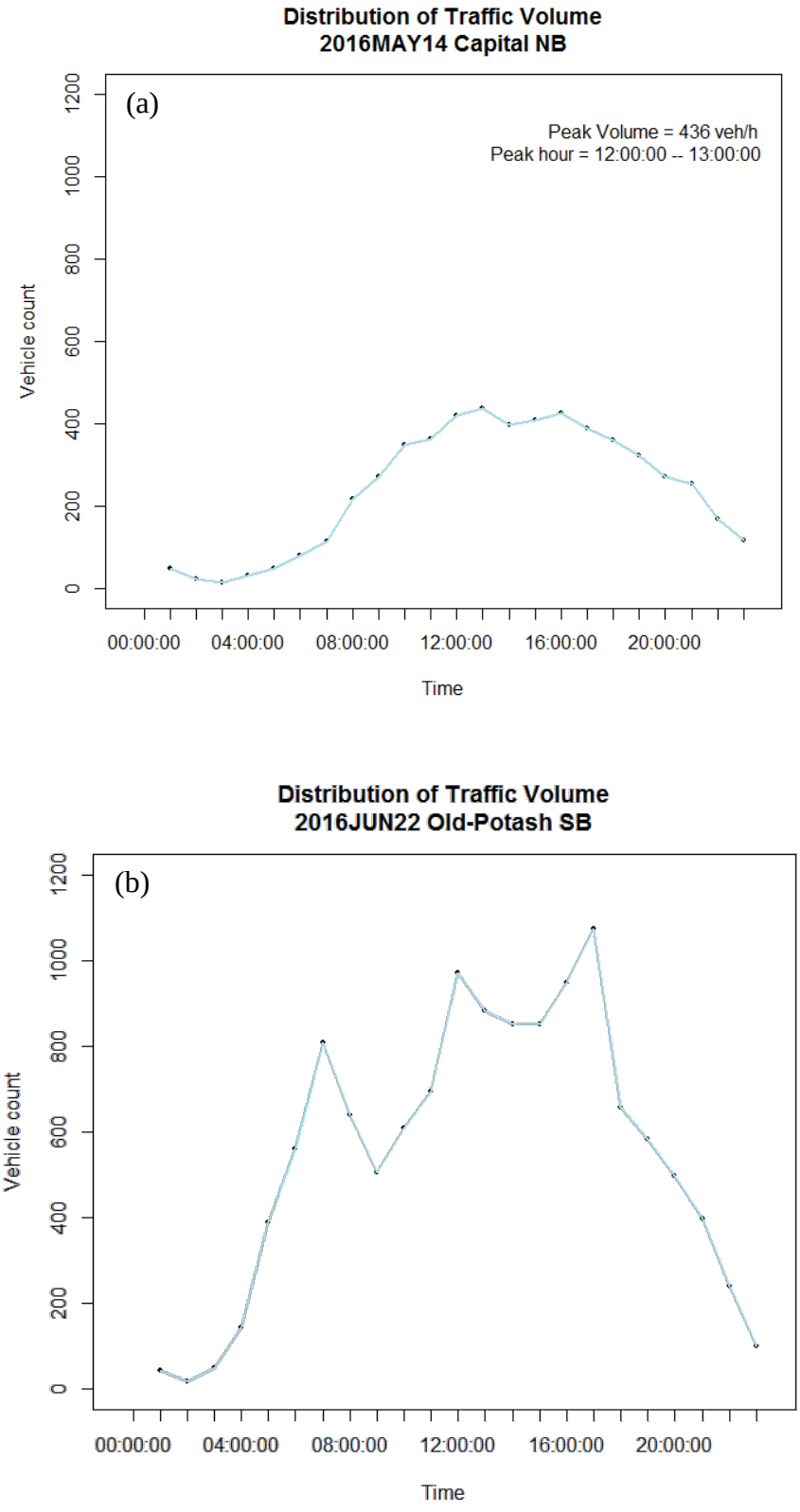

Figure 4.2 Examples of two sites with low and high traffic volume over a day

In general, the traffic volume is bimodal with the peaks around 6-7 am, 12-13 pm, and/or 16-17 pm. The exact time varies by site. These volumes depict the early morning period, lunch breaks, and evening peak. Traffic volumes for the other sites are also obtained in the same manner, as shown in table 4.2.

Table 4.2 provides the highest hourly volumes for the nine approaches studied. Note that because the data was collected on different dates, it would not be expected that the volume would be highly correlated.

Table 4.2 Traffic volume characteristic at different sites

No.	Approach	Volume Analysis Date	Volume Analysis Weekday	Highest Hourly Volume	Hour of Highest Volume
1	Capital SB	5/17-5/18	Tue-Wed	511	6-7
2	Capital NB	5/14	Saturday	436	12-13
3	State St. SB	5/19-5/20	Thu-Fri	780	10-11
4	State St. NB	5/27-5/28	Fri-Sat	635	6-7
5	13th St. SB	5/4-5/5	Wed-Thu	944	6-7
6	13th St. NB	4/22-4/23	Fri-Sat	814	7-8
7	Faidley SB	4/3, 4/8	Sun, Fri	819	16-17
8	Faidley NB	4/12-4/13	Tue-Wed	952	11-12
9	Old-Potash SB	6/22	Wednesday	1074	16-17

4.1.3 Speed

Figure 4.3 (a) and Figure 4.3 (b) are graphs of the instantaneous speed, obtained by the sensors on traffic adjacent to the trailer, as a function of the time of day for NB Capital Street and SB Old Potash Street, respectively. It may be seen in Figure 4.3 (a) that there is a wide distribution in speed. This would be expected on an arterial roadway that has coordinated signals. Figure 4.3 (b) shows a similar scatter, and it should be noted that there are three distinct times when speeds are noticeably lower. These times correspond to the peak demonstrated in figure 4.2, and it is hypothesized that they represent "congestion" during the peak periods.

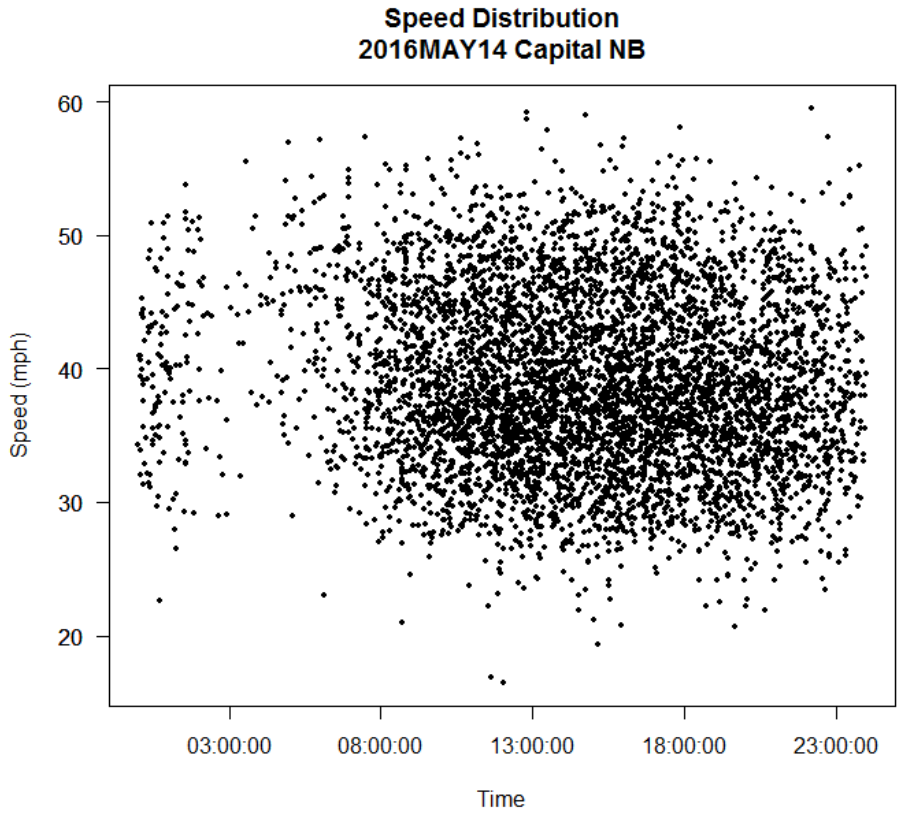

(a) Speed distribution in the low traffic volume scenario

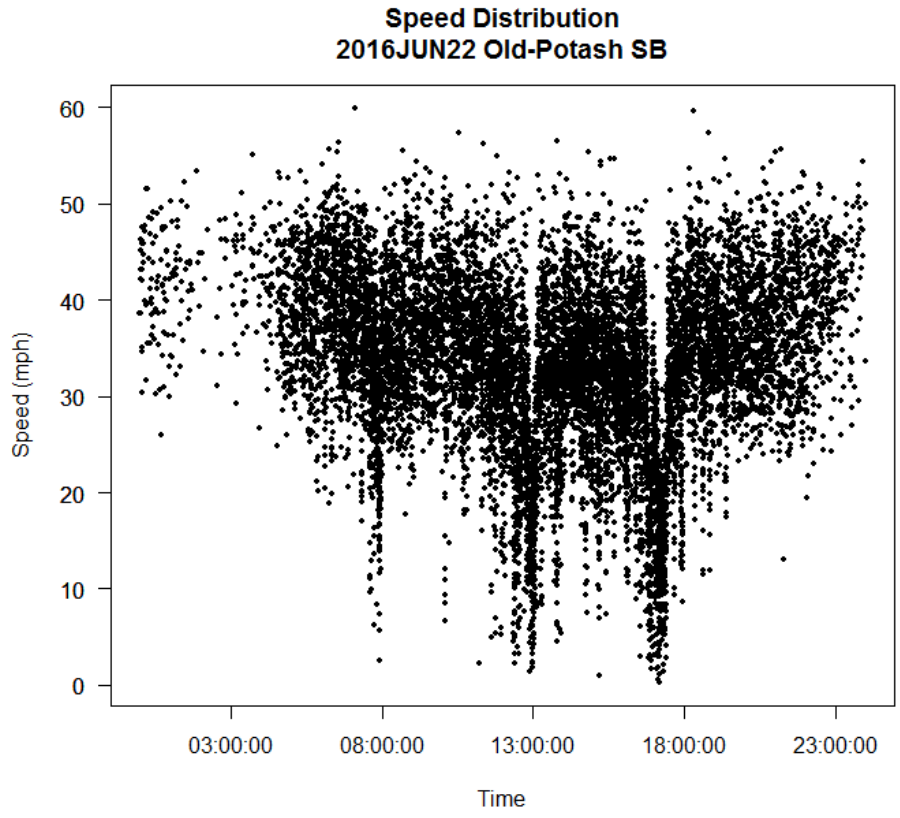

(b) Speed distribution in the high traffic volume scenario

Figure 4.3 Examples of speed scatter distribution over a day

Not surprisingly, the speed distribution is correlated to the traffic volume distribution in that as volume increases, the speed decreases. The speed drops indicate congestion during the peak hour periods.

A histogram of instantaneous speed, measured at the mobile trailer location, for SB 13th street (e.g., site 5), is shown in figure 4.4. Because the speed limit is 45 mph, any vehicle traveling faster than this value is considered speeding. For this site, approximately 12.5% of the vehicles are speeding.

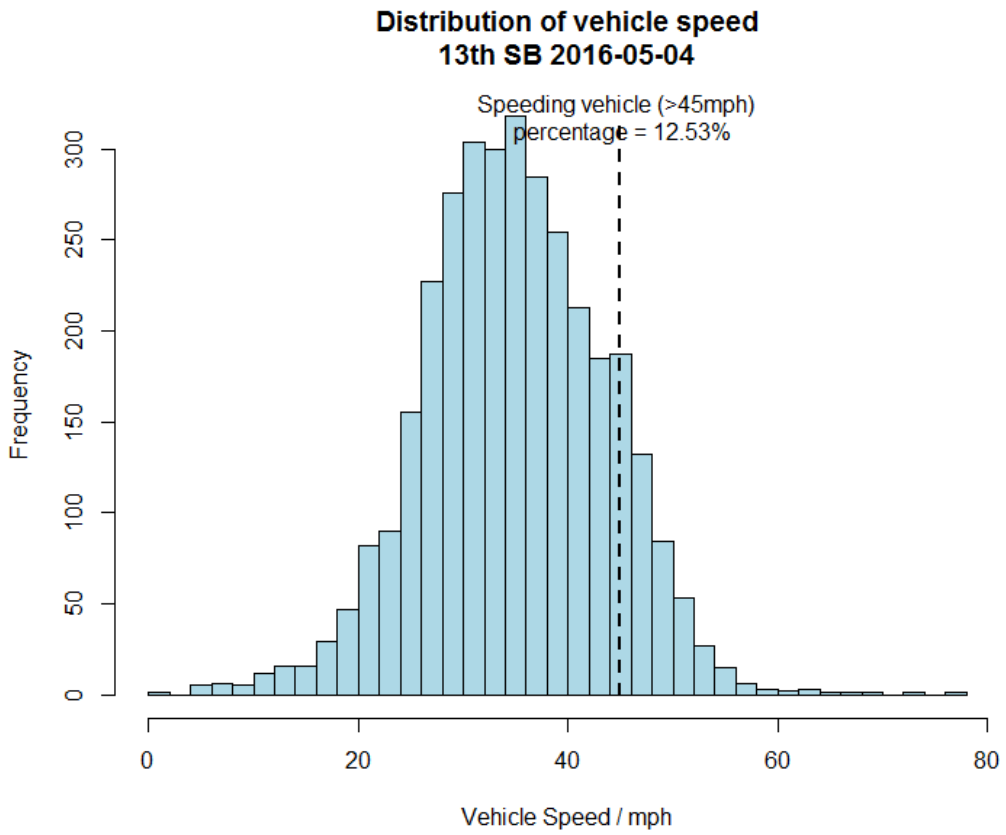

Figure 4.4 Histogram of vehicle's instantaneous speed at the trailer location for each site

The instantaneous speed histograms for the other eight sites may be found in Appendix B. Table 4.3 shows the average speed, standard deviation, and percentage of speeding for all nine sites. It may be seen that the range in percentage of speeding vehicles is from 6.93% to 21.72%, with an average of 15.0% and a standard deviation of 5.8%.

Table 4.3 Summary of vehicular instantaneous speed

No.	Approach	Average speed (mph)	Std. dev. (mph)	Percent of speeding
1	Capital SB	38.6	7.4	19.85%
2	Capital NB	39.0	6.6	20.66%
3	State St. SB	36.4	8.4	19.58%
4	State St. NB	39.1	6.8	21.72%
5	13th St. SB	34.8	8.7	12.53%
6	13th St. NB	40.2	7.8	8.04%
7	Faidley SB	35.6	8.1	16%
8	Faidley NB	36.3	6.4	6.93%
9	Old-Po. SB	35.4	7.7	9.84%

4.1.4 Vehicle Classification

Vehicle classification in this study is based on the measured length of the vehicle. Vehicle classification was conducted by the Wavetronix HD detector, where vehicles are classified based on their lengths. In this analysis, any vehicle over 25 feet was considered a large vehicle, and anything less was considered a passenger car. The 25 ft cut-off values was derived from an earlier report (16).

Previous researchers compared the results of the Wavetronix SmartSensor HD length data to manually-measured vehicle lengths. This comparison was conducted with highway data

collected during free-flow traffic periods. It was found that the average error among passenger vehicles was 0.6 feet with an absolute average error of 1.6 feet. The average error for trucks was 1.7 feet with an absolute average error of 2.8 feet. The reported percent errors were -2.3%, -15.3%, and -3.0% for passenger cars, trucks only, and total vehicles, respectively.

A histogram of vehicle length, measured at the mobile trailer location, for NB Highway 281 at Capital Street (e.g., site 2) is shown in figure 4.45. For this site, approximately 7% of the vehicles are classified as large.

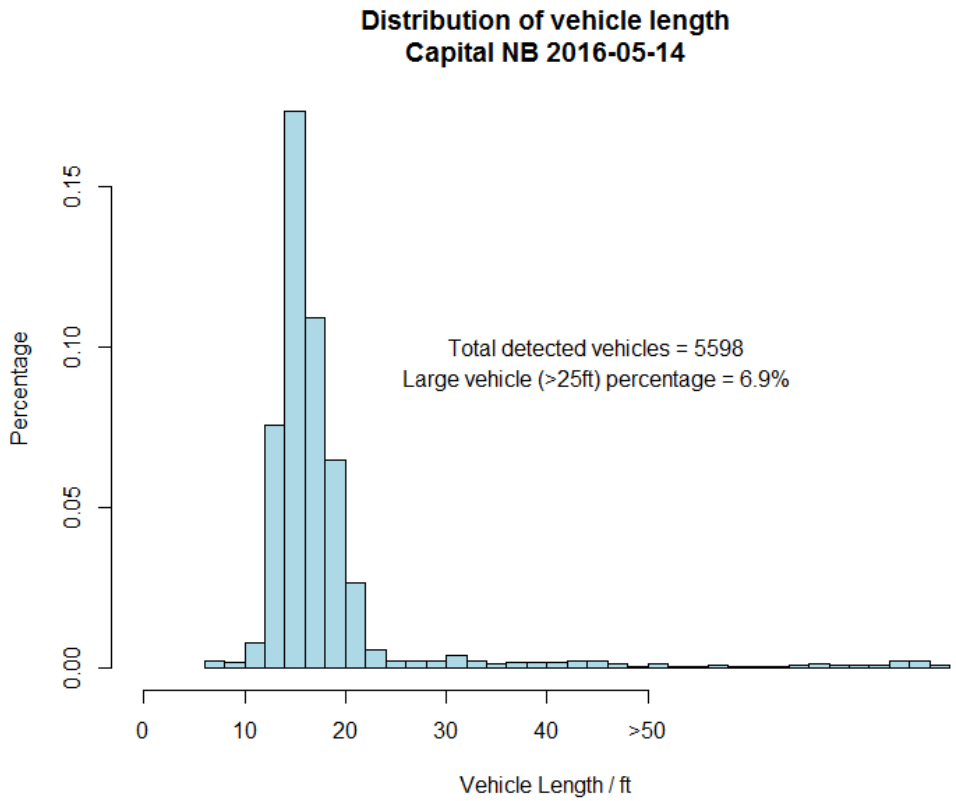

Figure 4.5 Distribution of the vehicle length at each site

The vehicle length histograms for the other eight sites may be found in Appendix C. Table 4.4 shows the average vehicle length, standard deviation, and percentage of large vehicles

for all nine sites. It may be seen that the percentage of large vehicles ranges from 6.9% to 13.2%, with an average of 9.6% and a standard deviation of 1.8%.

Table 4.4 Summary of vehicle length

No.	Approach	Average vehicle length (ft)	Std. dev. (ft)	Percent of large vehicles
1	Capital SB	19.4	7.7	8.5%
2	Capital NB	17.7	5.8	6.9%
3	State St. SB	18.7	6.9	9.9%
4	State St. NB	17.9	6.6	8.2%
5	13th St. SB	18.7	7.6	10.9%
6	13th St. NB	19.5	7.9	9.5%
7	Faidley SB	19.6	8.8	13.2%
8	Faidley NB	20.0	7.5	10.3%
9	Old-Po. SB	18.5	6.6	8.9%

4.2 Vehicle Trajectory

The two AD sensors track vehicles traveling from the upstream intersection to the downstream intersection. The distance covered by each sensor is measured relative to the location of the sensor (i.e., sensor location is as baseline as 0 ft). After the trailer distance to the stop-line is determined, all the detected vehicle travel distances are transformed into distance

from the upstream stop-line. Note that when a vehicle is within 50 ft of the sensor, it ceases to be tracked because the sensor has trouble detecting vehicles that are “under” the sensor.

Because the AD sensors operate independently, each AD sensor assigns a separate ID to each vehicle. It is not easy to identify which two ID numbers correspond to the same vehicle. This is especially true in busy traffic where multiple vehicles can be under surveillance at the same time. In this report, a filtering methodology was developed to estimate a complete trajectory. This methodology uses the distance, vehicle type, and time gaps to match the vehicles.

In addition to the speed trajectories from AD sensor, the HD sensor also provides a spot speed of the vehicle passing by at the trailer location. Information from all three sensors can be used to identify and match the two parts of the speed profiles of a particular vehicle.

4.2.1 Example 1: Stopping for a Red Signal during an AWS Activation

To illustrate the procedure, a vehicle was identified from the video recording and its two trajectories were identified manually. Figure 4.6 (a) shows the vehicle speed as a function of distance from the upstream stop-line. The orange line represents the location of the AWS flashers, the black line represents the location of the trailer, and the red line represents the upstream stop-line location. The blue data points represent the speed measured from the AD sensor pointed upstream, and the purple data points represent the speed measured from the AD sensor pointed downstream. Note that neither AD sensor can measure vehicle speed within 50 ft of the trailer. The green dot represents the spot speed, measured by the HD sensor. The goal is to develop a methodology for identifying these three measurements which all come from the same vehicle.

Figure 4.6 (b) shows the vehicle’s speed as a function of time. The orange dotted line, green-yellow dotted line, and the red-yellow dotted line show when the AWS flasher is turned

on, when the upstream signal transitions from green to yellow, and when the upstream signal transitions from yellow to red, respectively.

Observations of the speed profiles in figure 4.6 are described below.

1) The first capture of the vehicle is at around 690 ft, where it is still upstream of the AWS, the signal phase is green, and the AWS has not been activated yet.
2) The vehicle travels at a constant speed of approximately 40 mph which is lower than the 45 mph speed limit. When the vehicle is approximately 450 ft from the AWS sign, the AWS begins to flash, and the driver reduces the speed to 30 mph at the end of the detected upstream trajectory.
3) As the vehicle passes by the trailer, its speed is measured at 30 mph by the HD sensor.
4) After passing the trailer location, the vehicle is identified about 300 ft from the stop-line by the downstream AD sensor traveling at approximate 30 mph. Note that it is still in the lead flash period (i.e., AWS is active while the signal is still green).
5) The signal phase turns to amber and the vehicle continues to decelerate until it comes to a complete stop at the stop-line.

As can be seen, this vehicle behaves a typical process of compliance to the traffic rules. The driver is not speeding and begins to slow down when the AWS flasher is activated. The vehicle continues to decelerate until it comes to a complete stop. It is hypothesized that for this driver, the AWS worked effectively in helping alert the driver of the impending end of green.

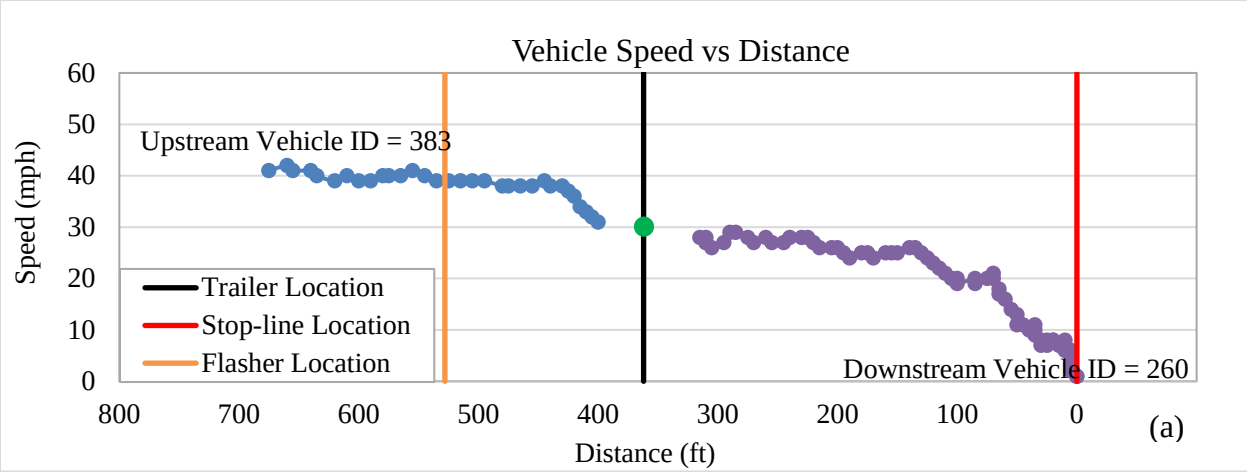

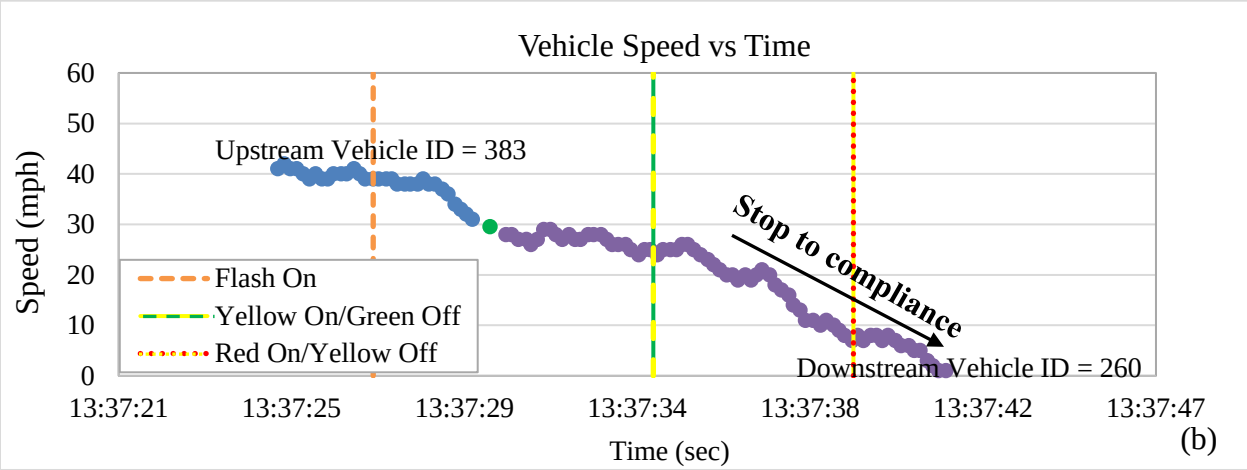

Figure 4.6 An example of compliance stopping vehicle during the actuation of AWS

4.2.2 Example 2: Red-light Running during the Actuation of AWS

Similar to example 1 in section 4.2.1, figure 4.7 (a) shows the speed versus distance graph of a driver who ultimately enters the upstream intersection after the signal turns red (e.g., "red-light runner"). The same color coding of figure 4.6 (a) applies. Similarly, figure 4.7 (b) shows the vehicle speed as a function of time. The same color coding of figure 4.6 (b) applies. The speed profiles in figure 4.7 (a) and figure 4.7 (b) indicate the following information.

1) The first identification of the vehicle is at around 730 ft, where it is upstream of the AWS, the signal phase is green, and the AWS has not been activated yet.

2) Before arriving at the AWS location, the vehicle travels at approximately 43 mph (close to the 45mph speed limit). After the start of the AWS flasher, the vehicle speed decreases below 40 mph.

3) As the vehicle passes by the trailer, its speed is measured at 39 mph by the HD sensor.

4) After passing the trailer location, the vehicle is identified at approximately 300 ft from the stop-line. Its speed is approximately 35 mph. Note that it is still in the lead flash period (i.e., AWS is active while the signal is still green) and the vehicle reduces its speed to approximately 25 mph. It is about 200 ft away from the stop-line at the onset of amber.

5) During the amber (4.5 seconds), the vehicle accelerates to a speed over 40 mph. The vehicle passes the stop-line after the onset of the red signal.

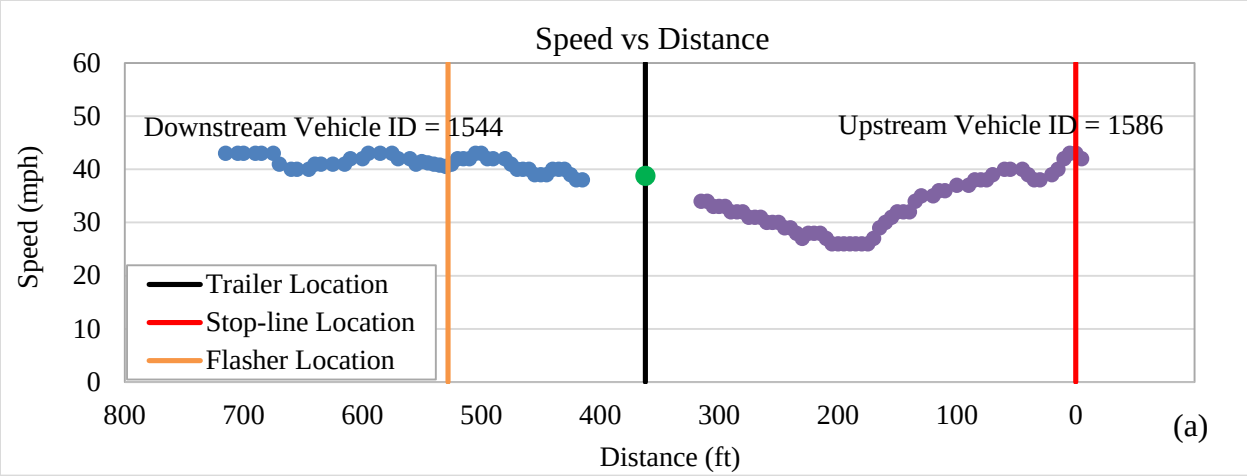

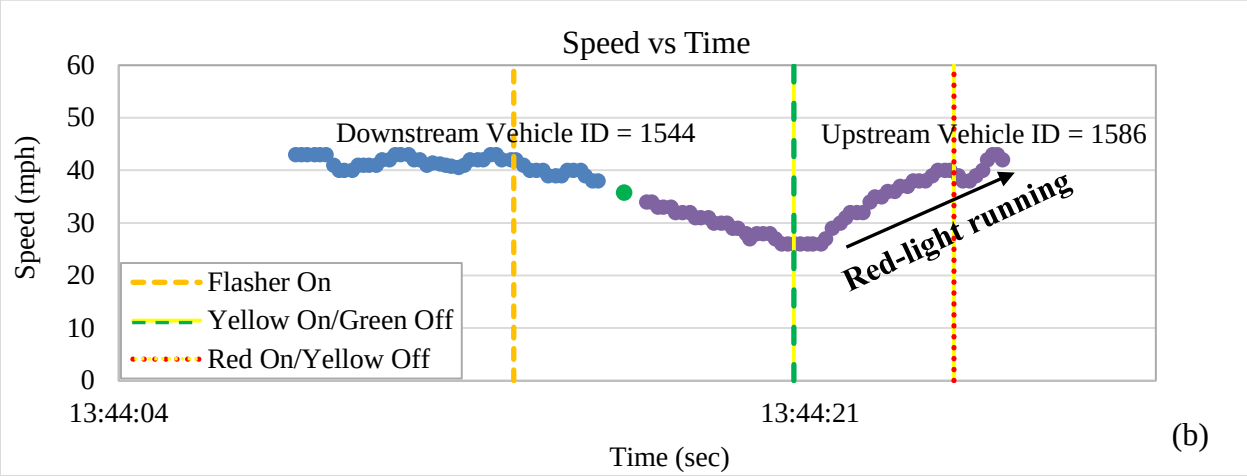

Figure 4.7 An example of red-light running vehicle during the actuation of AWS

As can be seen in figure 4.7, this vehicle is a red-light runner, meaning this vehicle crossed the stop-line after the onset of the red signal. It should be noted that the driver reduced the speed after the activation of the AWS and could have stopped safely. It is assumed that this driver changed his or her mind approximately 200 ft from the stop-line, and that the original decision was to stop (slow down). Because the vehicle began to slow down initially during the green phase, it is hypothesized that the driver's speed reduction is a result of the AWS activation. This example also indicates that the AWS does not always lead to safer behavior. Interestingly, if

the driver had not maintained his or her initial speed, and did not slow down when the AWS began to flash, the driver could have entered the intersection safely. The critical question, of course, is whether safety is improved at the crossing.

4.3 Summary

In this chapter, basic traffic flow and operational information were obtained, including the distribution of green time, the distribution of traffic volume as a function of time, the distribution of speed as a function of time, and the classification of vehicle length.

Three Wavetronix devices: upstream AD, HD, and downstream AD, were used to record the trajectory of each vehicle traveling from 600 ft upstream of the trailer to 600 ft downstream of the trailer. The goal was to develop a methodology for identifying these three measurements, which all come from the same vehicle, for later data analysis usage.

For illustration purposes, two manually extracted vehicular trajectory examples were used to show the vehicle trajectory of the speed over distance and time. The interpretation from the trajectory showed two examples of driver behaviors as they approached an intersection. This information, in conjunction with the signal information, can be used to identify whether a vehicle is a red-light runner or not.

Chapter 5 Operational Performance Analysis

When optimizing traffic signals on a corridor, the start of green at a downstream intersection is often set so that the waiting vehicles discharge prior to the platoon arrival from the upstream intersection. A key input to an optimal signal coordination strategy is understanding how the platoon of vehicles that are released from the upstream intersection arrives at the downstream intersection. This chapter studies the operational performance of the AWFs on the coordinated Highway 281 corridor in Grand Island. In particular, the effect of AWS on platoon dispersion is analyzed.

5.1 Platoon Dispersion

When the green phase at the upstream intersection starts, it releases a platoon of vehicles that travel to the downstream signalized intersection. As this platoon moves downstream, the vehicles that comprise the platoon disperse or spread out. In other words, the headway between vehicles increases due to the differences in vehicle speed, vehicle interactions (lane changing, merging, etc.), and roadway "friction" (e.g., on-road parking, pedestrians, etc.). This phenomenon is called platoon dispersion (PD). When a platoon of vehicles is released from an upstream traffic signal, the degree to which this platoon has dispersed at the next downstream signalized intersection, in part, determines whether significant benefits can be achieved from signal coordination. The effectiveness of signal timing and progression diminishes when platoons are fully dispersed.

It is important to understand how AWS affects the platoon dispersion so that this can be accounted for in the signal coordination methodology. The manner in which the platoon is affected will also indicate whether the AWS is working effectively. This section focuses on the performance of the signal coordination among intersections in terms of platoon dispersion.

Figure 5.1 shows the percentage saturation, which is a measure of the flow rate, as a function of time step t at the two intersections A and B. For a coordinated corridor, the two signalized intersections A and B will have a common cycle length. Note that the green time t_{gA} and t_{gB} are not necessarily the same. Robertson's platoon dispersion model is used to describe the dispersion behavior (17). The model assumes an upstream departure flow q_A, which discharges at the saturation flow starting at the beginning of the effective green. The first vehicle shifts a lag time of T when arriving at intersection B. The average travel time of the arrival vehicles is denoted by t_o. It is assumed that for each time step the arrival flow q_B follows a geometric distribution after the dispersion, as illustrated in the first time step in figure 5.1 (shaded area).

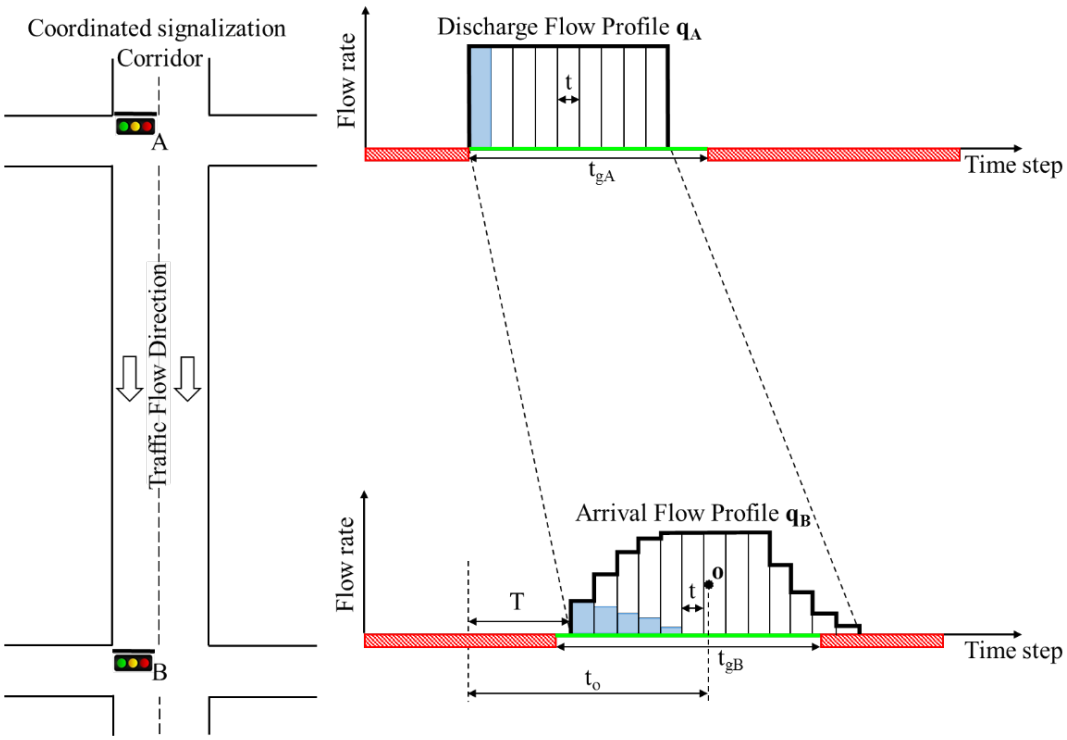

Figure 5.1 Robertson's platoon dispersion model illustration

The process can be described by Robertson's platoon dispersion model in equation 5.1.

$$q_B(t) = Fq_A(t - T) + (1 - F)q_B(t - 1) \quad (5.1)$$

Where q_A = discharge flow at upstream location A of the link (in units of veh/time step)

q_B = arrival flow at downstream location B of the link (in units of veh/time step)

T = a lag time for the arrival of the first vehicle in platoon, a.k.a., platoon arrival time (in units of time step)

F = smoothing factor (unitless)

The Robertson's platoon dispersion model in eq. 5.1 indicates that any arrival flow to the downstream location B is a weighted combination of: i) the traffic flow at the upstream location A, where the traffic flow departed *T* time ago, and ii) the arrival flow at location B in the previous second (*t-1*).

The variable *F*, which is a smoothing factor, is a function of the platoon travel time to the downstream signal and roadway impedance to traffic flow or "friction." Platoon travel time is defined as the average running time of all vehicles in a platoon from the upstream location to the downstream location. With reference to the start of the green at the upstream intersection, the average platoon travel time (e.g., travel time of vehicles in platoon) is marked as t_o in figure 5.1, where point *o* is a virtual point that represents the average of the platoon vehicles. Based on empirical evidence, Robertson (17) found that the platoon arrival time *T* is a portion of the average of the platoon travel time t_o, and *F* is a function of two parameters: the platoon dispersion factor α ($0 \leq \alpha \leq 1$), and the travel time factor β ($0 \leq \beta \leq 1$). These can be estimated using eqs. (5.2) and (5.3).

$$T = \beta t_o \tag{5.2}$$

$$F = \frac{1}{1 + \alpha\beta t_o} \tag{5.3}$$

Note that the average platoon travel time t_o (in units of time step) can be estimated by the field observation of the vehicles, which travel as a platoon after the start of the green signal at the upstream intersection. It has been found that different link travel times result in the selection of different α and β values, even when road conditions are similar (18). A successful application of Robertson's platoon dispersion model relies on the appropriate calibration of several model parameters. In TRANSYT, the default value of β is 0.8 for all α, while 0.35 is recommended for α in the United Kingdom (19), and 0.25-0.5 is recommended for α in North America (20). In general, as roadway friction increases (e.g., parking on road, high pedestrian volumes, narrow lane widths), α increases.

Some researchers (21 and 22) have also recommended that α and β values should be calibrated at each site in order to capture various geometric and traffic conditions. Based on an assumption that the travel time follows a shifted geometric distribution, Yu and Van Aerde (18) proposed a simplified calibration method based on the average platoon travel time t_o and it's variance ${\sigma_{t_o}}^2$, as shown in eqs. (5.4) and (5.5).

$$\alpha = \frac{\sqrt{1 + 4{\sigma_{t_o}}^2} - 1}{2t_o + 1 - \sqrt{1 + 4{\sigma_{t_o}}^2}} \tag{5.4}$$

$$\beta = \frac{2t_o + 1 - \sqrt{1 + 4{\sigma_{t_o}}^2}}{2t_o} \qquad (5.1)$$

In essence, the dispersion factors α and β are related to the average travel time required to travel from the upstream location to the downstream location (t_o) and the variance of the travel time (${\sigma_{t_o}}^2$). It can be seen that as ${\sigma_{t_o}}^2$ increases, the dispersion factor α becomes larger and β becomes smaller, which indicates that the platoon will be more dispersed at the downstream intersection.

When an AWS flasher is located between the upstream and downstream intersection, a natural question is whether the flashing signal impacts platoon dispersion, as illustrated in figure 5.2. Based on prior research, it is easy to hypothesize that the signal might cause some drivers to slow down, and others to speed up. If so, the platoon dispersion factors would be different, which would impact the signal coordination. These factors would also provide evidence for whether the AWS was having a positive effect on safety.

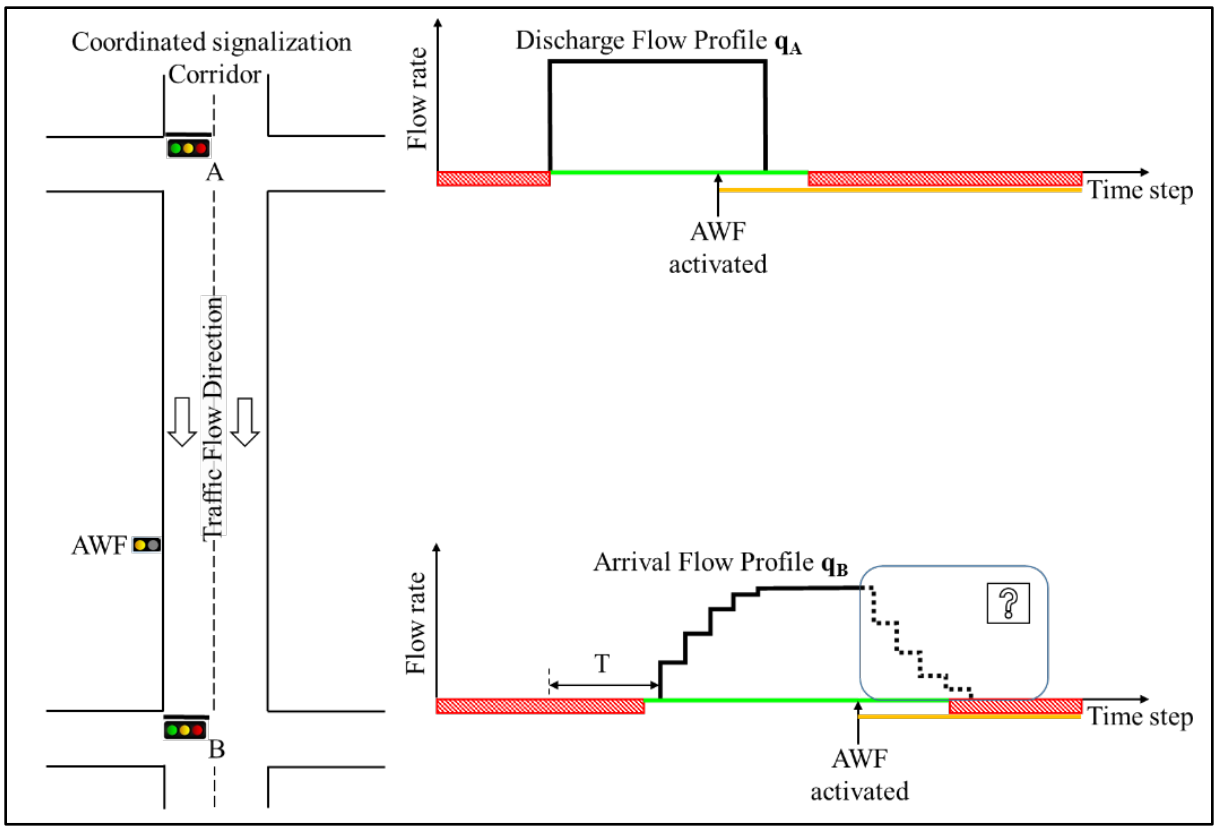

Figure 5.2 The AWS involved platoon dispersion model

A comprehensive literature review found that none of the existing research has considered the effect of AWS on PD or signal coordination. It is hypothesized that ignoring this effect will lead to sub-optimal signal coordination.

5.2 Data Preparation

Three test sites were used in the operational platoon performance study. They are site 1: SB link from Capital St to State St; site 2: NB link from 13th St to State St; and site 3: SB link from Faidley St to Old Potash St.

A generic representation of the data collection setup is shown in figure 5.3. Trailer 1 is the one that is used for data collection, and it was described in chapter 3. Its location was selected so that it could measure the effect of the AWS on vehicle speed. Note that the

measurements would not be impacted by any queueing on the downstream intersection. For each site, an additional trailer, marked as trailer 2 in figure 5.3, is used to collect discharge platoon information at the upstream intersection of the link. Trailer 2 is located 100 ft away from the nearest edge of the upstream intersection. This location is chosen because the immediate traffic outflow from the upstream intersection can be readily identified. On trailer 2, a camera and a Wavetronix SmartSensor HD (SSD) sensor were installed perpendicular to the traffic flow. The camera was used to videotape the traffic passing the trailer in case the SSD data need to be checked visually. It should be noted that the video range of the upstream camera (i.e., camera on trailer 2) covers the upstream intersection signal so that the time of signal change can be recorded. Thus, the average travel speed for each vehicle can be estimated by dividing the running time by the distance between the two data collection points. The SSD was used to automatically record the time that each vehicle passes the trailer location. A Mikrotik SXT 5HnD router was used to wirelessly connect the two trailers so that all the data were synchronized in time and saved in the local server which was located in the trailer 1 cabinet.

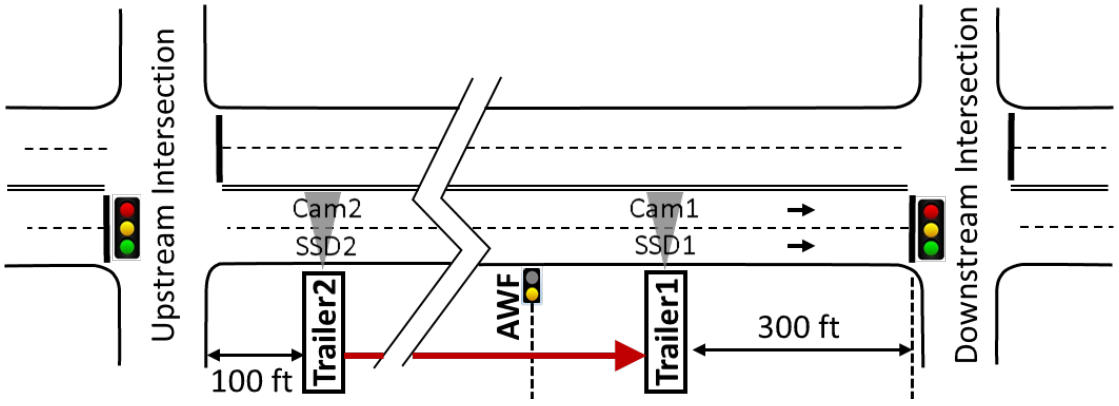

Figure 5.3 Layout of the generic data collection system

The time step of the vehicle count for both the SSD and video data collection was set to a one second interval. The signal timing from the upstream intersection was obtained from the traffic signal control cabinets.

Data was collected using both trailers on May 17 and 18, May 27 and 28, and Jun 4 and 5, 2016 at sites 1, 2, and 3, respectively. The data from the first day at 8 pm to the second day at 6 am was removed because of low traffic volume and corresponding small platoon sizes. A statistical summary of the data from the three sites are listed in table 5.1.

Table 5.1 Summary of study site characteristics

Site	Upstream (from)	Downstream (to)	Peak hour volume (veh/h/ln)	Signal cycles	Speed at Trailer 1 (mph)		Speed at Trailer 2 (mph)	
					Mean	85%	Mean	85%
1	Capital St	State St	283	638	30.8	41.4	36.3	45.1
2	13th St	State St	385	637	33.7	42.2	36.6	45.9
3	Faidley	Old Potash	596	637	32.9	42.2	36.6	45.8

The platoon for each signal cycle is determined using the following three steps.

1) Identify the “on” of the green phase (t_{on}) and the “off” of the green phase (t_{off}) at the upstream signal intersection. Match the SSD data at the upstream trailer 2 to the downstream trailer 1.

2) Use the count data from the upstream trailer to identify the discharge platoon as a function of time for each cycle. The discharge platoon in each cycle starts when the green time is on and ends when the green time is off, as shown in eqs. (5.6) and (5.7).

$$t_{1,start} = t_{g\_on} \tag{5.6}$$

$$t_{1,end} = t_{g\_off} \tag{5.7}$$

3) Use the count data from the downstream trailer to identify the arrival platoon as a function of time for each cycle. Based on an average running speed, the time offset between the two trailers is approximately 35 seconds. The start and end of the arrival platoon can be estimated using eqs. (5.8) and (5.9).

$$t_{2,start} = t_{on} + \frac{D_i}{V_i} \tag{5.8}$$

$$t_{2,end} = t_{off} + \frac{D_i}{V_i} \tag{5.9}$$

Where, D_i represents the distance from the upstream to the downstream trailer at site *i* (feet);

V is the average platoon running speed at site *i* (ft/s).

The focus in this chapter is on through vehicles in the platoon traveling from the downstream intersection to the upstream intersection. Note that for any green signal there may be

two distinct platoons. The first platoon is made up of through vehicles and the second consists of right turning vehicles from the minor street. There is a natural time gap between these two platoons. It was unclear which time gap/platoon headway was best to use in order to decide where one platoon ends and the other begins. Consequently, a sensitivity analysis was conducted to identify the best value. Platoon headways from 2 seconds to 10 seconds were tested. The objective was to optimally match the identified arrival platoons to the discharge platoons in terms of the platoon numbers and platoon sizes. It was found that a 5-second headway gave the best results with respect to matching the total number of platoons and the size of each platoon at the upstream and downstream trailers.

5.3 Calibration of Travel Time

In this section, two methods were used to extract data for identifying the platoon and the platoon travel time. Firstly, 25 continuous signal cycles (about half an hour) were extracted from the SSD data to manually verify the quality of the data. There were 25 cycles during this period, and each cycle resulted in one platoon. The travel time was recorded from SSD 2 (upstream) to SSD 1 (downstream) for all vehicles in each of the 25 platoons.

Video recordings from the two cameras were also observed at each site to verify the platoon data collected by SSD. It should be noted that unlike the video from two cameras, the platoon vehicles recorded by the SSD 1 and SSD 2 could not be matched automatically due to lane-changing and overtaking behaviors. However, it does not affect the average platoon travel time because: 1) the overtaking vehicles were still considered part of the platoon, and 2) the time differences for the pair of upstream and downstream recordings were cancelled out when they were averaged. Note that the platoons manually observed from the video were used only for model calibration while the whole SSD data was used in the data analysis.

Figure 5.4 shows the vehicles in the 25 platoons as a function of the green time at the upstream signal of site 3. As discussed in chapter 4, the signals for this corridor are actuated, which means they can have different offsets and different green times depending on the cross street volumes. Therefore the start of each upstream green phase was normalized to zero seconds for comparison purposes. For example, $T_r^{(25)}$ in figure 5.4 is the running time between the first recorded discharge vehicle and the first recorded arrival vehicle in the 25^{th} platoon. In the same manner, the running times for the other vehicles in the 25^{th} platoon can be obtained. The average of the vehicle running time of all the vehicles in the platoon yielded the average travel time for this particular platoon. The average of all the platoons' running time is the average platoon travel time (t_o), which will be used for calibration of platoon dispersion parameters at this site.

Figure 5.4 Examples of discharge and arrival platoon vehicles at site 3, June 4, 2016.

It may be seen in figure 5.4 that the time headways of the vehicles in the platoon at the upstream location are much "tighter" compared to the time headways of the vehicles in the downstream platoon. Note that Van Aerde and Yu's platoon dispersion parameter estimation method (18) only requires the platoon travel time t_o and the variance $\sigma_{t_o}{}^2$. Both of these variables are collected from all the 25 platoons at each site and are listed in table 5.2.

Table 5.2 Data reduction statistics for study sites

Site	Method	No. of platoons	Space mean speed (mph)	Std. dev. of speed (mph)	Mean of travel time (s)	Variance of travel time (s)
1	SSD	25	45.2	3.3	32.71	5.47
	Video	25	46.3	2.9	30.18	3.06
2	SSD	25	41.2	2.6	35.43	4.84
	-	-	-	-	-	-
3	SSD	25	41.7	4.1	37.62	14.21
	Video	25	43.4	4.6	36.24	15.76

The mean and standard error of travel time obtained from the video observations indicated a difference of less than 10% compared to the SSD data from site 1 and site 3. It was concluded that the travel time estimation by the SSD method was appropriate. It was unfortunate that the recorded video at site 2 was lost because of a camera malfunction. An effort was made to manually observe the running time between the two trailer locations on site by driving through site 2 several times. The average of the running time beginning at the upstream trailer to the

downstream trailer was 34.27 seconds, with a variance of 2.79 seconds. This provided a reference of comparison to the SSD data at site 2, and it may be seen that the values were close.

5.4 Effect of AWS on Arrival Flow Profiles Calibration

Assuming that all vehicles in a platoon travel at the same speed (e.g., at speed limit), there will be no dispersion, as illustrated by the blue dashed lines in figure 5.5. However, in reality, not all vehicles travel at speed limit, and the platoon will disperse such that the first portion of the arrival platoon vehicles will pass by the AWS before it is active. Vehicles in this part of the platoon will not be affected by the AWS. These vehicles are indicated by the red rectangle in figure 5.5. When the AWS flasher is actuated, it is assumed that all the drivers in the vehicles upstream of the AWS flasher will recognize and react to the flashing signal.

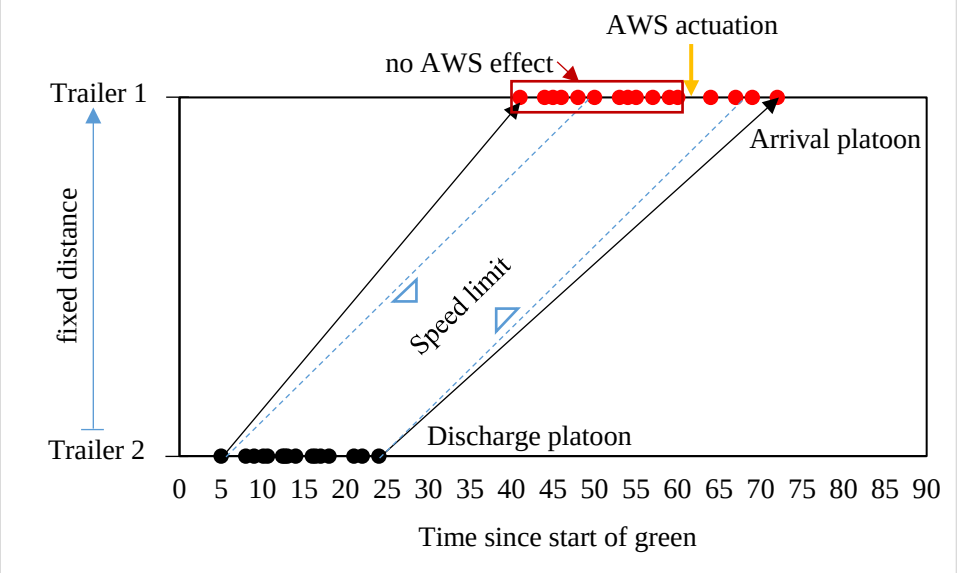

Figure 5.5 An Example of platoon vehicles encounter the actuated AWS at site 3

Robertson's PD model was calibrated to the two different regimes: AWS inactive and AWS active. If the AWS does not affect traffic, it is hypnotized that there will be no difference

in the calibration parameters. Eqs. (5.3-5.5) were used to estimate the platoon dispersion parameters for each site and for each regime (e.g., AWS active and AWS inactive). The results are listed in table 5.3.

Table 5.3 Comparing of the platoon dispersion parameters with and without AWS effect

Site	Platoon vehicles regime	Calibrated platoon dispersion coefficient α	Calibrated platoon arrival time coefficient β	Calibrated smoothing factor F
1	AWS Inactive	0.085	0.921	0.28
	AWS Active	0.224	0.817	0.13
2	AWS Inactive	0.118	0.895	0.21
	AWS Active	0.222	0.819	0.13
3	AWS Inactive	0.137	0.879	0.19
	AWS Active	0.287	0.777	0.11

As can be seen from table 5.3, the dispersion coefficient α for the three sites ranges from 0.085 to 0.137 when the AWF is inactive, and from 0.222 to 0.287 when the AWF is active. Both of these ranges are lower than the default value of 0.35 recommended by Roberson (17). Note that the higher value of α associated with the AWF effect indicates an increase in roadway friction (i.e., longer platoon travel time). The platoon arrival time coefficient β ranges from 0.777 to 0.819 when the AWF is active. This is approximately the same as the default value of 0.8

recommended by Roberson (17). The smoothing factor *F* ranges from 0.11 to 0.13 when the AWF effect is included in the parameter estimation. This is smaller than the smoothing factor for platoons without considering the AWF effect.

Next, the arrival flow profiles were predicted in Robertson's model using the estimated coefficients. Figure 5.6 shows the observed flow rates at the upstream and downstream trailers, and the predicted flow rate at the downstream trailer for sites 1, 2, and 3, respectively. For the three sites, the black solid-point curves represent the discharge flow profile observed at the upstream trailer, and the red sold curves represent the arrival flow profile observed at the downstream trailer. The arrival flow rates, at one-second time step from the start of green in each cycle, were averaged for all signal cycles during the data analysis period.

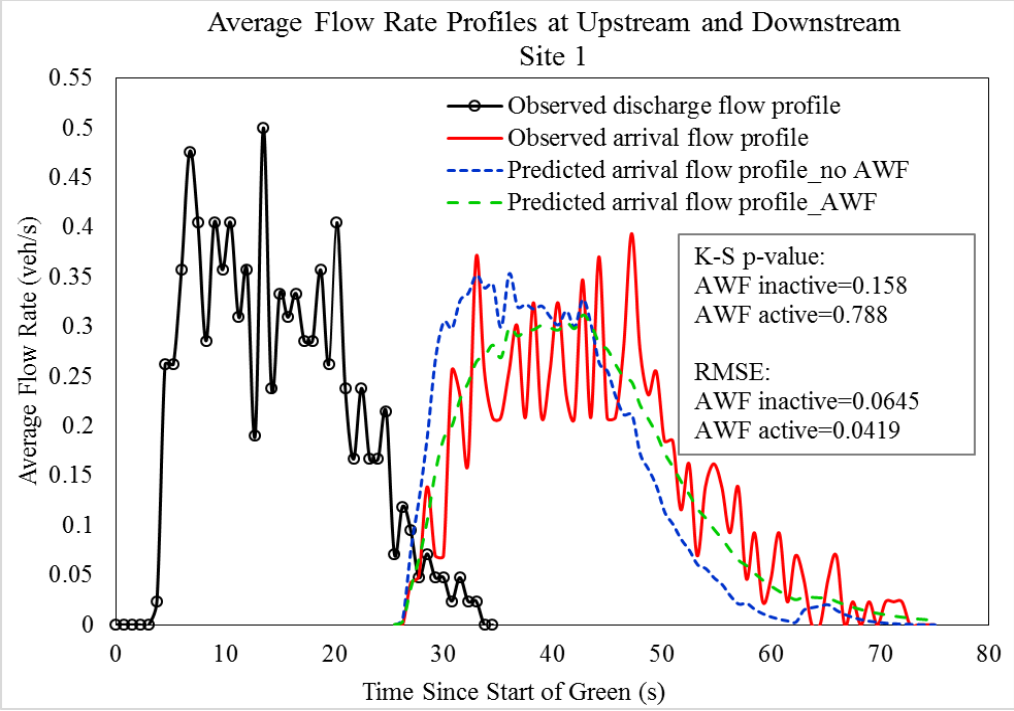

(a) site 1

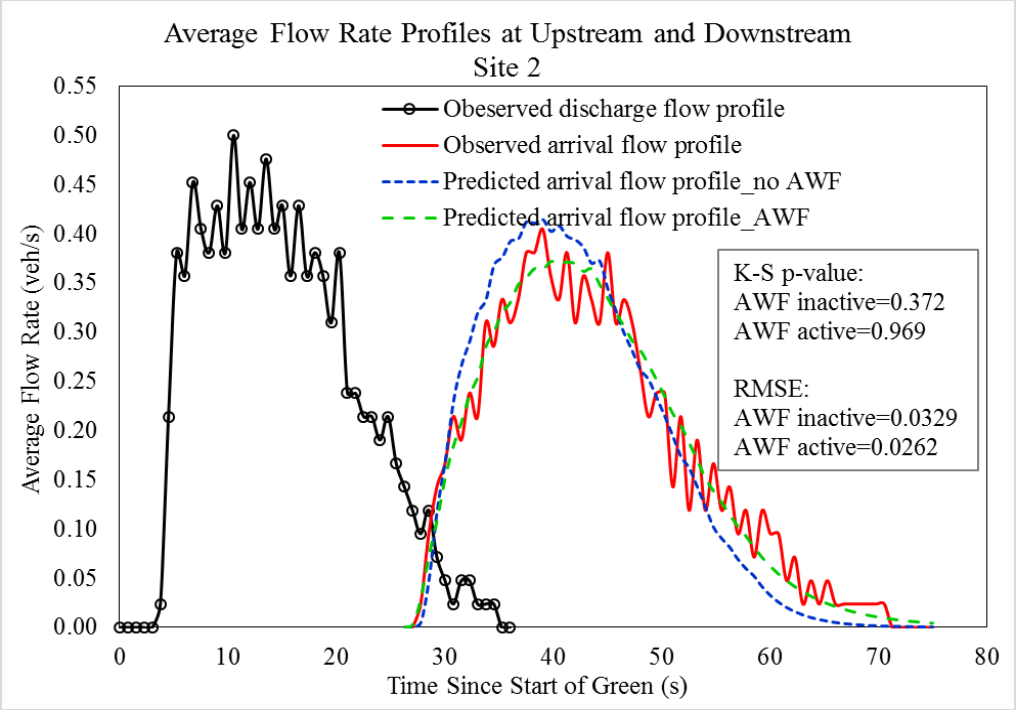

(b) site 2

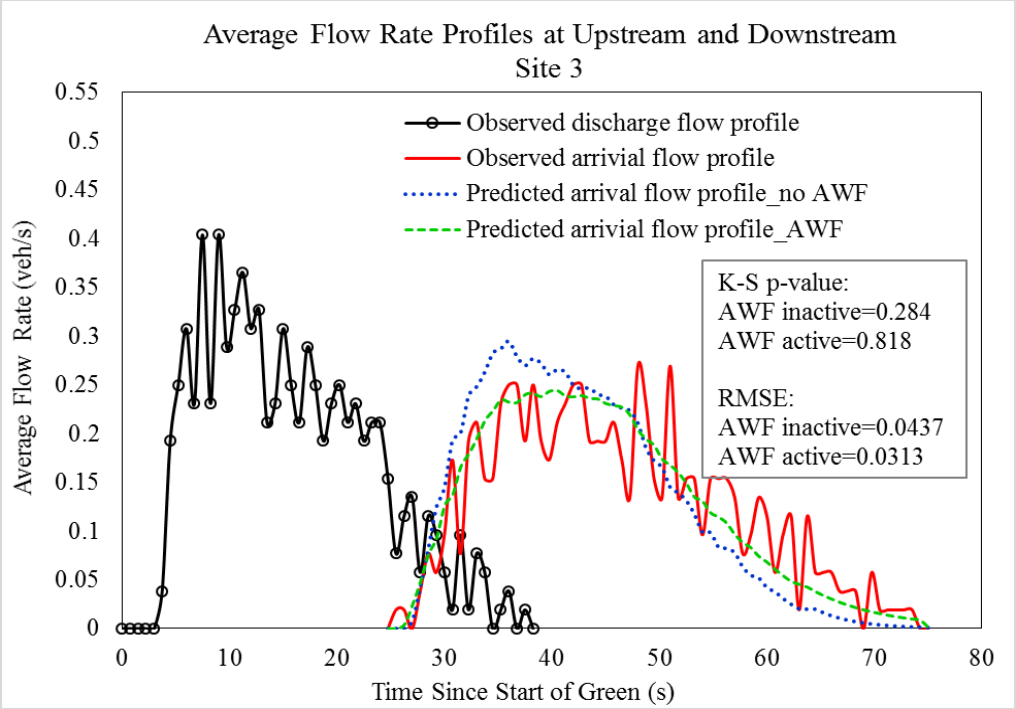

(c) site 3

Figure 5.6 The fitted arrival flow profiles for both AWF inactive and AWF active regimes

Given the observed discharge flow and arrival flow profiles, the predicted arrival flow profile can be estimated by using the two sets of coefficients from table 5.3. As compared in figure 5.6, the blue dotted curves are the fitted arrival profiles assuming an AWF inactive regime, while the green dashed curves are the fitted arrival flow profiles assuming an AWF active regime. It is worth mentioning that under the AWF active regime, the total platoon constitutes vehicles that are both unaffected by the AWF (e.g., front portion of a platoon) and affected by the AWF (e.g., tail portion of the platoon). The average number of vehicles in a platoon that were affected by the AWF was 3.44 vehicles, with a standard deviation of 1.8 vehicles. Seventy-five platoons were used in the calibration process.

In general, the arrival flow dispersion is underestimated when the AWF effect is not included in the calibrated model. As can be seen in the AWF inactive regime (i.e., blue dotted curves) in figure 5.6, the right-hand tails of the predicted arrival flow profiles "shrink" earlier than the observed arrival flow profiles after the actuation of the AWF. This is particularly true when the observed discharge flow rates have a lot of fluctuation (e.g., sites 1 and 3). From a visual check of the fit of the model, the observed arrival flow profiles are better fit by the AWF active regime (i.e., green dashed curves) in figure 5.6. In other words, the effect of AWF is to elongate or delay the arrival platoon. This conclusion supports the finding that the calibrated α value was higher for the AWF active regime as compared to the AWF inactive regime in table 5.3.

In addition, a Kolmogorov-Smirnov test is used to statistically compare the goodness of fit of the two models. The null hypothesis is that the observed arrival flow and the predicted arrival flow (e.g., in the two regimes) have the same distribution. A small p-value indicates any violation of that null hypothesis, such as different medians, different variances, or different

distributions. As the p-values shown in figure 5.6 indicate, the arrival profiles incorporating the AWF effect are better fitted compared to those that do not incorporate the AWF effect. Also shown in figure 5.6 is the Root-Mean-Square-Error (RMSE), which measures the predicted arrival flow profiles with the observed arrival flow profiles for both regimes. The smaller RMSE associated with the AWF active regime indicates that it reduces the error, as compared to the AWF inactive regime, by 20% to 35%.

5.5 Summary

This chapter studied the operational performance of the AWS in terms of how platoons are affected in the test corridor. The traffic flow dispersion patterns at coordinated signalization corridors were examined by calibrating Robertson's platoon dispersion model. The dispersion parameters were calibrated with and without the AWS active in order to test the hypothesis of whether there is an effect of AWS on dispersion parameters.

The three test sites have the same speed limits, similar traffic compositions, and similar signal timing. The smoothing factor F ranged from 0.19 to 0.28 when the AWS flashers were not active. This confirms that the dispersion parameters are site specific.

When the AWS effect is included in the calibration, the smoothing factor F was lower and ranged from 0.11 to 0.13, the platoon dispersion coefficient α increased from an average of 0.11 to 0.24, which indicated an increase of friction in the road traffic. As the only change was the activation of the AWS, it was concluded that the AWS indeed affects (i.e., increase) the dispersion parameter. It was hypothesized that the AWS caused the vehicles to slow down which lead to a small platoon dispersion compared to the AWS inactive case.

A goal of a good design for signal coordination is to reduce the number of stragglers at the rear who miss the green phase. As the AWS will affect the rear part of the arrival platoon

vehicles, it is recommended to consider the calibration with the AWS effect when applying the dispersion parameters in signal coordination.

Chapter 6 Safety Performance Analysis

This chapter analyzes the safety performance of AWS in coordinated systems with respect to three aspects: dilemma zone entrapment, red-light running, and the acceleration and deceleration behavior of drivers with and without the flasher activated.

6.1 Dilemma Zone Analysis

As a traffic signal changes from green to amber, a driver who is approaching the intersection has to decide whether to stop or proceed through the intersection. Under certain circumstances, either choice may result in a violation of traffic laws. The section of the roadway upstream of the intersection where this occurs is known as the dilemma zone. As shown in figure 6.1, the dilemma zone is defined by two boundaries. The upper boundary, D_{bz}, is the beginning of the dilemma zone where vehicles downstream of the boundary cannot stop comfortably at the stop-line. The lower boundary, D_{ez}, is the end of the dilemma zone where vehicles upstream of the boundary cannot proceed through the intersection safely before the onset of red. If there is overlap between the two boundaries (i.e., $D_{bz} - D_{ez} > 0$), then a dilemma zone exists.

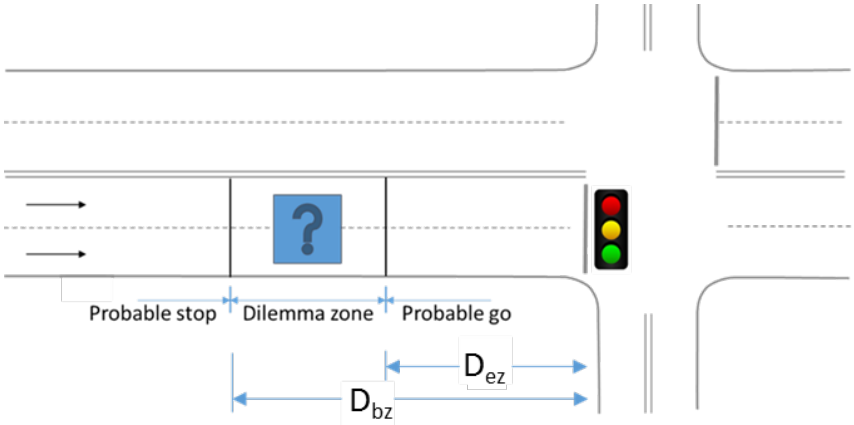

Figure 6.1 Tradition definition of dilemma zone

In other words, a driver upstream of the dilemma zone, who is traveling at the legal speed limit at the onset of the amber indication, can decelerate at a comfortable rate and come to a stop without entering the intersection. A driver downstream of the dilemma zone, who is traveling at the legal speed limit at the onset of the amber indication will be able to maintain their speed and enter the intersection before the end of the amber. However, if the driver has neither sufficient distance to bring the vehicle to a complete stop nor sufficient time to proceed safely through the stop-line before the onset of red, it causes a dilemma zone situation. The beginning of dilemma zone D_{bz} and the ending of dilemma zone D_{ez} can be calculated using eqs. (6.1) and (6.2).

$$D_{bz} = t_{PRT}V + \frac{V^2}{2a} \quad (6.1)$$

$$D_{ez} = \text{Vt} \quad (6.2)$$

Where

V	initial speed at the start of the flashing light (km/s)
t_{PRT}	perception reaction time for stopping vehicles (s)
t	lead flash time duration (s)
a	deceleration rate for stopping vehicles (m/s^2)

Theoretically, it is possible to eliminate the dilemma zone with proper signal timing. However, because of the stochastic nature of driver behavior some drivers may have issues in deciding whether to stop or go when the amber becomes active. For example, they may misjudge the distances to the stop-line and choose to stop when they should proceed, they may have slower perception-reaction times than the designed value, or their vehicles may lack the necessary braking power required.

Drivers exhibit distinct differences in their desires or abilities to stop at the onset of the amber. Some drivers may stop abruptly, therefore increasing the risk of a rear-end collision. Other drivers might proceed through the intersection which increases the risk of red-light running and the possibility of a right-angle collisions with vehicles entering the intersection from the cross road.

The potentially negative impact of dilemma zones on the operational capacity and safety of signalized intersections, particularly at high-speed locations, has prompted a great deal of effort focused on the mitigation of the dilemma zone issue. These mitigation efforts include: 1) reducing the likelihood of a driver being located in the dilemma zone at the onset of the amber; 2) increasing the awareness of the driver that the signal phase will be changing from green to amber shortly, thus requiring them to take an appropriate action; or 3) both options 1 and 2 (23). Typically, dilemma zone protection at high-speed signalized intersections is provided by the use of advanced detection, advance warning flashers, or a combination of both advance detection and advance warning flashers.

6.2 NDOR-defined Dilemma Zone Entrapment with AWS

AWS has been proven as an effective method to provide dilemma zone protection at isolated, high-speed signalized intersections (23). The AWS provides information on whether the traffic signal will transition from green to amber, via flashing beacons and warning signs, to drivers as they approach a signalized intersection. The goal is to alert drivers to the impending end of the green to hopefully reduce indecision and variability in driver behaviors during the amber interval. The flashing signal heads are activated at a predetermined time (e.g., lead flash time t) before the end of the green interval, which is calculated using eq. (6.3).

$$t = \frac{D_M}{V} \tag{6.3}$$

Note that at a signalized intersection operated under semi-actuated control, the major road does not have a green extension because there is no advance detector. Therefore, the green phase will end at the predetermined regardless of the traffic volume.

According to the NDOR dilemma zone definition, the beginning of a vehicle's dilemma zone is based on the stopping distance, and the end of the dilemma zone is the stop-line of the intersection (1). Because the stopping distance (i.e., the beginning of the dilemma zone D_{bz}) is a function of speed, the speed distribution on the approach is an important design component. Vehicles traveling at or above the design speed, up to the practical maximum speed V_m, will reach the stop line before the onset of amber and are therefore provided dilemma zone protection. The local maximum speed V_{m0}, at which a slower-moving vehicle (e.g., traveling at a speed less than design speed) could travel, is used to define the vehicles that will not reach the beginning of its dilemma zone. Assuming a 2 s perception-reaction time and a 10 ft/s^2 deceleration rate, the maximum speed value V_m and the local maximum speed V_{m0} can be calculated by using eq. (6.4) and eq. (6.5) (1).

$$V_m = -2 * 10 + 2 * \sqrt{100 + 5 * D} \tag{6.4}$$

$$V_{m0} = -10 * (2 + t) + \sqrt{100(2 + t)^2 + 20D} \tag{6.5}$$

Where D = distance between advance detector and the stop-line (ft)

t = lead flash time duration (second)

Vehicles traveling at speeds lower than the design speed will not reach the stop-line before the onset of amber and may be in a dilemma zone. A slower vehicle would be provided dilemma zone protection only if it had not reached the beginning of its dilemma zone by the time the amber indication started. Therefore, a vehicle approaching an intersection equipped with NDOR AWS devices will be provided dilemma zone protection if it travels at speed V (1), as determined by equation 6.6.

$$V \in \{0 < V \leq V_{m0} \cup V_{85} \leq V \leq V_m\} \quad (6.6)$$

Where V_{85} = the design speed, mph

V = vehicle travel speed, mph

Vehicles traveling at speeds outside these ranges will not be provided dilemma zone protection. That is, they will be traveling in their dilemma zones at the onset of amber. If the distribution of speeds as vehicles pass the AWS flasher location at the onset of amber is known, and it is assumed the driver continues at their speed, then the probability that a vehicle would be in its dilemma zone can be calculated. Assuming that the speed data were approximately normally distributed, the expected probability of the dilemma zone entrapment rate P_{DZ} can be expressed in eq. (6.7).

$$P_{DZ} = p(V_{m0} < V < V_{85}) \quad (6.7)$$

The estimated DZ entrapment is calculated by assuming that all vehicles at the start of the flashing signals maintain their speed at the time the signals begin flashing. The number of vehicles that would be in the DZ at the start of amber are then tabulated. Results of the DZ entrapment rate analysis are shown in table 6.1.

Table 6.1 Dilemma zone entrapment rates

Street Name	Vehicle at Flasher at Onset of Yellow		Dist. from Flasher to Stop-line (D) (ft)	Dilemma Zone Range $[0,D_{bz}]$ (ft)	Speed Range with DZ Protection		DZ Entrapment $p(V_{m0}<V<V_m)$	
	Mean Speed (mph)	Std. Dev. (mph)			Lower Range $(0, V_{m0}]$ (mph)	Upper Range $[V_{85}, V_m]$ (mph)	Expected %	Observed %
Capital SB	34.3	6.77	507	(0, 350)	(0, 31]	[45, 56]	60.7%	8.8%
Capital NB	36.3	6.40	495	(0, 350)	(0, 30]	[45, 56]	73.2%	11.1%
State St. SB	36.5	8.54	550	(0, 350)	(0, 31]	[45, 59]	58.0%	14.3%
State St. NB	37.2	7.24	519	(0, 350)	(0, 29]	[45, 57]	73.1%	39.1%
13th St. SB	34.9	8.95	554	(0, 350)	(0, 33]	[45, 59]	45.5%	12.5%
13th St. NB	39.8	5.85	535	(0, 350)	(0, 32]	[45, 58]	72.2%	16.4%
Faidley SB	40.2	7.88	528	(0, 350)	(0, 32]	[45, 58]	57.6%	31.2%
Faidley NB	39.0	6.60	528	(0, 350)	(0, 32]	[45, 58]	66.2%	23.6%
Old-Po. SB	35.5	8.02	526	(0, 350)	(0, 32]	[45, 58]	55.1%	13.7%

In general, a lower percent of vehicles in their dilemma zones at the onset of amber indicates a higher degree of dilemma zone protection. It may be seen from table 6.1 that the observed percentage of vehicles caught in the NDOR-defined DZ were much lower than the estimated number based on the vehicle speed of the HD detection. In particular, as shown in the comparison of the last two columns, the percentage of vehicles in their dilemma zones when the signal changed from green to amber ranged from 8.8% to 39.1%. This was, on average, 81% smaller than what would have been expected if the NDOR AWS was not installed. The lower than expected number of vehicles in the NDOR-defined dilemma zones at the onset of amber indicates that the NDOR AWS devices increased the propensity of drivers to begin to slow down when the warning device flashers become active. This is consistent with the speed profile results shown in chapter 4, which indicated that drivers upstream of the flasher had a tendency to: 1) lower their speeds during the lead flash period, and 2) lower their speeds even more when the traffic signal transitioned from green to amber.

6.3 Driver's Accelerating/Decelerating Behavior

The number of drivers who accelerate at the onset of amber has been used as a surrogate measure for unsafe behavior because it is linked to red-light running and an increased potential for right-angle collisions. A previous study at isolated high-speed signalized intersections in Nebraska showed that drivers respond positively to the AWS by slowing down as they approach the intersection (24). However, the results of studies conducted by other states (8 and 12) and the Federal Highway Administration (25) show that the active advance warning signs may encourage drivers to accelerate at the onset of yellow in an attempt to enter the intersection before the start of red.

6.3.1 Driving Behavior following the Onset of Amber

Vehicle's acceleration behavior was examined by studying the average acceleration rates at two segments of the approach. The first segment is close to the stop-line. It was important to choose a location where queuing vehicles would not be identified by the AD sensor. Therefore, a location between 100 ft and 200 ft upstream of the stop-line was chosen for analysis. The second segment was chosen so that the AWS flasher location was included. The average acceleration rate was calculated using the speed at the beginning and end of each segment and the segment length. Figure 6.2 shows the calculation of the acceleration rate for the two segments.

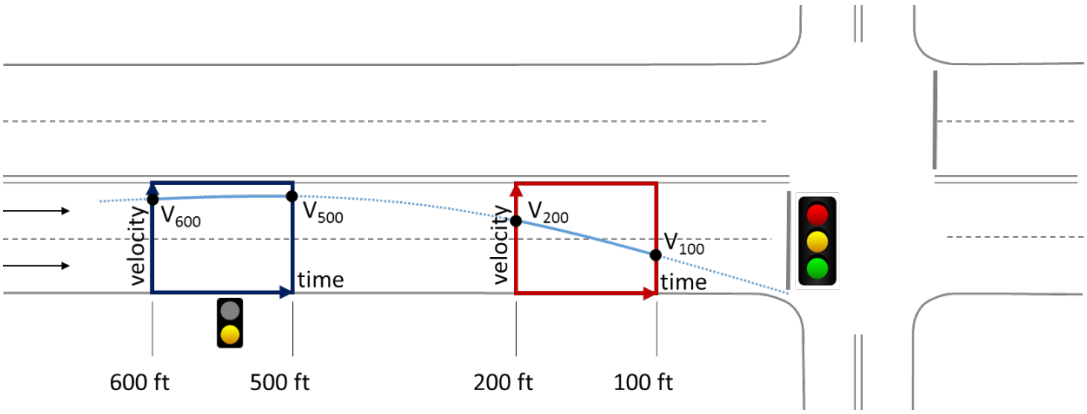

Figure 6.2 Illustration of calculating the acceleration rate

Figure 6.2 shows an idealized example. The blue dotted curve in figure 6.2 is a hypothesized speed profile over time and distance. The instantaneous speeds at a distance of 600 ft, 500 ft, 200 ft, and 100 ft are used to calculate the average acceleration rates in the 500-600 ft and 100-200 ft segments, respectively. It is assumed that the acceleration rate does not change within the segment.

The first segment is shown as a red rectangle and the second segment is shown as a dark blue rectangle. The x axis on each rectangle represents the time to the stop-line and the y axis represents instantaneous speed. The acceleration for the first segment (e.g., $a_{200\text{-}100}$) and the acceleration for the second segment ($a_{600\text{-}500}$) are calculated using eq. (6.8) and eq. (6.9), respectively.

$$a_{200-100} = \frac{V_{200} - V_{100}}{t_{200} - t_{100}} \tag{6.8}$$

$$a_{600-500} = \frac{V_{600} - V_{500}}{t_{600} - t_{500}} \tag{6.9}$$

The acceleration rate ($a_{200\text{-}100}$) in the first segment is used to reflect the driver's acceleration behavior in response to the amber signal phase. The acceleration rate in the second segment ($a_{600\text{-}500}$) is used to reflect the driver's acceleration behavior in response to the AWS flashers.

Figure 6.3 (a) and figure 6.3 (b) show drivers' acceleration distributions at the first segment and the second segment, respectively. These figures were developed using data from the SB State Street site. It was found that 16.4% of vehicles in the second segment accelerate after the onset of amber. This also means that the remaining 83.6% of vehicles decelerate after the onset of amber. The percentage of acceleration vehicles in the first segment was comparatively smaller at 8.8%.

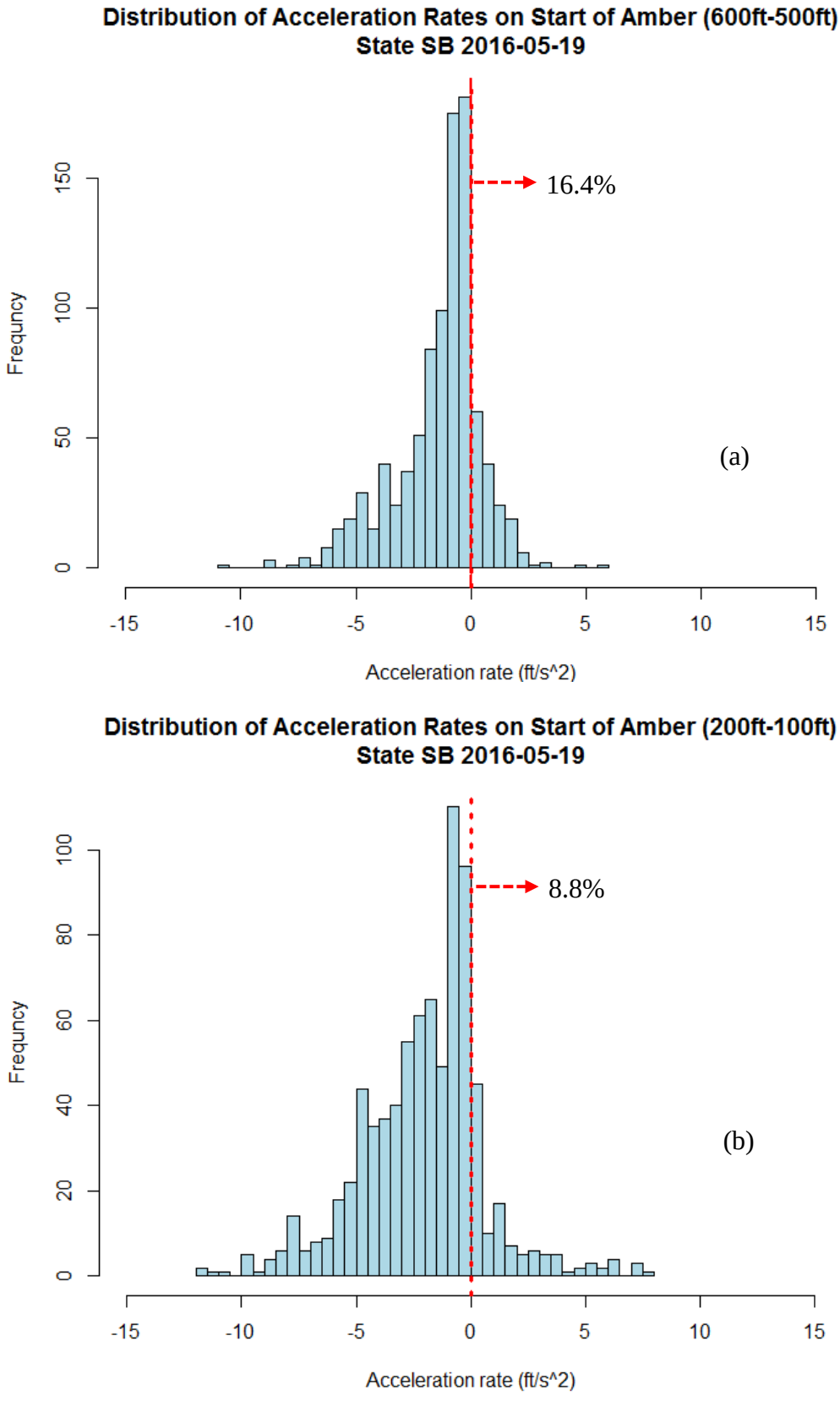

Figure 6.3 Example of the acceleration rate distribution at (a) 600 ft -500 ft, (b) 200 ft -100 ft

Note that for most of vehicles (94%) at this site, their acceleration/deceleration rates in the first segment are within ±7 ft/s^2. This range is considered a "comfortable" acceleration or deceleration rate (24). These results indicate that drivers are complying with the amber signal, given the hypothesis that the "uncomfortable" acceleration (i.e., acceleration rate higher than 7 ft/s^2) is more likely to be involved in red-light running events.

In the same manner, the vehicles' acceleration behavior at the other 8 sites were also analyzed. Table 6.2 shows the total number of cycles analyzed and the percent of vehicles conducting acceleration behavior after the start of amber for each site.

Table 6.2 Vehicle acceleration rate on start of amber

Site	No. of cyc.	No. of veh.	Acceleration rate $a_{200\text{-}100}$ in the first segment (200-100 ft)		Acceleration rate $a_{600\text{-}500}$ in the second segment (600-500 ft)	
			Comfortable ($0<a_{200\text{-}100}<7$ ft/s^2)	Uncomfortable (>7 ft/s^2)	Comfortable ($0<a_{600\text{-}500}<7$ ft/s^2)	Uncomfortable (>7 ft/s^2)
1	382	916	8.6%	0	6.5%	0
2	1078	3977	12.0%	2.6%	23.3%	0
3	1094	3045	8.3%	0.5%	16.4%	0
4	773	2162	10.8%	0	16.7%	0
5	438	2746	4.1%	0	12.5%	0
6	519	1255	3.2%	0	10.7%	0
7	483	2299	4.1%	0	9.5%	0
8	1236	4771	5.3%	0	18.9%	0.40%
9	718	2719	13.8%	1.1%	16.3%	0.20%
Ave			7.86%	0.47%	14.53%	0.07%

As can be seen in table 6.2, the ratio of the comfortable deceleration rate in the first and second segments can be calculated by (1- $a_{200\text{-}100}$)*100% and (1- $a_{600\text{-}500}$)*100%, respectively. On average, 8.32% vehicles accelerated in the 200-100 ft segment. This indicated that about 92% vehicles decelerated when close to the stop-line (i.e., 200-100 ft segment).On average, 14.53% vehicles accelerated in the 600-500 ft segment. This indicated that about 85% vehicles decelerated when passed the AWS (i.e., 600-500 ft segment).

6.3.2 Driving Behavior Following the Activation of the AWS Flasher

In comparison, the deceleration rate after the start of the AWS at the two segments (as shown in figure 6.2) for each site was calculated to indicate how the drivers react to the AWS. The upstream AD sensor data was used to calculate the deceleration rate in the 500-600 ft segment (e.g., where the AWS was located).

As shown in table 6.3, the majority of vehicles chose to decelerate after the warning signal started, and most of the drivers decelerated at a "comfortable" rate. The percentage of vehicles that decelerated or maintained their speed after the onset of the AWS ranged from 56.2% to 83.9%, with an average of 69.7%. The percentage of vehicles that accelerated after the AWS flashers were activated ranged from 4.5% to 20.7%, with an average of 12.5%. Note the rest of the percentage (i.e., besides the acceleration and deceleration) indicated the vehicles that kept their speed when passing through the AWS. These results correlate well to the entrapment results that indicated fewer vehicles were found in the NDOR dilemma zone than would be expected.

Table 6.3 Vehicle deceleration rate after start of AWS

Site	Number of cycles	Number of vehicles	Acceleration/Deceleration rate in 600-500 ft	
			Deceleration ($-7<a_{600-500}<0$ ft/s2)	Acceleration ($0<a_{600-500}<7$ ft/s2)
1	382	916	73.3%	20.7%
2	1078	3977	83.9%	12.6%
3	1094	3045	67.2%	19.3%
4	773	2162	75.4%	14.2%
5	438	2746	56.2%	4.5%
6	519	1255	82.1%	13.6%
7	483	2299	57.9%	5.9%
8	1236	4771	70.8%	14.4%
9	718	2719	60.9%	7.3%
Ave			69.7%	12.5%

6.4 Red-Light Running Rates

Vehicles that enter the intersection at or after the onset of the red signal are defined as red-light runners. Red-light running behavior is an indication that the dilemma zone protection may not be working. In this study, trajectory data was used to identify red-light runners. The steps used are described below, and the logic is shown in the flow chart of figure 6.4.

Step 1: When the amber starts, vehicle IDs and the trajectories of all the vehicles detected by the downstream AD sensor (coverage 0 - 400 ft) are identified.

Step 2: These vehicles are tracked in time and distance to the stop-line. At the same time, the start of the red phase is identified from the TSPI data (see section 3.1.2).

Step 3: If a vehicle proceeds through the stop-line prior to the start of red, it is defined as a compliant proceeding vehicle. If a vehicle stops at or before the stop-line, it is defined as a compliant stopping vehicle.

Step 4: If the red has started and the vehicle's speed at the stop-line is greater than a predefined threshold, it is identified as a non-compliant proceeding vehicle or a red-light runner. If its instantaneous speed is less than the threshold, it is identified as a non-compliant stopping vehicle. In this report, the speed threshold is 10 mph.

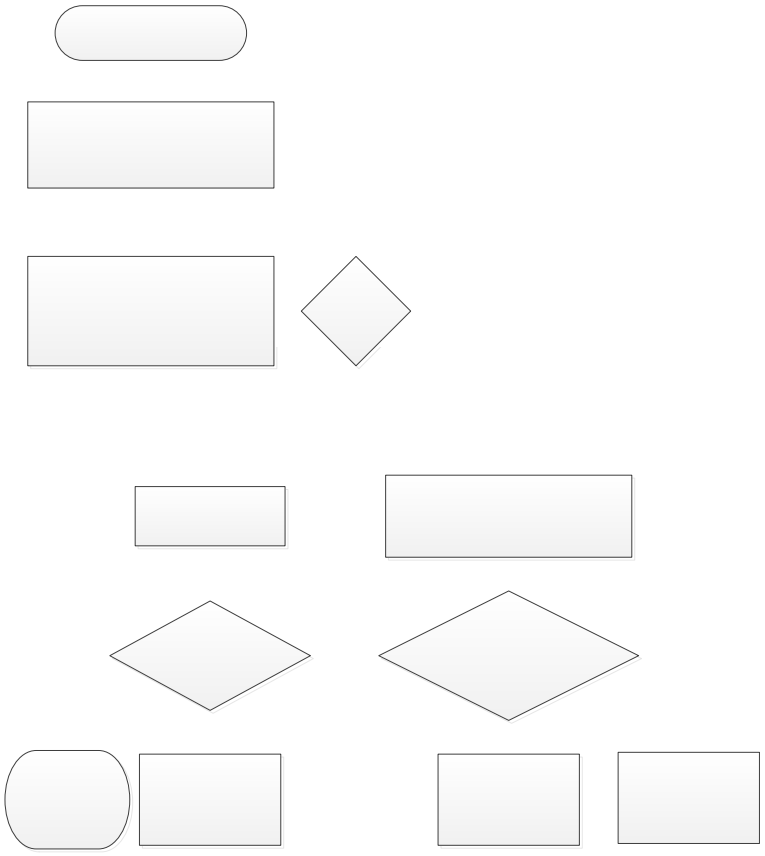

Figure 6.4 Flow chart of determination of red-light running vehicles

The percent of vehicles running the red light at each study site is shown in table 6.4. Note that the number of total detected vehicles *N* and the number of red-light running vehicles n_r is defined in figure 6.4. There are different metrics for measuring red-light running (RLR) activity. Three are used in this report and they are described below.

Table 6.4 Vehicle red-light running rates

Site	No. of Cycles (cyc)	Total Detected Vehicles *N** (veh)	RLR Vehicles n_r (veh)	RLR Metric 1 (%)	RLR Metric 2 (cyc/veh)	RLR Metric 3 (veh/h)
1	789	1427	24	1.7	33	1.4
2	1078	2216	35	1.6	31	1.5
3	1093	2436	46	1.9	24	1.9
4	773	1867	30	1.6	26	1.8
5	838	1743	15	0.9	56	0.8
6	519	1205	17	1.4	31	1.5
7	683	1435	29	2.0	24	1.9
8	572	1133	11	1.0	52	0.9
9	1093	1930	30	1.6	36	1.3

* Vehicles located between AWS signal and stop-line at start of red

RLR metric 1: The first metric is the total red-light running vehicles n_r divided by the total detected vehicles *N*. This is shown in column 4, and this metric ranges from 0.9% to 2.0%,

with an average of 1.5% and a standard deviation of 0.4%. These results indicate that on average, 1.5 out of 100 drivers who find themselves located between the stopping distance (determined by eq. (6.1)) and the stop-line when the signal transitions to amber will choose to run the red-light. It is important to note that the total number of vehicles in the NDOR-defined dilemma zone is much less than what would be expected with the AWS, as described in section 6.2.

RLR metric 2: In this metric, the red-light running vehicles n_r are divided by the number of cycles. It may be seen in column 5 that the value ranges from 24 to 56 cycles per red-light-running (RLR) vehicle, with an average of 35 cyc/RLR-veh and a standard deviation of 12 cyc/RLR-veh. These results indicate that, on average, for every 35 cycles there is one red-light running vehicle.

RLR metric 3: In the third metric, the red-light running vehicles n_r are divided by the period of study time (units in hour). The period of study is found by the product of the number of cycles at the intersection, the time per cycle (e.g., 79 s), and the number of the seconds in an hour. It was found that the values of the RLR metric 3 ranges from 0.8 to 1.9 vehicles per hour, with an average of 1.4 RLR-veh/h and a standard deviation of 0.4 RLR-veh/h. These results indicate that, on average, there are 1.4 red-light runners per hour on each approach in the corridor.

The relatively small amount of red-light running vehicles indicates that drivers, in general, follow the traffic rules at each site. Because there are fewer vehicles in the NDOR defined DZ at the onset of amber, it is hypothesized that RLR is reduced on these approaches. However, the only way to test this hypothesis statistically is to conduct a before-after analysis of an AWS implementation.

6.5 Summary

In summary, this chapter studied the safety performance of the AWS from three aspects of unsafe behavior: 1) the NDOR dilemma zone entrapment, 2) red-light running, and 3) the acceleration rate. The NDOR dilemma zone entrapment rates showed that that the percentage of vehicles in their dilemma zones when the signal changed from green to amber ranged from 8.8% to 39.1%, which was on average 81% smaller than that would have been expected if the NDOR AWS was not installed. The lower than expected number of vehicles in their dilemma zones at the onset of amber was an indication that the NDOR AWS devices increased the inclination of drivers to stop when they saw the warning devices flashing before the onset of amber.

The accelerating and decelerating behavior toward the amber signal shows that, for most of the vehicles (94%), the acceleration/deceleration rates close to the stop-line were within the comfortable range (i.e., ± 7 ft/s^2). On average, 92.1% of the vehicles (with a standard deviation of 3.9%) decelerated when close to the stop-line after the start of amber. This is a good indication of the driver's complying with the onset of amber, given the hypothesis that the "uncomfortable" acceleration (i.e., acceleration rate higher than 7 ft/s^2) was more likely to be involved in red-light running events.

The accelerating and decelerating behavior in relation to the activation of the AWS shows that the percentage of vehicles that decelerate or maintain their speed after the onset of the AWS ranges from 56.2% to 83.9%, with an average of 69.7%. The percentage of vehicles that conduct accelerating behavior after the onset of AWS is from 4.5% to 20.7%, with an average of 12.5%. The majority (82.2%) of vehicles accelerate or decelerate in a "comfortable" manner after the start of AWS.

The red-light running study showed that the percentage of a red-light running occurrence ranges from 0.9% to 2.0%, with an average of 1.5% and a standard deviation of 0.4%. Most of the vehicles analyzed were in compliance and stopped safety. The large amount of compliant vehicles indicates that vehicles followed the traffic rules in this corridor.

Chapter 7 Microsimulation Analysis

The Federal Highway Administration (FHWA) has suggested microsimulation as a viable approach to safety analysis for: 1) new facilities, and 2) in situations where there is not enough crash data to allow for reliable statistical analysis. As noted by the FHWA, the use of microsimulation circumvents the need to wait for “abnormally high” crashes to actually occur and allows assessments of hypothetical alternatives (26).

This chapter utilized the Surrogate Safety Assessment Model (SSAM), a tool developed by the FHWA that combines microsimulation and automated conflict analysis, to assess the AWS in Grand Island. SSAM analyzes vehicle trajectory files, produced by microsimulation models such as VISSIM, to identify and classify conflict events on the basis of conflict angle and a variety of surrogate safety measures, including post-encroachment time and time-to-collision, which are considered "valid and reliable precursors of actual crashes" (26).

7.1 Traffic Microsimulation: VISSIM

VISSIM is a discrete, stochastic time step-based microscopic traffic simulation model with driver-vehicle-units modeled as single entities. It was developed by Planung Transport Verkehr (PTV) in Germany. The model consists of two distinct components that communicate through an interface. The first component is a traffic simulator that simulates the movement of vehicles and generates output. The second component is a signal state generator that determines and updates the signal status using detector information from the traffic simulator on a discrete time step basis. The input data required for VISSIM includes network geometry, traffic demands, phase assignments, signal control timing plans, vehicle speed distributions, and the acceleration and deceleration characteristics of vehicles. VISSIM allows the user to model traffic signals using different control types, such as pre-timed, an RBC standard signal control emulator (which

can operate in fully actuated, coordinated, or semi-actuated coordinated modes), and vehicle actuated programming (VAP). The model is also capable of producing measures of effectiveness commonly used in the traffic engineering profession, including average delay, queue lengths, and fuel emissions (27).

7.2 Microsimulation Model Development

The Grand Island network was modeled with and without the presence of the AWS. Subsequently, the Grand Island network, with the AWS, is modeled. The AWS is simulated by using a yellow flashing signal that is either on or off. The activation follows the NDOR AWS logic discussed in chapter 2. Figure 7.1 (a) shows the simulation network after the AWS was added. Note that the AWS are included on all locations in the corridor. Figure 7.1 (b) shows a screen shot of the northbound Highway 281 of 13th Street. It can be seen that the lead flash of the AWS is active and the NB through movement signal is green. The AWS begins to flash 7-8 seconds before the through movement green indication begins, as shown in table 3.2. The AWS flasher will stay active during the red phase of the traffic signal, as shown in figure 7.1 (c). Note that modelling on AWS it is not simply a matter of putting a flasher into the network. The reaction of the driver to the flasher also needs to be modeled. The AWS is modeled using a "binary" speed distribution. When the AWS is inactive, the drivers who "see" the flashers will follow one speed distribution, and when it is active they will follow a different speed distribution. It is assumed that all the drivers will "see" and react to the AWS when it is active. This is accomplished by inputting a speed distribution. When the flasher is activated the drivers follow this distribution. The input distribution replicates the observation in the field.

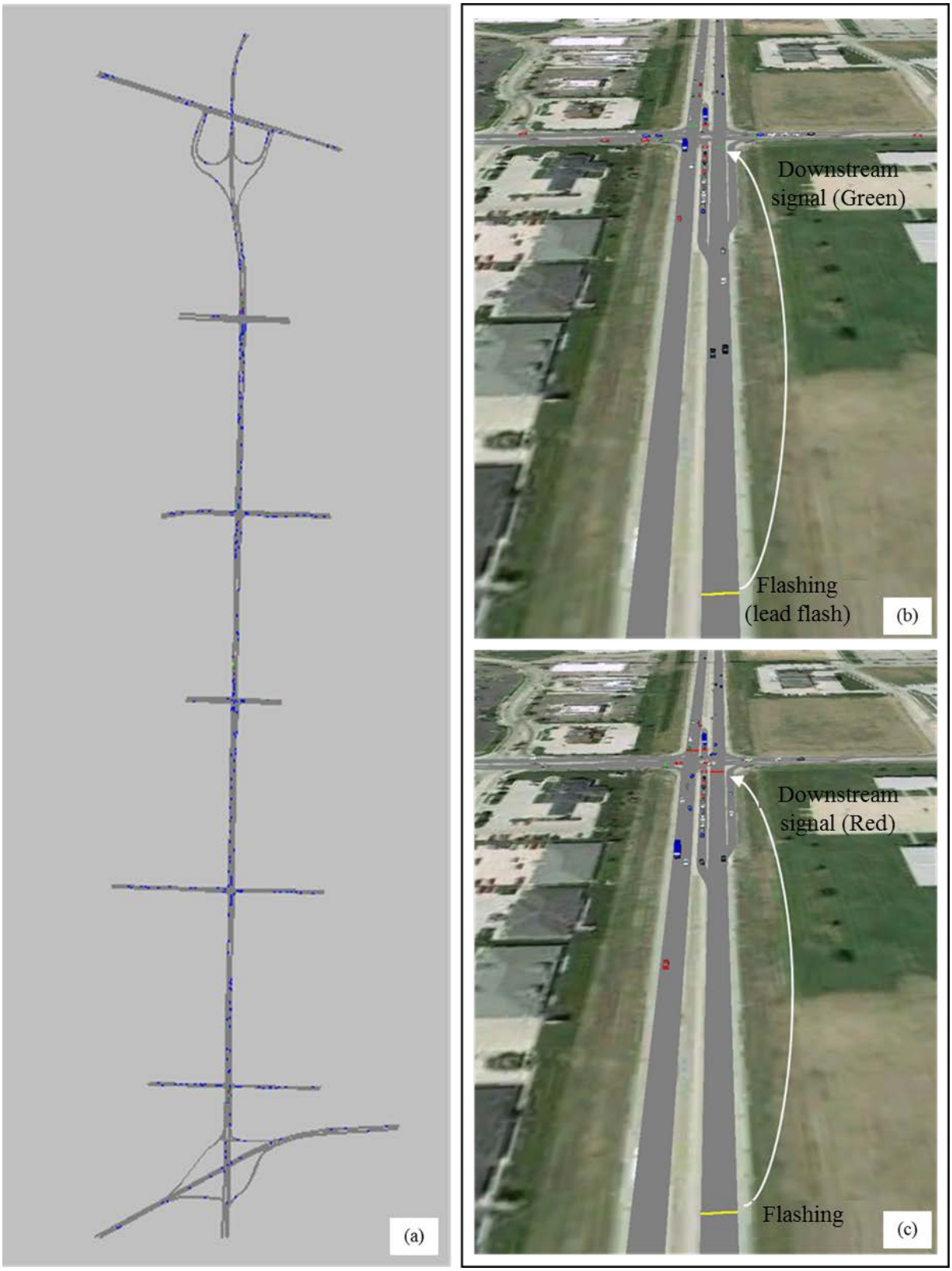

Figure 7.1 Simulation model development

7.2.1 Traffic Demand Input

The traffic demand input was obtained from field data and the signal timing plans were provided by the public works department of Grand Island. This included phase assignments, the maximum and minimum green time allocations per phase, detector length and location, passage times, and all detector call options for each intersection along the study corridor. The basic information of the simulation input is listed in table 7.1.

These inputs were first used to model the base situation (i.e., without the actuated advance warning system). Secondly, an alternative model with the NDOR AWS system logic, as described earlier, was modeled. The results were then compared.

Table 7.1 Simulation input of traffic conditions for each intersection

Category	Parameter	Capital St		State St		13th St		Faidley St		Old Potash St	
		Main Rd	Cross Rd	Main Rd	Cross Rd	Main Rd	Cross Rd	Main Rd	Cross Rd	Main Rd	Cross Rd
Geometry	Through/right-turn lanes	3	1	3	1	3	1	3	1	3	1
	Exclusive left-turn lanes	1	1	1	1	1	1	1	1	1	1
	Lane width (ft)	12	12	12	12	12	12	12	12	12	12
	Grade (%)	0	0	0	0	0	0	0	0	0	0
Traffic	Through + right volume (veh/h)	440	374	658	639	817	427	824	352	961	293
	Turning volume (%)	7	13	20	14	26	16	24	27	12	25

Table 7.2 Simulation input of traffic conditions for each intersection (cont.d)

	Approach speed (trailer loc.) (mph)	39	-	37	-	40	-	36	-	36	-
	Heavy vehicles (%)	7.7%	-	9.1%	-	10.2%	-	11.7%	-	9.0%	-
	Pedestrians	none	none	none	none	none	none	none	none	none	none
AWS	Advance flasher location (ft)	507(SB) 495(NB)	-	550(SB) 519(NB)	-	554(SB) 535(NB)	-	528(SB) 528(NB)	-	526(SB)	-
	Lead flash (s)	7	-	8	-	7	-	7	-	7	-
Signal Timing	Min green (s)	10	10	8	10	10	10	18	15	10	10
	Max green (s)	20	30	20	30	20	30	39	24	27	27
	Yellow (s)	4.5	3.5	4.5	4.0	4.5	4.0	4.5	3.5	4.5	3.5
	All-red (s)	1.5	1.0	1.5	1.0	1.5	1.0	2.0	1.5	2.0	1.5
	Passage time (s)	0	2	0	4	0	3	0	2	0	2

In VISSIM, the input of the desired speed distribution is the speed at which vehicles will travel when there is little or no impedance. The user first identifies the shape of the speed distribution as well as the minimum and maximum speed values. The speed limit for Highway 281 and the minor approaches are 45 mph and 30 mph, respectively. It was observed that the operational speed ranges between 5 mph above and 5 mph below the speed limit. Therefore, a range of 40 to 50 mph was used to model for vehicles on the main highway (281), and a range of 25 to 35 mph was used to model vehicles on the minor approaches. At the location of the AWS, another desired speed distribution is modeled to allow for unknown drivers' responses (whether increased or decreased speeds) as identified by McCoy and Pesti. Here, a normal distribution is used within the range of 35 to 55 mph and 5 to 10 mph, respectively.

7.2.2 Signal Timing

The signal timing for the 5 coordinated intersections are shown in figure 7.2. SG22 represents the signal group for the northbound AWS timing, and SG 62 represents the signal group for the southbound AWS timing. As can be seen, the SG 22 phase and the SG 62 phase are programmed to be coordinated with phase 2 (i.e., northbound through movement) and phase 6 (i.e., southbound through movement), respectively. The AWS flashers are programmed to begin flashing 7 to 8 seconds prior to the start of the amber of phase 2 (NB) and phase 6 (SB). The AWS flashers are programmed to end simultaneously with the end of phase 2 (NB) and phase 6 (SB). The signal control logic for the AWS flashers and the signal controllers are coded in VisVAP. Details can be found in Appendix D.

Figure 7.2 Actuated signal timing for the 5 coordinated intersections

Both VISSIM models (e.g., with AWS active and without) were simulated for 1 hour, which included a warm-up period of 10 minutes so that the system could reach steady-state. Each alternative was modeled with the same arrival flow pattern, and 20 random seeds were selected for each model. The model input and output logic is shown in figure 7.3.

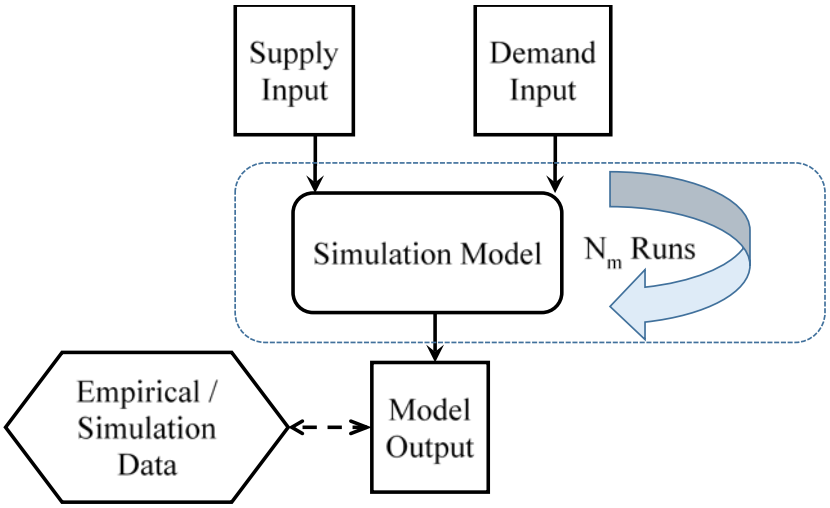

Figure 7.3 Simulation model input and output logic

7.2.3 Traffic Volume Output

A key check of any simulation is to ensure the output matches the observed values. In this report, an important metric was the number of vehicles that are processed by the simulation system during a specified analysis period. For this study, the number of vehicles of through traffic in each simulation was output, and it was compared with the through volumes that were input. The goal was to have the difference in input and output be as small as possible. The results are shown in table 7.3. As can be seen, the output volumes were very close to the input volumes as evident by the fact that their absolute differences range from 0.7% to 5.2%, with an average of 0.8% and standard deviation of 3.7%. It was concluded that simulation network adequately modeled vehicle throughput.

Table 7.3 Throughput of traffic volume comparison

Site	Input volume of through traffic (veh/h)	Output volume of through traffic (veh/h)	Diff. (veh/h)	Diff. (percent)
1	447	470	-23	-5.2
2	369	355	14	3.8
3	588	559	29	4.9
4	508	523	-15	-2.9
5	702	717	-15	-2.1
6	522	529	-7	-1.3
7	586	557	29	5.0
8	673	687	-14	-2.1
9	749	744	5	0.7

7.3 Traffic Conflict Analysis

The number of traffic conflicts is a common non-accident surrogate safety analysis measure. This has been used by highway engineers when direct crash analyses are not appropriate. In 1977, Hyden (28) defined traffic conflict as “an observable situation in which two or more road users approach each other in space and time to such an extent that there is a risk of collision if their movements remained unchanged.” The measure most often used for the severity of the traffic conflict between vehicles is time-to-collision (TTC). The smaller the TTC, the more severe the conflict.

TTC is the projected time for two vehicles to collide if they continue at their present speed and stay on the same path. The potential benefits of using the AWS in the test bed can be shown by comparing the frequency of conflicts (i.e., TTC counts) and the severity of the conflicts (i.e., distribution of TTC) under both the base (i.e., without AWS) and AWS situations. The TTC was modeled using FHWA's SSAM software. The vehicle trajectory output from the VISSM simulations were input into SSAM and the conflict metric output. In this chapter, a maximum threshold TTC value of 3 seconds is used to identify conflicts that might indicate a safety hazard (23). Conflict data and surrogate safety measures for vehicle-to-vehicle interactions with less than the user-defined threshold were output and analyzed for all of the nine test sites. Only through traffic in the N-S direction was analyzed over the 1-hour simulation period.

The TTC counts are shown in table 7.4. Based on the conflicting angle of the two vehicles, three types of conflict in the SSAM results were examined: rear-end conflict, lane-change conflict, and crossing conflict.

Table 7.4 Conflict frequency by conflict type

	All Conflict Types	Rear-End	Lane-Change	Crossing
Without AWS	4405	3674	637	94
With AWS	2251	1643	562	46
Percentage Reduction	49%	55%	12%	51%

It can be seen from table 7.4 that there is a reduction in all the three conflict types when the NDOR AWS logic was implemented. On average, there are 55%, 12%, and 51% reductions in rear-end, lane-change, and crossing conflicts, respectively, for all nine study sites. This is not surprising because the AWS reduces the number of vehicles in the NDOR-defined dilemma zone and hence reduces the number of conflicts.

An alternative way to check the severity of the conflicts in the corridor is to examine the distribution of TTC. In general, the smaller the TTC, the more hazardous the conflict. The extreme case is that the TTC equals zero when the two subject vehicles collide with each other. VISSIM will never simulate a crash, so the TTC will always be greater than zero. Figure 7.4 shows the TTC distribution for both the AWF inactive regime and the AWF active regime.

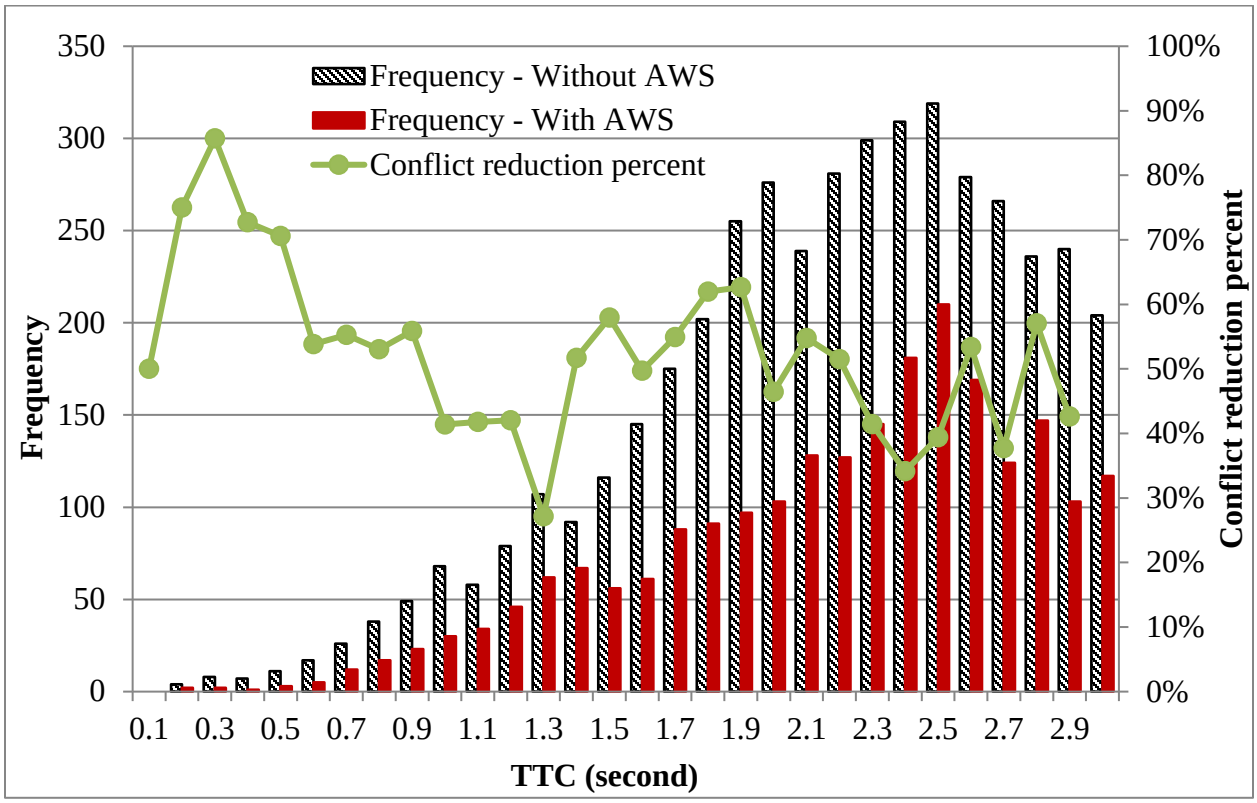

Figure 7.4 Simulation result of TTC frequency distributions with and without AWS on site

The means of the TTC are 2.15 seconds and 2.18 seconds, and the standard deviations of the TTC are 0.57 seconds and 0.57 seconds for the AWS inactive and active regimes, respectively. As seen in figure 7.4, the frequency of conflict occurrence under the AWS scenario is much less than that without the AWS. The frequency distribution (indicated in the histogram) shows that there are approximately 50% fewer conflicts when the AWS is implemented in the corridor. Moreover, conflict reduction from the AWS inactive regime to the AWS active regime, as indicated in the green line in figure 7.4, indicates that the AWS helps to reduce the severity conflict (e.g., TTC<1 second). This surrogate measure indicates that, in terms of the number of conflicts, AWS helps to reduce the conflict occurrence, which makes the corridor safer.

7.4 Summary

This chapter developed a simulation model to study the potential conflicts along the Grand Island test bed. The AWS was simulated by using a flash yellow signal. The signal timing plan and the actuated signal control logic was coded in VisVAP. The AWS inactive regime was compared to the AWS active regime. Traffic conflicts were analyzed using the SSAM software, and the TTC was used as the surrogate indicator of safety.

On average, it was estimated that there were 55%, 12%, and 51% fewer rear-end, lane-change, and crossing conflicts, respectively, for all nine study sites when the AWS system was applied. The frequency distribution also shows an average of an approximate 50% reduction in total traffic conflicts when the AWS was implemented in the system. It suggests that having the AWS system in place with signal coordination improves safety by removing conflicts.

Chapter 8 Conclusions and Recommendations

The objective for this project was to study the cost and benefits of deploying AWS on high speed arterials operating in a coordinated mode and to develop guidelines for their implementation. The guidelines are used to determine whether to remove the existing AWS at corridors or to install AWS at coordinated intersections, and under what conditions they can be used.

Field data was collected by using two Wavetronix ADs and two cameras, for upstream and downstream traffic, and one Wavetronix HD. The equipment was mounted on a trailer. The advanced sensor detected the speed of the approaching vehicle and tracked it through-out the intersection. The camera recorded traffic in case there was a need for verification. The HD sensor was used to perform volume and classification of these vehicles. The signal timing was recorded by a Raspberry PI sensor system that was located in the traffic cabinet. The intersection signal and the AWS flashing time was used to match the time stamp of the data and synchronize them. All data was saved on the on-board computer in the trailer cabinet.

A detailed operational analysis was performed to evaluate the platoon dispersion along the coordinated corridor. A detailed safety analysis was conducted using speed profiles. Three areas were examined: dilemma zone entrapments, acceleration rates after the AWS system becomes active, and red-light running rates. A detailed microsimulation was developed to estimate traffic conflicts when: 1) the AWS was active, and 2) the AWS was not active. The data included traffic counts and vehicle classification, traffic signals and AWS time stamps, approach speed as a function of time and distance, dilemma zone entrapment rates, red light running rates, and number of conflicts.

The results showed that the safety effect of AWS in a coordinated system is positive. These results are specified below.

1) The dilemma zone entrapment rates show that that the percentage of vehicles in their dilemma zones when the signal changed from green to amber was, on average, 81% smaller than what would have been expected if the NDOR AWS was not installed. The lower than expected number of vehicles in their dilemma zones was an indication that the NDOR AWS devices increased the inclination of drivers to stop as they saw the AWS flashing before the onset of amber.
2) The accelerating and decelerating behavior of drivers within 200 feet of the intersection during the amber interval showed that 94% of the acceleration/deceleration rates were within the comfortable range (i.e., ±7 ft/s^2). On average, 92.1% of the vehicles (with a standard deviation of 3.9%) decelerated when close to the stop-line after the start of amber. This was a good indication of the vehicle's compliance with the onset of amber, given the hypothesis that the "uncomfortable" acceleration (i.e., acceleration rate higher than 7 ft/s^2) was more likely to be involved in red-light running events.
3) The red-light running study shows that the percentage of red-light running occurrence is from 0.9% to 2.0%, with an average of 1.5% and a standard deviation of 0.4%. Most of the vehicles chose to stop and did so in a safe and legal manner. The large amount of compliant vehicles indicates that drivers follow the traffic rules at each site. It is hypothesized that the AWS lead to the low red-light running rates.
4) The conflict analysis results from the simulation showed that, on average, there are 55%, 12%, and 51% lower rear-end, lane-change, and crossing conflicts, respectively,

for all nine study sites when the AWS system was applied. The frequency distribution also showed an average of about a 50% reduction in the total traffic conflict when the AWS was included in the system. This surrogate measure indicates that the AWS helped to reduce the number of severity conflicts. It is hypothesized that having an AWS system in a corridor with signal coordination improves safety. It is unclear how these results would translate geographically (e.g., New York or California).

Based on the analyses of the results, it is determined that AWS has a positive effect on safety in the US 281 corridor and should be considered at other high-speed signalized intersections or corridors.

The guidelines regarding installation or removal of the NDOR AWS on the state highway system should be in accordance with the NDOR previous report by McCoy and Pesti in 2002 (1). However, because the installation of the AWS should be site specific, a simulation study at the site would be beneficial.

References

1. McCoy, P. T., and G. Pesti, 2002. Advance Detection on High-Speed Signalized Intersection Approaches. Report No. SPR-PL-1(035) P525. Department of Civil Engineering, University of Nebraska-Lincoln, NE.

2. Messer, C.J, S.R. Sunkari, H.A. Charara, and R.T. Parker, 2004. Design and Installation Guidelines for Advance Warning Systems for End-of-Green Phase at High-Speed Traffic Signals. Report FHWA/TX-04/0-4260-4. FHWA, U.S. Department of Transportation.

3. Bonneson, J., D. Middleton, K. Zimmerman, H. Charara, and M. Abbas, 2002. Development and Evaluation of a Detection-Control System for Rural Intersections. TTI Research Report TX-02/4022-1. Texas Transportation Institute, College Station, TX.

4. Knodler, M. A., and D. S. Hurwitz, 2009. An Evaluation of Dilemma Zone Protection Practices for Signalized Intersection Control. Report No. 2009-6. University of Massachusetts Transportation Center.

5. Appiah, J., B. Naik, R. Wojtal and L. R. Rilett. 2011. Safety Effectiveness of Actuated Advance Warning Systems. Transportation Research Record: Journal of the Transportation Research Board, No. 2250: pp. 19-24.

6. Eck, R.W., and Z.A. Sabra, 1985. Active Advance Warning Signs at High-Speed Signalized Intersections: A Survey of Practice (Abridgement). Transportation Research Record: Journal of the Transportation Research Board, No. 1010: pp. 62-64.

7. Gibby, A.R., S.P. Washington, and T.C. Ferrara, 1992. Evaluation of High-Speed Isolated Signalized Intersections in California. Transportation Research Record: Journal of the Transportation Research Board, No. 1376: pp. 45-56.

8. Klugman, A., B. Boje, and M. Belrose, 1992. A Study of the Use and Operation of Advance Warning Flashers at Signalized Intersections. Report MN/RC-93/01. Minnesota Department of Transportation, Saint Paul, MN.

9. Agent, K.R., and J.G. Pigman, 1994. Evaluation of Change Interval Treatments for Traffic Signals at High-Speed Intersections. Report KTC-94-26. Kentucky Transportation Center, Lexington, KY.

10. Sayed, T., V. Homoyaoun, and F. Rodriquez, 1999. Advance Warning Flashers, Do They Improve Safety? Transportation Research Record: Journal of the Transportation Research Board, No. 1692: pp. 30-38.

11. Farraher, B.A., B.R. Wenholzer, and M.P. Kowski, 1999. The Effect of Advance Warning Flashers on Red-Light-Running–A Study Using Motion Imaging Recording System Technology at Trunk Highway 169 and Pioneer Trail in Bloomington, Minnesota. Proceedings of the ITE 69th Annual Meeting, Las Vegas, NV.

12. Pant, P.D., and Y. Xie, 1995. Comparative Study of Advance Warning Signs at High-Speed Signalized Intersections. Transportation Research Record: Journal of the Transportation Research Board, No. 1495: pp. 28-35.

13. Sunkari S., C. Messer, and H. Charara. 2005. Performance of advance warning for end of green system for high-speed signalized intersections. Transportation Research Record: Journal of the Transportation Research Board, No. 1925: 176-184.

14. Sharma, A., Rilett, L., Wu, Z., & Wang, S. (2012). Speed Limit Recommendation in Vicinity of Signalized, High-Speed Intersection.

15. Minge, Erik, Jerry Kotzenmacher, and Scott Peterson. Evaluation of non-intrusive technologies for traffic detection. No. MN/RC 2010-36. Minnesota Department of Transportation, Research Services Section, 2010.

16. MAG internal truck travel survey and truck model development study. Cambridge Systematics, Inc. Final Report, 2007. https://www.azmag.gov/Documents/TRANS_2011-02-25_mag-internal-truck-travel-survey-and-truck-model-development-study.pdf. Acccessed on Aug. 20, 2016.

17. Robertson, D.I. TRANSYT: A Traffic Network Study Tool. Road Research Laboratory Report No. RL-253, Grothorne, Berkshire, England, 1969.

18. Yu, L. and M. Van Aerde. Implementing TRANSYT's Macroscopic Platoon Dispersion in Microscopic Traffic Simulation Models. Transportation Research Board of the National Academies, Washington D.C., 1995.

19. Courage, K., C. E. Wallace, and M. A. Hadi. TRANSYT-7F Users Guide. Federal Highway Administration, Washington, D.C., 1991.

20. Tarnoff, P. J., and P. S. Parsonson. Selecting Traffic Signal Control at Individual Intersections, Vol. 1. National Cooperative Highway Research Program Report 233, PRC Engineering, 1981.

21. Yu, L. Real-time Calibration of Platoon Dispersion Model to Optimize the Coordinated Traffic Signal Timing in ATMS Networks. No. PB-99-160046/XAB; SWUTC--99/472840-00044-1. Texas Southern University, Center for Transportation Training and Research, Houston, Texas, 1999.

22. Guebert, A. A., and G. Sparks. Timing Plan Sensitivity to Changes in Platoon Dispersion Settings. Traffic Control Methods. Proceedings of The Fifth NG foundation Conference, Santa Barbara, California, 1990.

23. Naik, Bhaven, and Justice Appiah. Dilemma Zone Protection on High-Speed Arterials. No. 25-1121-0003-055. 2014.

24. Justice Appiah, Laurence Rilett, and Zifeng Wu. Evaluation of NDOR's Actuated Advance Warning Systems, 2011.

25. T.K. Datta, D.D. Perkins, J.I. Taylor, and H.T. Thompson. Accident Surrogates for Use in Analyzing Highway Safety Hazards. Final Report FHWA/RD-82/105. Federal Highway Administration, U.S. Department of Transportation. Washington, D.C. July 1982.

26. Gettman, D., L. Pu, T. Sayed, and S. Shelby. 2008. Surrogate Safety Assessment Model and Validation: Final Report. Report FHWA-HRT-08-051. Turner-Fairbank Highway Research Center, McLean, VA.

27. Ambadipudi, R., P. Dorothy, and R. Kill. 2006. Development and Validation of Large-Scale Microscopic Models. Transportation Research Board, Compendium of Papers CDROM, 85th Annual Meeting, Washington, DC.

28. Hydén, C., and L. Linderholm. The Swedish traffic-conflicts technique. International Calibration Study of Traffic Conflict Techniques. Springer Berlin Heidelberg, 1984. 133-139.

Appendix A: Green Time at Each Site

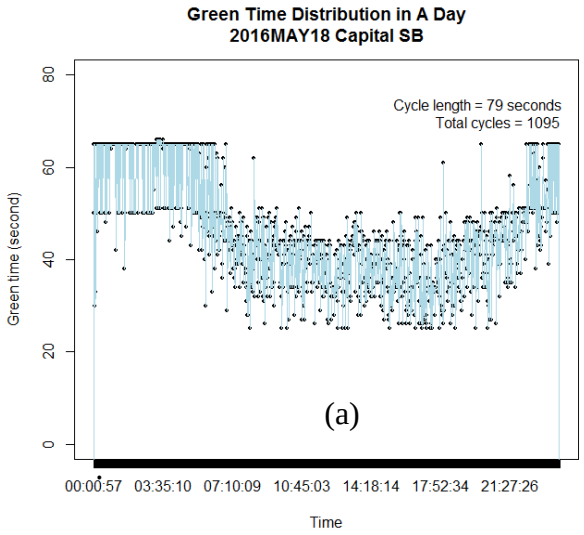

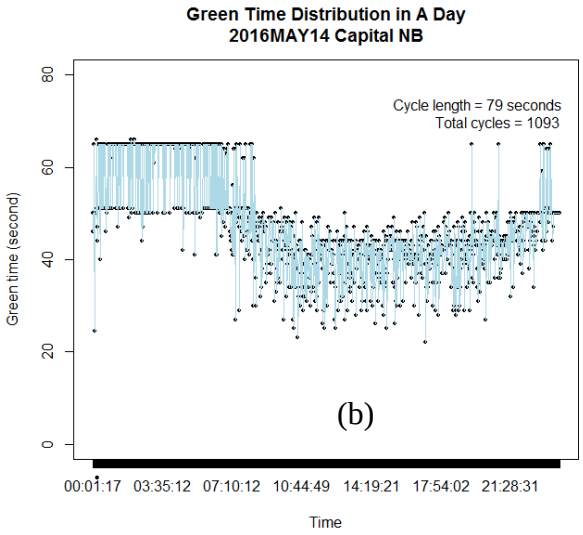

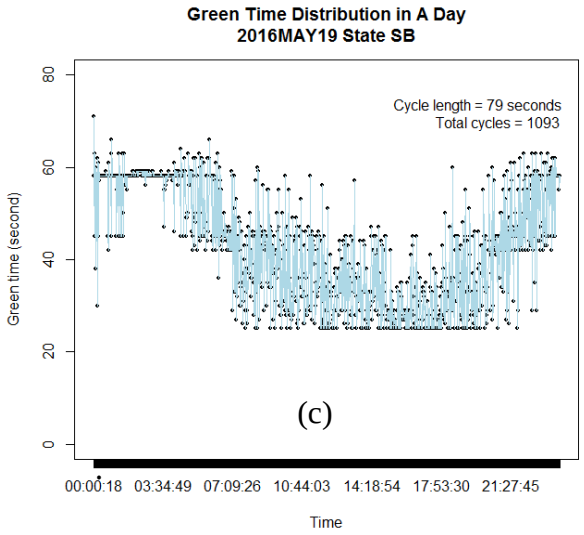

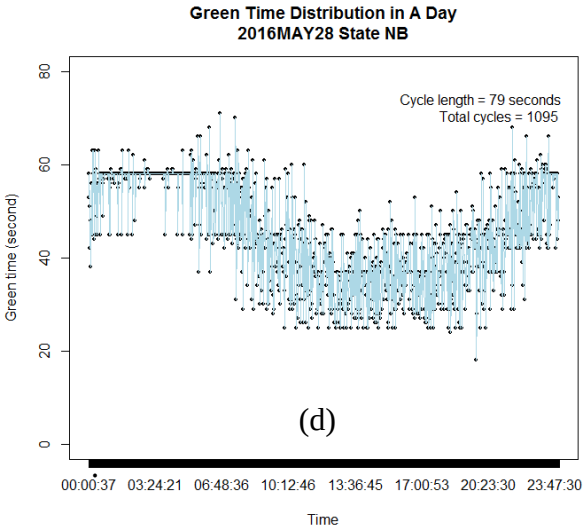

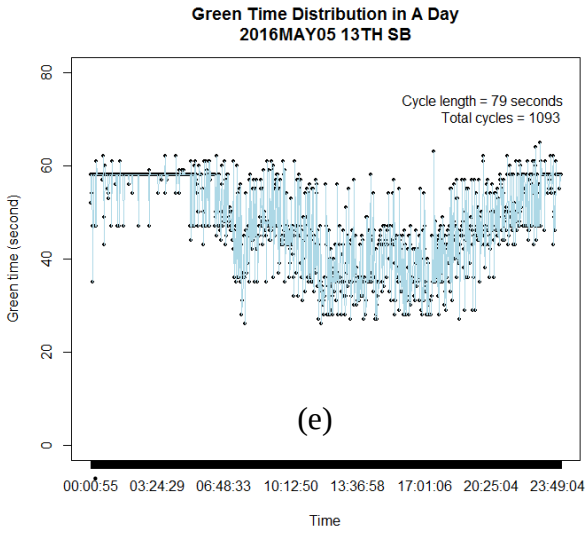
Green Time Distribution in A Day
2016MAY05 13TH SB
Cycle length = 79 seconds
Total cycles = 1093
Green time (second)
0
20
40
60
80
00:00:55
03:24:29
06:48:33
10:12:50
13:36:58
17:01:06
20:25:04
23:49:04
Time

(e)

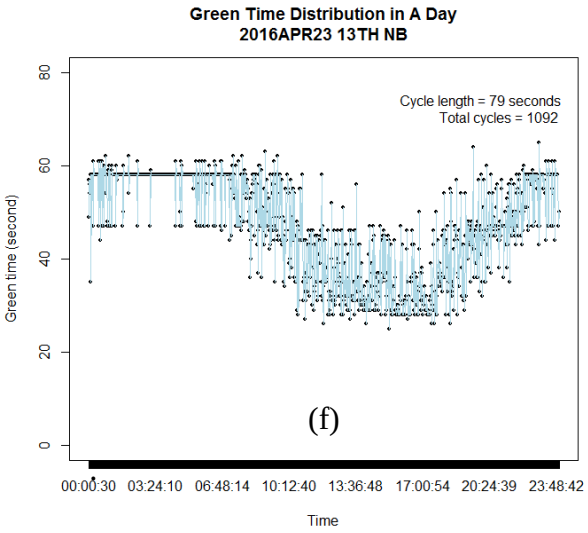
Green Time Distribution in A Day
2016APR23 13TH NB
Cycle length = 79 seconds
Total cycles = 1092
Green time (second)
0
20
40
60
80
00:00:30
03:24:10
06:48:14
10:12:40
13:36:48
17:00:54
20:24:39
23:48:42
Time

(f)

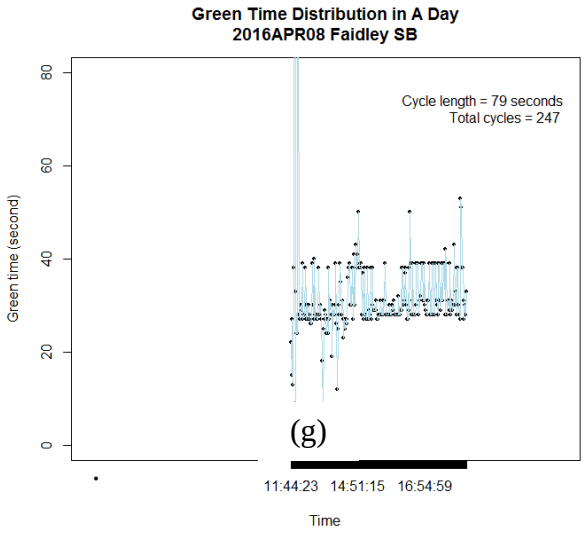
Green Time Distribution in A Day
2016APR08 Faidley SB
Cycle length = 79 seconds
Total cycles = 247
Green time (second)
0
20
40
60
80
11:44:23
14:51:15
16:54:59
Time

(g)

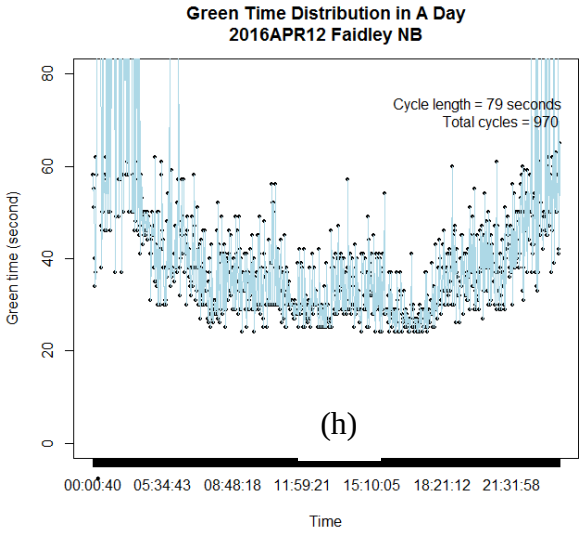
Green Time Distribution in A Day
2016APR12 Faidley NB
Cycle length = 79 seconds
Total cycles = 970
Green time (second)
0
20
40
60
80
00:00:40
05:34:43
08:48:18
11:59:21
15:10:05
18:21:12
21:31:58
Time

(h)

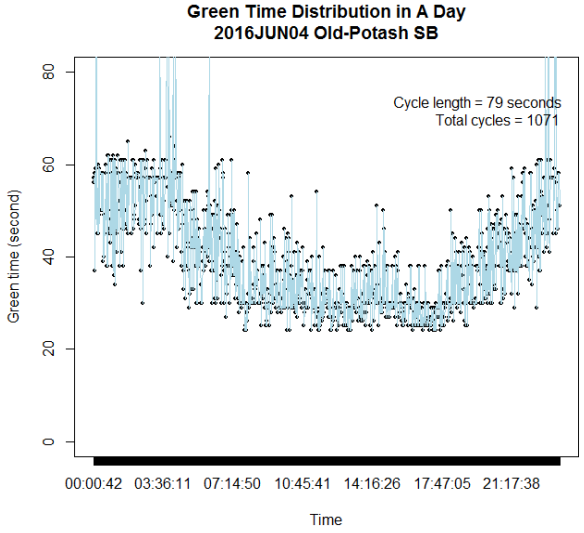
Green Time Distribution in A Day
2016JUN04 Old-Potash SB
Cycle length = 79 seconds
Total cycles = 1071
Green time (second)
0
20
40
60
80
00:00:42
03:36:11
07:14:50
10:45:41
14:16:26
17:47:05
21:17:38
Time

(i)

Appendix B: Vehicle Speed at Each Site

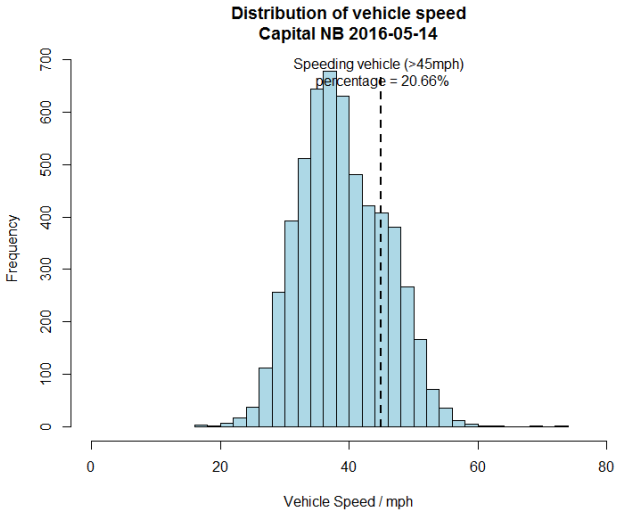

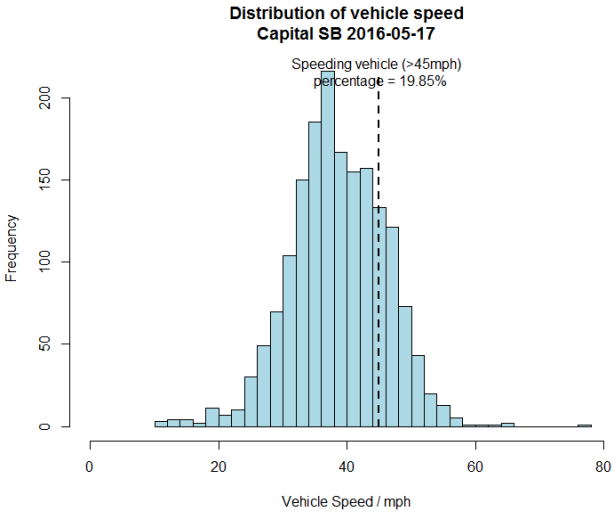

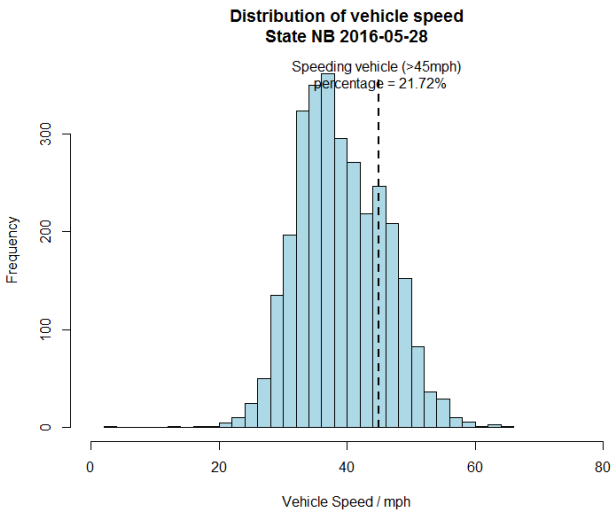

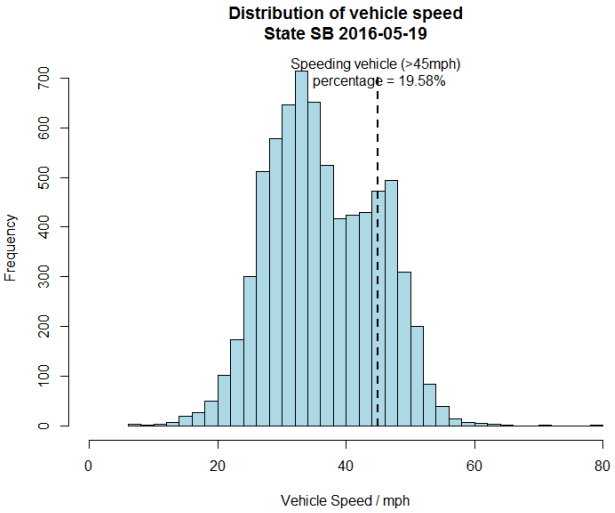

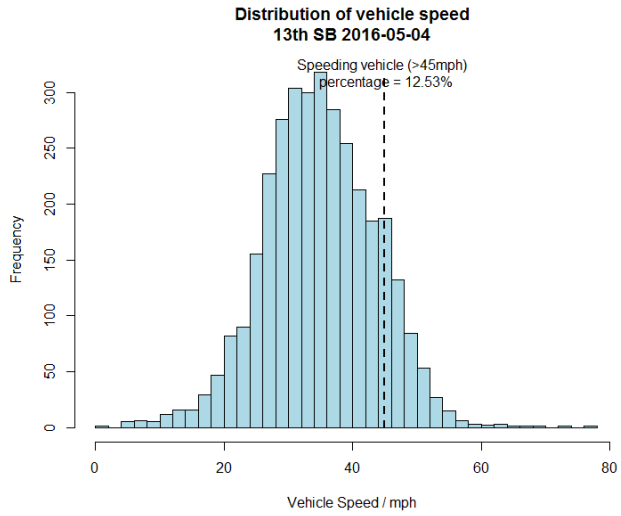
Distribution of vehicle speed
13th SB 2016-05-04
Speeding vehicle (>45mph)
percentage = 12.53%
Frequency
Vehicle Speed / mph

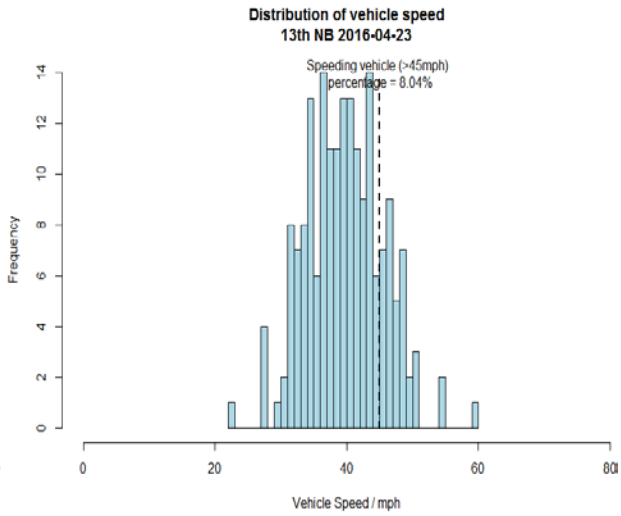
Distribution of vehicle speed
13th NB 2016-04-23
Speeding vehicle (>45mph)
percentage = 8.04%
Frequency
Vehicle Speed / mph

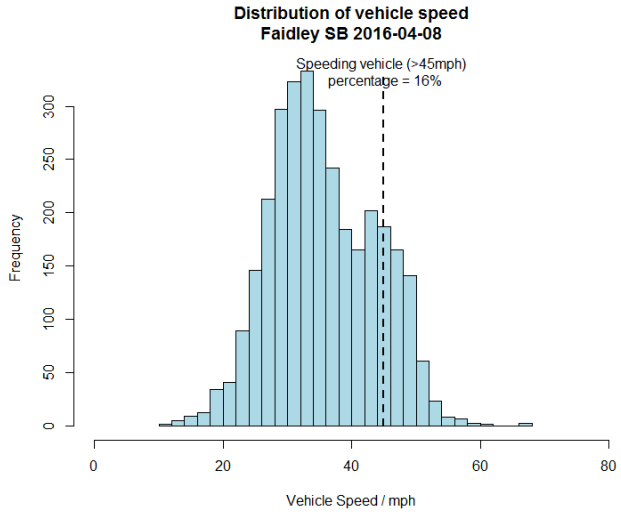
Distribution of vehicle speed
Faidley SB 2016-04-08
Speeding vehicle (>45mph)
percentage = 16%
Frequency
Vehicle Speed / mph

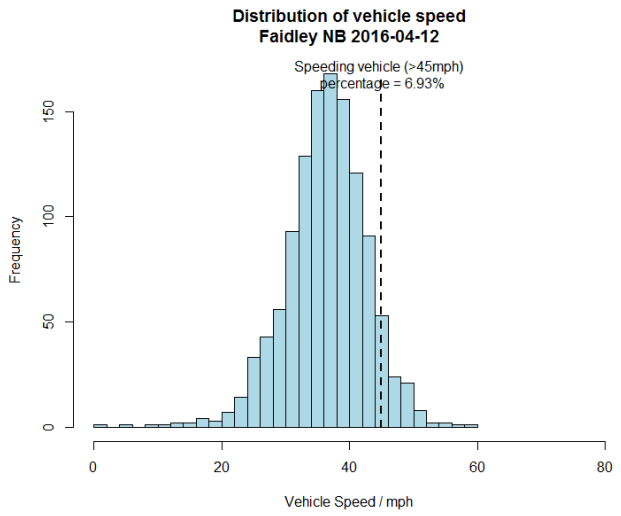
Distribution of vehicle speed
Faidley NB 2016-04-12
Speeding vehicle (>45mph)
percentage = 6.93%
Frequency
Vehicle Speed / mph

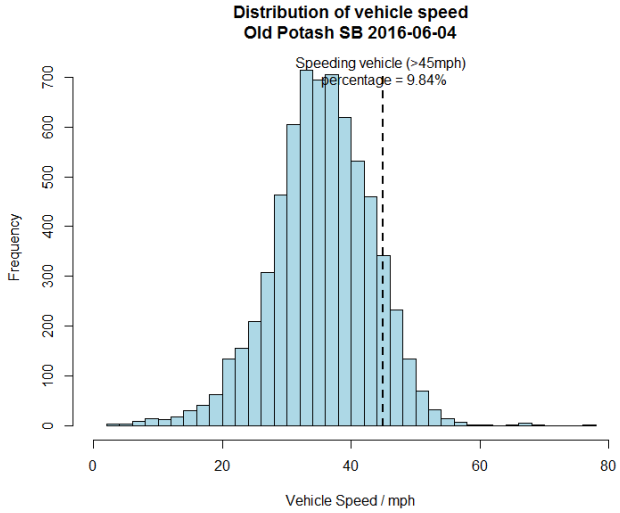
Distribution of vehicle speed
Old Potash SB 2016-06-04
Speeding vehicle (>45mph)
percentage = 9.84%
Frequency
Vehicle Speed / mph

Appendix C: Vehicle Classification at Each Site

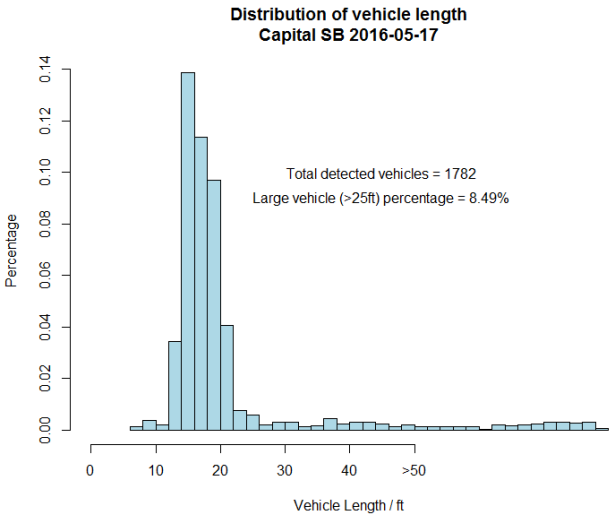

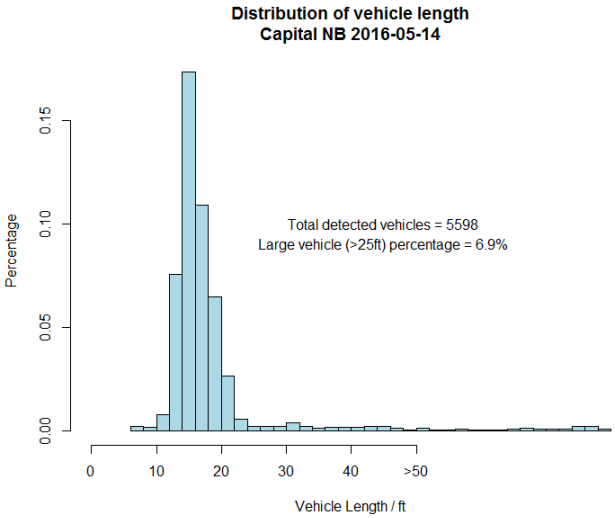

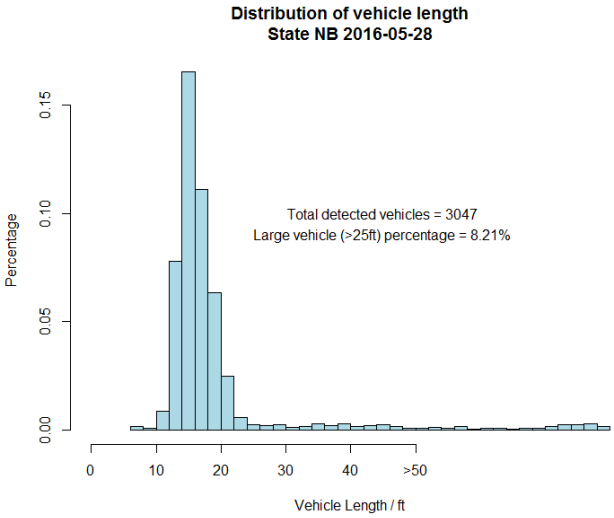

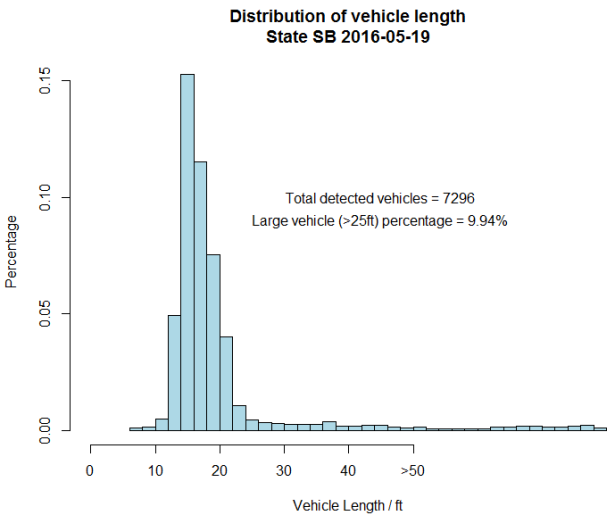

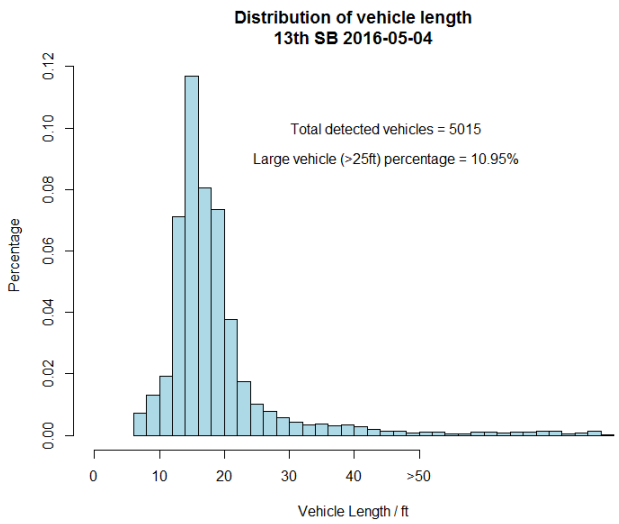
Distribution of vehicle length
13th SB 2016-05-04
Total detected vehicles = 5015
Large vehicle (>25ft) percentage = 10.95%
Percentage
0.00
0.02
0.04
0.06
0.08
0.10
0.12
0
10
20
30
40
>50
Vehicle Length / ft

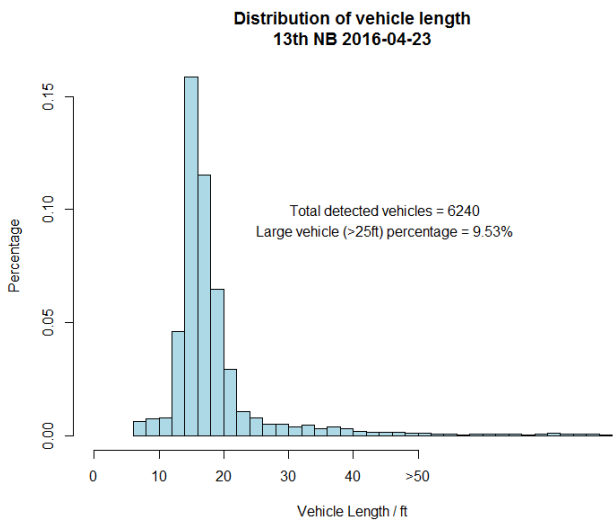
Distribution of vehicle length
13th NB 2016-04-23
Total detected vehicles = 6240
Large vehicle (>25ft) percentage = 9.53%
Percentage
0.00
0.05
0.10
0.15
0
10
20
30
40
>50
Vehicle Length / ft

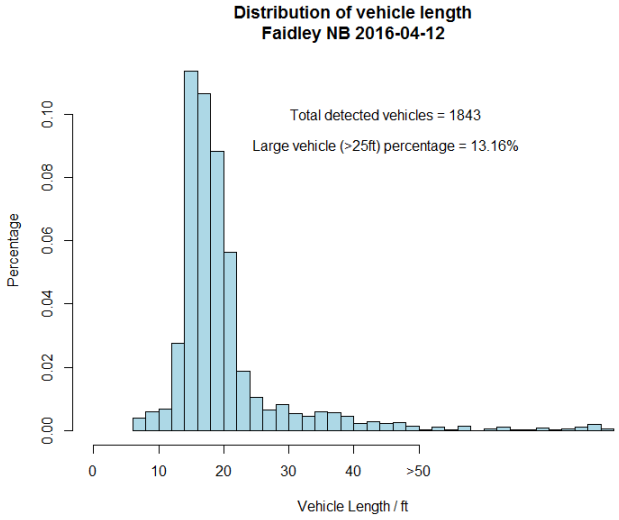
Distribution of vehicle length
Faidley NB 2016-04-12
Total detected vehicles = 1843
Large vehicle (>25ft) percentage = 13.16%
Percentage
0.00
0.02
0.04
0.06
0.08
0.10
0
10
20
30
40
>50
Vehicle Length / ft

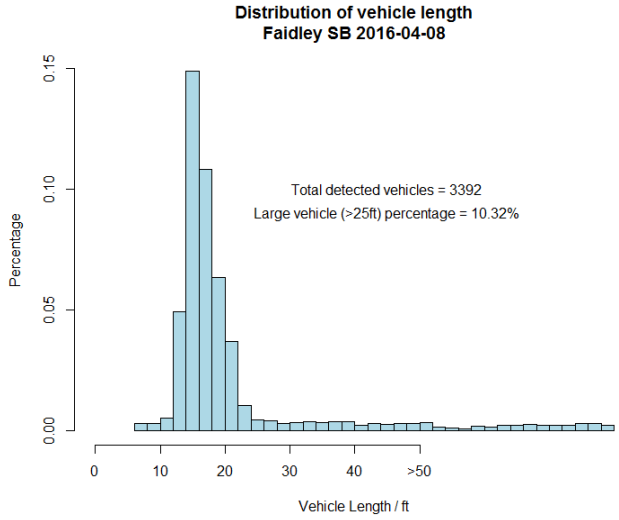
Distribution of vehicle length
Faidley SB 2016-04-08
Total detected vehicles = 3392
Large vehicle (>25ft) percentage = 10.32%
Percentage
0.00
0.05
0.10
0.15
0
10
20
30
40
>50
Vehicle Length / ft

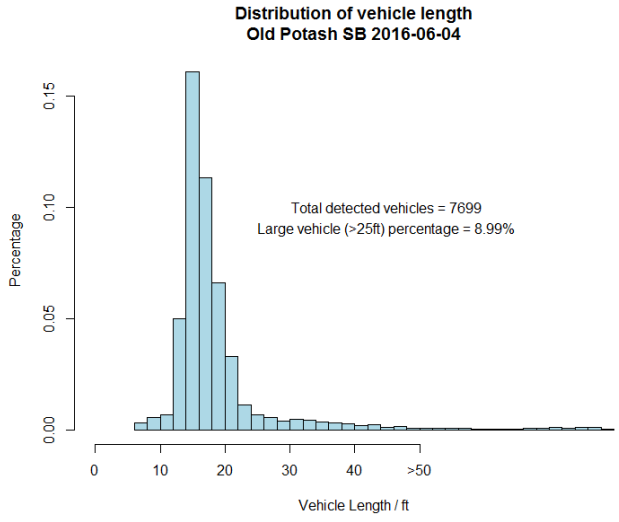
Distribution of vehicle length
Old Potash SB 2016-06-04
Total detected vehicles = 7699
Large vehicle (>25ft) percentage = 8.99%
Percentage
0.00
0.05
0.10
0.15
0
10
20
30
40
>50
Vehicle Length / ft

Appendix D: AWS Signal Programming (VisVAP)

```
PROGRAM W_Faidley_St_and_Hwy_281; /* take Faidley intersection as an example */
VAP_FREQUENCY 1;
CONST
        offset = 0,
         Leadflash = 7;
ARRAY
        tamber[ 8 ] = [3.0, 4.5, 3.0, 3.5, 3.0, 4.5, 3.0, 3.5],
        RedClear[ 8 ] = [0, 2.0, 0, 1.5, 0, 2.0, 0, 1.5],
        MinGreen[ 8 ] = [5, 18, 0, 15, 5, 18, 0, 15],
        MaxGreen[ 8 ] = [5, 34, 0, 20, 8, 34, 0, 20],
        forceoff[ 8 ] = [73.5, 34, 0, 60.5, 73.5, 34, 0, 60.5],
        Recall[ 8 ] = [0, 1, 0, 0, 0, 1, 0, 0],
        Passage[ 8 ] = [1.0, 0, 0, 2, 1.0, 0, 1, 2],
SUBROUTINE master_clock; /* .\master_clock.vv */
        D01S00Z002: t_actual:=t-offset;
        D01S04Z002: IF t_actual<0 THEN
        D01S05Z002: t_actual:=t_actual+tc
            END;
        D01S00Z004: IF t_actual=tc THEN
        D01S04Z004: t_actual:=0
            END
```

```
D01PROG_ENDE: .
/* PARAMETERS DEPENDENT ON SCJ-PROGRAM */
/* EXPRESSIONS */
    call1 := presence(1) or occupancy(1);
    call2 := recall[2];
    call3 := presence(3) or occupancy(3);
    call4 := presence(4) or occupancy(4) or callped4;
    call5 := presence(5) or occupancy(5);
    call6 := recall[6];
    call7 := presence(7) or occupancy(7);
    call8 := presence(8) or occupancy(8) or callped4;
    call15 := call1 or call5;
    call26 := call2 or call6;
    call37 := call3 or call7;
    call48 := call4 or call8;
    gapout1 := headway(1)>Passage[1];
    gapout3 := headway(3)>passage[3];
    gapout4 := headway(4)>Passage[4];
    gapout5 := headway(5)>Passage[5];
    gapout7 := headway(7)>Passage[7];
    gapout8 := headway(8)>passage[8];
    minover1 := t_green(1)>=minGreen[1];
    minover3 := t_green(3)>=minGreen[3];
```

```
minover4 := t_green(4)>=minGreen[4];
minover5 := t_green(5)>=minGreen[5];
minover7 := t_green(7)>=minGreen[7];
minover8 := t_green(8)>=minGreen[8];
maxout1 := t_green(1)>=maxGreen[1];
maxout2 := t_green(2)>=maxGreen[2];
maxout3 := t_green(3)>=maxGreen[3];
maxout4 := t_green(4)>=maxGreen[4];
maxout5 := t_green(5)>=maxGreen[5];
maxout6 := t_green(6)>=maxGreen[6];
maxout7 := t_green(7)>=maxGreen[7];
maxout8 := t_green(8)>=maxGreen[8];
minover15 := Minover1 and Minover5;
minover48 := Minover4 and Minover8;
minover37 := Minover3 and Minover7;
gapout15 := Gapout1 and Gapout5;
gapout48 := Gapout4 and Gapout8;
gapout37 := Gapout3 and Gapout7;
maxout15 := Maxout1 and Maxout5;
maxout26 := Maxout2 and Maxout6;
maxout48 := Maxout4 and Maxout8;
maxout37 := Maxout3 and Maxout7;
```

```
        callPed4 := presence(104) or occupancy (104) or presence(108)
                or occupancy(108);
    minoverPed2 := (t_green(102)>=Pedwalk[1]) or (t_green(106)>=Pedwalk[3]);
    minoverPed4 := (t_green(104)>=Pedwalk[2]) or (t_green(108)>=Pedwalk[4]);
    MaxtoFlash2 := (t_actual>=forceoff[2]-Leadflash-tamber[2]-RedClear[2]) and
                        (t_actual<=forceoff[2]-Leadflash-tamber[2]-RedClear[2]+1);
    MaxtoFlash6 := (t_actual>=forceoff[6]-Leadflash-tamber[6]-RedClear[6]) and
                        (t_actual<=forceoff[6]-Leadflash-tamber[6]-RedClear[6]+1);
    MaxtoFlash26 := MaxtoFlash2 and MaxtoFlash6;
/*-------------------------------------------------------------------------*/
/* MAIN PROGRAM */
S00Z002:  IF initial=0 THEN
S03Z002:  set_sg_direct(22, off); set_sg_direct(62, off);initial:=1
  END;
S00Z004:  GOSUB master_clock;
S00Z013:  IF t_green(1) and t_green(5) THEN
S03Z013:  IF call26 and minover15 and (gapout15 or maxout15) THEN
S04Z013:  sg_red(1); sg_red(5); start(Phase5ClearTimer); NextRing1Phase:=2;
        NextRing2Phase:=6
            END
  END;
S00Z015:  IF t_green(2) and t_green(6) THEN
S01Z015:  IF MaxtoFlash26 THEN
```

```
S02Z015:  set_sg_direct(22,amber_f);set_sg_direct(62,amber_f); start(Flasher26Timer);
S03Z015:  IF call37 and maxout26 THEN
S04Z015:  set_sg_direct(22,amber_f);set_sg_direct(62,amber_f);
            start(Phase26ClearTimer); NextRing1Phase:=3;NextRing2Phase:=7
          ELSE
S03Z017:  IF call48 and maxout26 and (Ped2Active=0) THEN
S04Z017:  set_sg_direct(22,amber_f);set_sg_direct(62,amber_f);
            start(Phase26ClearTimer); NextRing1Phase:=4;NextRing2Phase:=8
          ELSE
S03Z019:  IF call15 and maxout26 and (Ped2Active=0) THEN
S04Z019:  set_sg_direct(22,amber_f);set_sg_direct(62,amber_f);
            start(Phase26ClearTimer); NextRing1Phase:=1;NextRing2Phase:=5
          END
        END
       END
      END
    END;
S00Z021:  IF Flasher26Timer = LeadFlash THEN
S01Z021:  stop(Flasher26Timer);reset(Flasher26Timer); sg_red(2); sg_red(6)
  END;
S00Z023:  IF t_green(3) and t_green(7) THEN
S03Z023:  IF call48 and minover37 and (gapout37 or maxout37) THEN
S04Z023:  sg_red(3); sg_red(7); start(Phase7ClearTimer);NextRing1Phase:=4;
```

```
            NextRing2Phase:=8
        ELSE
S03Z025:  IF call15 and minover37 and (gapout37 or maxout37) THEN
S04Z025:  sg_red(3); sg_red(7); start(Phase7ClearTimer);NextRing1Phase:=1;
            NextRing2Phase:=5
        ELSE
S03Z027:  IF call26 and minover37 and (gapout37 or maxout37) THEN
S04Z027:  sg_red(3); sg_red(7); start(Phase7ClearTimer);NextRing1Phase:=2;
            NextRing2Phase:=6
        END
      END
    END
  END;
S00Z029:  IF t_green(4) and t_green(8) THEN
S03Z029:  IF call15 and minover48 and (gapout48 or maxout48) THEN
S04Z029:  sg_red(4);sg_red(8); start(Phase48ClearTimer);NextRing1Phase:=1;
            NextRing2Phase:=5
        ELSE
S03Z031:  IF call26 and minover48 and (gapout48 or maxout48) THEN
S04Z031:  sg_red(4);sg_red(8); start(Phase48ClearTimer);NextRing1Phase:=2;
            NextRing2Phase:=6
        END
      END
```

```
  END;
S00Z034:  IF Phase5ClearTimer>=tAmber[5]+RedClear[5] THEN
S03Z034:  IF (NextRing2Phase=6) or (NextRing1Phase=2) THEN
S04Z034:  sg_green(2); sg_green(6);stop(Phase5ClearTimer);reset(Phase5ClearTimer);
          set_sg_direct(22, off); set_sg_direct(62, off);
S05Z034:  sg_green(102);sg_green(106);Ped2Active:=1
      END
  END;
S00Z036:  IF Phase26ClearTimer>=tAmber[2]+RedClear[2] THEN
S03Z036:  IF (NextRing1Phase=3) and (NextRing2Phase=7) THEN
S04Z036:  sg_green(3);sg_green(7);stop(Phase26ClearTimer);
      reset(Phase26ClearTimer)
      ELSE
S03Z038:  IF (NextRing1Phase=4) and (NextRing2Phase=8) THEN
S04Z038:  sg_green(4);sg_green(8);stop(Phase26ClearTimer);
          reset(Phase26ClearTimer);
S05Z038:  IF CallPed4 THEN
S06Z038:  sg_green(104);sg_green(108)
      END
      ELSE
S03Z040:  IF (NextRing1Phase=1) and (NextRing2Phase=5) THEN
S04Z040:  sg_green(1);sg_green(5);stop(Phase26ClearTimer);
          reset(Phase26ClearTimer)
```

```
        END
       END
      END
    END;
S00Z042:  IF Phase7ClearTimer>=tAmber[7]+RedClear[7] THEN
S03Z042:  IF (NextRing1Phase=4) and (NextRing2Phase=8) THEN
S04Z042:  sg_green(4);sg_green(8);stop(Phase7ClearTimer);reset(Phase7ClearTimer);
S05Z042:  IF CallPed4 THEN
S06Z042:  sg_green(104);sg_green(108)
        END
        ELSE
S03Z044:   IF (NextRing1Phase=1) and (NextRing2Phase=5) THEN
S04Z044:   sg_green(1);sg_green(5);stop(Phase7ClearTimer);reset(Phase7ClearTimer)
         ELSE
S03Z046:   IF (NextRing1Phase=2) and (NextRing2Phase=6) THEN
S04Z046:   sg_green(2);sg_green(6);stop(Phase7ClearTimer);reset(Phase7ClearTimer);
             set_sg_direct(22, off); set_sg_direct(62, off);
S05Z046:   sg_green(102);sg_green(106);Ped2Active:=1
         END
       END
     END
   END;
S00Z048:  IF Phase48ClearTimer>=tAmber[8]+RedClear[8] THEN
```

```
S03Z048:  IF (NextRing1Phase=1) and (NextRing2Phase=5) THEN
S04Z048:  sg_green(1);sg_green(5);stop(Phase48ClearTimer);
            reset(Phase48ClearTimer)
        ELSE
S03Z050:   IF (NextRing1Phase=2) and (NextRing2Phase=6) THEN
S04Z050:   sg_green(2);sg_green(6);stop(Phase48ClearTimer);
            reset(Phase48ClearTimer); set_sg_direct(22, off); set_sg_direct(62, off);
S05Z050:   sg_green(102);sg_green(106)
         END
       END
      END
PROG_ENDE:  .
/*-------------------------------------------------------------------------*/
```